

Heavy Metal Ion Extraction and Electrochemical Detection with a Thermomorphonic Ionic Liquid

Dissertation
Fabian Schmitt



TECHNISCHE
UNIVERSITÄT
DARMSTADT



Heavy Metal Ion Extraction and Electrochemical Detection with a Thermomorphic Ionic Liquid

Extraktion und Elektrochemische Detektion von Schwermetallen mit einer
Thermomorphen Ionischen Flüssigkeit

Vom Fachbereich Chemie
der Technischen Universität Darmstadt

zur Erlangung des Grades

Doktor-Ingenieur
(Dr.-Ing.)

Dissertation
von Fabian Schmitt

Erstgutachter: Prof. Dr.-Ing. Dipl.-Kfm. Bastian J. M. Etzold

Zweitgutachter: Prof. Dr. rer. nat. Markus Biesalski

Darmstadt 2023

Schmitt, Fabian

Heavy Metal Ion Extraction and Electrochemical Detection
with a Thermomorphic Ionic Liquid

Darmstadt, Technische Universität Darmstadt,

Jahr der Veröffentlichung der Dissertation auf TUprints: 2023

Tag der mündlichen Prüfung: 23.11.2023

Veröffentlicht unter CC BY-SA 4.0 International

<https://creativecommons.org/licenses/>

Erklärungen laut Promotionsordnung

§8 Abs. 1 lit. c der Promotionsordnung der TU Darmstadt

Ich versichere hiermit, dass die elektronische Version meiner Dissertation mit der schriftlichen Version übereinstimmt und für die Durchführung des Promotionsverfahrens vorliegt.

§8 Abs. 1 lit. d der Promotionsordnung der TU Darmstadt

Ich versichere hiermit, dass zu einem vorherigen Zeitpunkt noch keine Promotion versucht wurde und zu keinem früheren Zeitpunkt an einer in- oder ausländischen Hochschule eingereicht wurde.

§9 Abs. 1 der Promotionsordnung der TU Darmstadt

Ich versichere hiermit, dass die vorliegende Dissertation selbständig und nur unter Verwendung der angegebenen Quellen verfasst wurde.

§9 Abs. 2 der Promotionsordnung der TU Darmstadt

Die Arbeit hat bisher noch nicht zu Prüfungszwecken gedient.

Darmstadt, den 09.10.2023

Fabian Schmitt

Danksagung

An dieser Stelle möchte ich all jenen Danken, die mich auf verschiedenste Art und Weise bei der Erstellung dieser Arbeit und rundherum unterstützt haben.

Zunächst gilt mein Dank Prof. Bastian Etzold für die Möglichkeit zur Promotion in seinem Arbeitskreis, die stets konstruktive Betreuung, das Einräumen von Freiräumen und die in jeglicher Hinsicht lehrreiche Zusammenarbeit in einer tollen Arbeitsumgebung.

Ebenso Bedanken möchte ich mich bei Prof. Biesalski für das Koreferat dieser Arbeit, die Leitung des Verbundprojektes FiPRe und die enge Kooperation. Tizian Venter und den weiteren Mitgliedern dieses Projektes möchte ich für die Zusammenarbeit danken und wünsche weiterhin viel Erfolg.

Ich möchte mich insbesondere bei allen Studierenden bedanken, die sich in ihren Praktika und Abschlussarbeiten mit diesem Forschungsgebiet beschäftigt haben: Benedikt Pollicino, Chandra Brabovo, Ipek Celik, Julia Hoffmann, Leander Biet, Luis Martini und Pascal Theis.

Daria Omralinov danke ich für die Erstellung des 3D-gedruckten, porigen Spacers als wiederverwendbare, definierte Zelle zur Annäherung an die Papier-basierten elektrochemischen Zellen.

Ein besonderer Dank gilt allen Kolleg*innen des Arbeitskreises Etzold. Neben dem fachlichen Austausch habe ich die tägliche Arbeit und das Miteinander freundschaftlich, lustig und vielseitig bereichernd erlebt. Marianne Blascak, Alfons Drochner und Jan Gläsel möchte ich für all die Organisationsarbeit und Unterstützung und die Gespräche rundherum danken.

Prägend für die gesamte Zeit an der TU Darmstadt bleiben allem voran die fachlichen als auch unfachlichen, stets bereichernden Diskussionen mit Konrad Krois, Maximilian Hungsberg, Felix Herold, Stephan Schultheis und vielen weiteren in bester Erinnerung.

Sowohl diese Arbeit als auch das vorangegangene Studium wären ohne den bedingungslosen Rückhalt meiner Familie so nicht möglich gewesen – Danke Martina und Karl, danke Sebastian! Einen besonderen Dank möchte ich an Laura und Noemi richten für die ausdauernde Unterstützung, das Aushalten, die Bereicherungen, Erheiterungen, Erinnerungen und Erlebnisse zur und während der Fertigstellung dieser Arbeit als auch drumherum!

Kurzfassung

Schwermetalle umfassen einen Großteil der Elemente im Periodensystem und können überall in der Erdkruste bis zum Erdkern gefunden werden. Abhängig von ihrer Konzentration übernehmen sie mitunter wichtige Funktionen in der belebten Natur, können jedoch auch eine Gefahr für Gesundheit, Leben und Umwelt darstellen. Im Gegensatz zu organischen Materialien sind sie nicht biologisch abbaubar und können sich so anreichern. Durch menschliche Aktivitäten werden Schwermetalle zudem an die Erdoberfläche befördert. Durch Korrosion entstehen ionische, wasserlösliche Spezies. Da diese bereits in geringen Konzentrationen eine Gefahr darstellen, schlägt die Weltgesundheitsorganisation (engl. World Health Organization, WHO) Grenzwerte vor, wie beispielsweise $5 \mu\text{g L}^{-1}$ für Blei (Pb) in Leitungswasser. Die Überprüfung der Konzentrationen erfolgt mittels etablierter, höchst sensibler Labormethoden wie der Atomabsorptionsspektrometrie (AAS) oder der induktiv gekoppelter Plasma - optischer Emissionsspektrometrie (ICP-OES). Diese sind jedoch ortsfeste investitionsintensive Methoden und erfordern eine entsprechende Infrastruktur und geschultes Personal. Um point-of-care (PoC) Anforderungen gerecht zu werden, wurden mobile Geräte für elektrochemische Nachweisverfahren entwickelt und deren Potential in wissenschaftlichen Arbeiten demonstriert. Bisher konnten sich diese Anwendungen jedoch nicht durchsetzen, während elektrochemische Sensoren in anderen Bereichen, z.B. für pH- und Blutzucker-Messungen, weit verbreitet sind.

Zur Erhöhung der Sensitivität und Selektivität bei der elektrochemischen Schwermetalldetektion können die eingesetzten Elektroden chemisch modifiziert werden. Üblicherweise bestehen modifizierte Elektroden aus verschiedenen Kohlenstoffmaterialien wie glasartigem Kohlenstoff, Graphit oder Nanoröhrchen, auf die Bismut, welches aus Umweltgründen Quecksilber in dieser Funktion ablöst, und Nafion[®], ein perfluoriertes Polymer mit Sulfonsäurefunktionalität, aufgebracht werden. Überdies kann die Ionenselektivität durch Modifikation mit Metallionen-komplexierenden Molekülen erhöht werden. In der wissenschaftlichen Literatur werden Elektrodenmaterialien beschrieben mit Nachweisgrenzen (engl. limit of detection, LOD) weit unterhalb der WHO-Vorgaben.

Die Extraktion von Schwermetallen ist neben der (Ab-)wasseraufbereitung auch durch die Rückgewinnung von Metallen aufgrund ihres ökonomischen Wertes motiviert. So wird im Themenfeld der Hydrometallurgie an Extraktionsmitteln geforscht, die möglichst selektiv sind und hohe Extraktionskoeffizienten ermöglichen. Dabei können unter anderem ionische Flüssigkeiten (engl. ionic liquid, IL) eingesetzt werden.

ILs sind Salze mit Schmelzpunkten unter $100 \text{ }^\circ\text{C}$ bzw. Raumtemperatur (RTIL) und bilden eine Klasse an Substanzen mit vernachlässigbarem Dampfdruck und elektrischer Leitfähigkeit. Aufgrund der großen Anzahl an Kombinationsmöglichkeiten von Anionen und Kationen und der Modifikation der chemischen Konstitution, insbesondere bei organischen Ionen, und den damit einhergehenden, einstellbaren, physikalisch-chemischen Eigenschaften, werden ILs für

die unterschiedlichsten und insbesondere elektrochemischen Anwendungen untersucht. In der elektrochemischen Schwermetalldetektion werden ILs bisher fast ausschließlich als Binder bei der Elektrodenpräparation eingesetzt. Die IL Betain Bis(trifluoromethylsulfonyl)imid [HBet][NTf₂], deren selektive Extraktionseigenschaften für Metallionen aus wässriger Lösung untersucht wurde, vermag verschiedene Metalloxide aufzulösen, wobei die anschließende elektrochemische Detektion dokumentiert wurde. Das Gemisch aus [HBet][NTf₂] und Wasser weist thermomorphes Phasenverhalten auf. Oberhalb der oberen kritischen Lösungstemperatur (engl. upper critical solution temperature, UCST) liegt bei allen Zusammensetzungen ein einphasiges System vor. Kühlt das Gemisch ab, trennen sich die IL-reiche und wasserreiche Phase. Dieses Verhalten kann sich bei der Extraktion zunutze gemacht werden, wodurch Rühren zur Vergrößerung der Phasenaustauschfläche umgangen werden kann. Dies könnte in einer mobilen Anwendung mit kleinen Volumina und hochviskosen ILs Vorteile mit sich bringen.

Eine weitere Disziplin innerhalb der PoC ist die Entwicklung integrierter, mikrofluidischer Sensoren. Für den Einmalgebrauch sollen diese klein sein und aus kostengünstigen, verfügbaren und unkritischen Materialien bestehen. Papier-basierte Materialien erfüllen diese Anforderungen als Fluidkanal und Substrat und stellen bereits einen prominenten Vertreter in dieser Funktion dar.

Um störende Interferenzen bei der Detektion mit anderen Ionen in einer Probe zu vermeiden und gleichzeitig den Einsatz kostengünstiger Arbeitselektroden zu ermöglichen, sollen in dieser Arbeit elektrochemische Methoden mit einer vorangeschalteten Extraktion des Analyten (hier Pb²⁺) untersucht werden. Eine IL soll dabei sowohl als Extraktionsmittel als auch als Elektrolyt fungieren. Schließlich soll dieses Konzept auf die Anwendung in Papier-basierten, mikrofluidischen Sensoren übertragen werden. Die IL muss daher die Anforderungen an ein Extraktionsmittel, an einen Elektrolyten und an ein Flussmittel in einem Papierkanal vereinen.

Trotz vergleichsweise hoher Wasseraufnahme eignet sich die IL [HBet][NTf₂] aufgrund der Extraktionseigenschaften durch die Carboxy-Funktion des Kations und wurde überdies aufgrund ihrer thermomorphen Eigenschaften für diese Arbeit gewählt. Wassergesättigte [HBet][NTf₂] konnte mithilfe der Anfertigung des Walden-Plots charakterisiert werden. Die Extraktion von Pb²⁺ aus wässrigem Medium nach Erwärmung über die UCST konnte mittels ICP-OES bestätigt werden. Die Analytkonzentration konnte dabei sowohl durch die Erhöhung des initialen Wasser-zu-IL-Verhältnis als auch durch die Zugabe von zwitterionischem Betain zu dem Gemisch erhöht werden. Eine Erhöhung der Wassermenge führte jedoch schließlich zu einer vollständigen Auflösung der IL-reichen Phase.

Pb²⁺ konnte in der IL nach der Extraktion mithilfe der SWV (engl. square wave voltammetry) detektiert werden, wobei Methodenparameter, übernommen von wässrigen Systemen, hin zu stärkeren Signalen optimiert werden können. Eine Messung bei erhöhten Temperaturen (42 °C) führt zu einer weiteren Signalverstärkung, was mit der geringeren Viskosität und der höheren elektrischen Leitfähigkeit begründet werden kann. Die Zugabe von zwitterionischem Betain kann die gemessenen Signale verstärken, jedoch sinkt die Leitfähigkeit mit zunehmender Zugabe und der Effekt ist nicht mehr detektierbar. Die starke Erhöhung der

Konzentration bei der Extraktion führt somit nur begrenzt zu größeren Signalen in der elektrochemischen Detektion.

Die Signalintensität der SWV konnte durch Modifikation der Arbeitselektroden mit Nafion® und Bismut weiter gesteigert werden. Der stärkste Effekt zeigte sich, wenn Bismut bei der Elektrodenpräparation gelöst vorlag. Die Zugabe von Kohlenstoffmaterialien (Ruß bzw. Graphit-Pulver) führte zu keiner Steigerung, offenbarte jedoch die Notwendigkeit weiterer Parameteranpassungen bei Änderung des Elektrodenmaterials.

Eine Kombination aus erhöhtem, initialem Wasser-zu-IL-Verhältnis und Betain-Zugabe bei der Extraktion mit Temperaturerhöhung und Elektrodenmodifikation bei der Detektion führte zu einer Nachweisgrenze (engl. limit of detection, LOD) von 30 ppb. Dies liegt oberhalb der WHO-Vorgaben, demonstriert jedoch das Potential der Kombination aus Extraktion und Detektion.

Schließlich konnte die Detektion von Pb^{2+} in [HBet][NTf₂] nach der Extraktion in einer Papier-basierten Zelle durchgeführt werden. Hierzu wurde aufgrund der Flussgeschwindigkeit der IL in Papieren Glasfaser-haltiges Material verwendet. Trotz kürzerer Zeiten zur Anreicherung des Analyten und mit nicht optimierten Extraktionen und Elektroden wurden um ein zehnfaches höhere Signalintensitäten gemessen, bei gleichzeitig um ein hundertfaches geringeren Widerständen. Zudem erlauben die kleinen Abmessungen der Papier-basierten Zelle mit dem geringen Elektrodenabstand den Einsatz von geringen Mengen Elektrolyt.

Zusammenfassend konnte in dieser Arbeit die Kombination der Extraktion mit anschließender elektrochemischer Detektion mithilfe der thermomorphen IL [HBet][NTf₂] demonstriert werden. Möglichkeiten zur Analytanreicherung im Elektrolyten und der Erhöhung der Signalintensitäten konnten ausgemacht und genutzt werden. Das Konzept konnte auf Papier-basierte Zellen übertragen werden. Die geringen Elektrodenabstände verringern den Zellwiderstand und höhere Signalintensitäten konnten gemessen werden.

Abstract

Heavy metals comprise a large proportion of the elements in the periodic table and can be found anywhere from the earth's crust to its core. Depending on their concentration, some perform important functions in living nature, but can also pose a risk to health, life, and the environment. Unlike organic materials, they are not biodegradable and can therefore accumulate. Human activities additionally bring heavy metals to the earth's surface. Corrosion produces ionic, water-soluble species. As these pose a risk even in low concentrations, the World Health Organization (WHO) proposes upper limits, such as $5 \mu\text{g L}^{-1}$ for lead (Pb) in tap water. The concentrations are usually monitored using established, highly sensitive laboratory methods such as atomic absorption spectrometry (AAS) or inductively coupled plasma optical emission spectrometry (ICP-OES). However, these are stationary, investment-intensive methods and require laboratory infrastructures and trained personnel. In order to meet point-of-care (PoC) requirements, mobile devices for electrochemical detection methods have been developed and their potential demonstrated in scientific work. So far, however, these applications have not been able to establish, while electrochemical sensors continue to be used in other areas, e.g., for pH and blood sugar measurements.

To increase the sensitivity and selectivity of electrochemical heavy metal detection, the electrodes used can be chemically modified. Modified electrodes usually consist of various carbon materials such as glassy carbon, graphite, or nanotubes to which bismuth, which has replaced mercury in this function for environmental reasons, and Nafion[®], a perfluorinated polymer with sulfonic acid functionality, are applied. In addition, ion selectivity can be increased by modification with metal ion-complexing molecules. Electrode materials with limits of detection (LOD) far below the WHO specifications are described in the scientific literature.

In addition to (waste) water treatment, the extraction of heavy metals is also motivated by the recovery of metals due to their economic value. In the field of hydrometallurgy, research is being conducted into extracting agents that are selective and enable high extraction coefficients. Ionic liquids (ILs) can be used for this purpose.

ILs are salts with melting points below $100 \text{ }^\circ\text{C}$ or room temperature (RTIL) and form a class of substances with negligible vapor pressure and electrical conductivity. Due to the large number of possible combinations of anions and cations and the modification of the chemical constitution, particularly in the case of organic ions, and the associated adjustable physico-chemical properties, ILs are intensively studied, and electrochemical applications are being investigated. In electrochemical heavy metal detection, ILs have so far been used almost exclusively as binders in electrode preparation. The IL betaine bis(trifluoromethylsulfonyl)imide [HBet][NTf₂], whose selective extraction properties for metal ions from aqueous solution were investigated, is able to dissolve various metal oxides, and the subsequent electrochemical detection was documented. The mixture of [HBet][NTf₂]

and water exhibits thermomorphic phase behaviour. Above the upper critical solution temperature (UCST), a single-phase system is present for all compositions. When the mixture cools down, the IL-rich and water-rich phases separate. This behaviour can be exploited for extraction, whereby stirring can be avoided to increase the phase exchange surface. This could have advantages in a mobile application with small volumes and highly viscous ILs.

Another discipline within PoC is the development of integrated, microfluidic sensors. For single use, these should be small and consist of inexpensive, available, and non-critical materials. Paper-based materials fulfil these requirements as a fluid channel and substrate and are already a prominent representative in this function.

In order to avoid disturbing interferences during detection with other metal ions in a sample and at the same time to enable the use of inexpensive working electrodes, electrochemical methods with upstream extraction of the analyte (here Pb^{2+}) are to be investigated in this work. An IL shall be employed as both the extraction agent and the electrolyte. Finally, this concept is to be transferred to the application in paper-based, microfluidic sensors. The IL must therefore combine the requirements of an extracting agent, an electrolyte, and a fluid in a paper channel.

Despite comparatively high water uptake, the IL [HBet][NTf₂] is suitable due to its extraction properties provided by the carboxy function in the cation and was chosen for this work. Additionally, it features thermomorphic properties. Water-saturated [HBet][NTf₂] could be characterized using the Walden plot. The extraction of Pb^{2+} from aqueous medium after heating above the UCST was confirmed by ICP-OES. The analyte concentration could be increased both by increasing the initial water-to-IL ratio and by adding zwitterionic betaine to the mixture. However, increasing the amount of water ultimately led to complete dissolution of the IL-rich phase.

Pb^{2+} could be detected in the IL after extraction using square wave voltammetry (SWV), whereby method parameters can be optimized for stronger signals starting from parameters for aqueous systems. Measurement at elevated temperatures (42 °C) leads to further signal amplification, which can be explained by the lower viscosity and higher electrical conductivity. The addition of zwitterionic betaine can amplify the measured signals, but the conductivity decreases with increasing mass ratio of the zwitterionic betaine, and the effect is no longer detectable. The strong increase in the concentration during extraction therefore only leads to larger signals in electrochemical detection to a limited extent.

The signal intensity of the SWV could be further increased by modifying the working electrodes with Nafion® and bismuth. The strongest effect was seen when bismuth was dissolved during electrode preparation. The addition of carbon materials (carbon black or graphite powder) did not lead to an increase but revealed the need for further parameter adjustments when changing the electrode material.

A combination of increased initial water-to-IL ratio and betaine addition during extraction with temperature increase and electrode modification during detection led to a limit of detection (LOD) of 30 ppb. This is above the WHO guidelines but demonstrates the potential of the combination of extraction and detection.

Finally, the detection of Pb^{2+} in $[\text{HBet}][\text{NTf}_2]$ after extraction was carried out in a paper-based cell. Due to the flow rate of IL in paper, material containing glass fibres was used for this purpose, although detection was conducted without flux. Despite shorter times for enrichment of the analyte and with non-optimized extractions and electrodes, signal intensities were measured that were ten times higher and resistances that were a hundred times lower compared to bulk cell experiments. In addition, the small dimensions of the paper-based cell with the small electrode spacing allow the use of small amounts of electrolyte.

In summary, this work demonstrated the combination of extraction with subsequent electrochemical detection using the thermomorphic IL $[\text{HBet}][\text{NTf}_2]$. Possibilities for analyte enrichment in the electrolyte and increasing the signal intensities were identified and utilized. The concept could be transferred to paper-based cells. The small electrode spacing reduces the cell resistance and higher signal intensities could be measured.

Table of Contents

1. Introduction	1
2. State of the Art	3
2.1. Electrochemical Heavy Metal Detection	3
2.1.1. Square Wave Anodic Stripping Voltammetry	5
2.1.2. Electrode Materials	9
2.1.3. Ionic Liquids in Electrochemical Heavy Metal Sensing	11
2.1.4. Ionic Liquids as Electrolytes	14
2.2. Extraction of Heavy Metal Ions	19
2.2.1. Ionic Liquids in Metal Ion Extraction	21
2.2.2. Homogeneous Liquid-Liquid Extraction	24
2.3. Microfluidic Devices	28
2.3.1. Flow Channels in Electrochemical Heavy Metal Sensing Devices	28
2.3.2. Paper Materials and Ionic Liquids	29
3. Objective and Scope	30
4. Experimental Setup, Materials and Methods	31
4.1. Physico-chemical Properties of ILs	31
4.1.1. Setting the Water Content	33
4.1.2. Karl Fischer Titration	33
4.1.3. Density	33
4.1.4. Viscosity	34
4.1.5. Electrical Conductivity	34
4.1.6. Walden Plot and Vogel-Fulcher-Tammann Equation	34
4.1.7. pH Measurements	35
4.1.8. Thermogravimetric Analysis	35
4.2. Homogeneous Liquid-Liquid Extraction	36
4.2.1. Water Saturation of [HBet][NTf ₂]	36
4.2.2. Lead Ion Extraction	36
4.2.3. Determination of Lead in the Extraction Process	37
4.3. Electrochemical Methods	39
4.3.1. Lead Detection with Square Wave Anodic Stripping Voltammetry	39
4.3.2. Resistance and Conductivity Determination	43
4.3.3. Electrochemical Stability	44

4.3.4. Introduction of a Paper Channel	44
5. Results and Discussion	46
5.1. Choice of the Ionic Liquid	46
5.1.1. Water Content of Saturated ILs	47
5.1.2. Physico-Chemical Properties after Water Exposure	48
5.2. Homogeneous Liquid-Liquid Extraction of Lead Ions with [HBet][NTf ₂]	50
5.2.1. Phase Behaviour	50
5.2.2. Extraction Behaviour	50
5.2.3. Effect of the Addition of Zwitterionic Betaine	53
5.3. Temperature Influence on Electrolyte Properties of [HBet][NTf ₂]	56
5.3.1. Viscosity	56
5.3.2. Electrical Conductivity	57
5.3.3. Walden Plot	59
5.3.4. Electrochemical and Thermal Stability	61
5.4. Electrochemical Heavy Metal Ion Detection	63
5.4.1. Adaptation of SWV Parameters	63
5.4.2. Temperature Influence on the Sensing Performance	66
5.4.3. Electrode Modification	68
5.4.4. Influence of Extraction Additives on the Sensing Performance	71
5.4.5. Limit of Detection	72
5.4.6. Integration of a Paper Channel	74
6. Summary	78
7. References	80
8. Appendix	I

Abbreviations

Abbreviation	Meaning
aq	(Dissolved in) aqueous phase
(s)	Solid phase
μ PAD	Microfluidic paper-based analytical device
μ PED	Microfluidic paper-based electrochemical device
AAS	Atomic absorption spectroscopy
AdSV	Adsorptive stripping voltammetry
AS	Anodic stripping
BDD	Boron doped diamond
CA	Chronoamperometry
CAD	Computer aided design
CB	Carbon black (here Vulcan XC-72, Cabot)
CE	Counter electrode
corr.	Baseline corrected
CV	Cyclic voltammetry
dep	Deposition
DPASV	Differential pulse anodic stripping voltammetry
DPV	Differential pulse voltammetry
geo	Geometrical
GP	Graphite powder
HER	Hydrogen evolution reaction
HLLE	Homogeneous liquid-liquid extraction
ICP OES	Inductively coupled plasma optical emission spectrometry
IfW	Institute of Materials Science
ini	initial
IL	Ionic liquid
ISE	Ion selective electrode
ITO	Indium tin oxide
IUPAC	International Union of Pure and Applied Chemistry
LCST	Lower critical solution temperature
lin.reg.	Linear regression
Lit.	Literature

LOD	Limit of detection
LSV	Linear sweep (or scan) voltammetry
max	Maximal
min	Minimal
misc	Miscibility
MPA	State Materials Testing Institute
OCV	Open circuit potential
org	(Dissolved in) organic phase
PEEK	Polyether ether ketone
PEIS	Potentiostatic Electrochemical Impedance Spectroscopy
PEMFC	Proton exchange membrane fuel cells
PIL	Protic ionic liquid
PoC	Point-of-care
ppb	Parts per billion
ppm	Parts per million
PTFE	Polytetrafluoroethylene
qRE	Quasi (or pseudo) reference electrode
RE	Reference electrode
RH	Relative humidity
RT	Room temperature
RTIL	Room temperature ionic liquid
sat.	(Water) saturated
SHE	Standard hydrogen electrode
SPE	Screen printed electrodes
Std.	Standard
SVR	Support vector regression
SWASV	Square wave anodic stripping voltammetry
SWV	Square wave (anodic stripping) voltammetry
TOPO	Trioctylphosphine oxide
TSIL	Task specific ionic liquid
TU	Technical University (Darmstadt)
UCST	Upper critical solution temperature
VFT	Vogel-Fulcher-Tammann
VOC	Volatile organic compounds
WHO	World Health Organization

WE	Working electrode
wt	Weight
zw. Bet	Zwitterionic betaine

Symbols

Symbol	Meaning	Unit
a_{Ox}	Activity of the oxidant	-
a_{Red}	Activity of the reductant	-
d	Average pore diameter of the paper material	m
N_A	Avogadro constant	mol^{-1}
k_B	Boltzmann constant	J K^{-1}
c	Concentration	mol L^{-1}
c_A	Concentration in phase A	mol L^{-1} , mg g^{-1}
c_B	Concentration in phase B	mol L^{-1} , mg g^{-1}
ρ	Density	g cm^3
$Diff$	Diffusion coefficient	$\text{m}^2 \text{s}^{-1}$
l	Distance covered by fluid	m
D	Distribution ratio	-
I	Electric current	A
κ	Electrical conductivity	S m^{-1}
E	Electrochemical Potential	V
E^\ominus	Electrochemical standard potential	V
e	Elementary charge	C
$\%E$	Extraction efficiency	%
F	Faraday constant	C mol^{-1}
η^{-1}	Fluidity	$\text{Pa}^{-1} \text{s}^{-1}$
f	Frequenzy	Hz
A_{geo}	Geometrical surface area	cm^2
θ	Liquid fibre contact angle	
σ	Liquid-air surface tension	N m^{-1}
$ Z $	Magnitude of electrical impedance	Ohm
$w_{\text{H}_2\text{O}}$	Mass fraction	g g^{-1}
x	Mol fraction	mol mol^{-1}
Λ_m	Molar conductivity	$\text{S m}^2 \text{mol}^{-1}$
M	Molecular mass	g mol^{-1}
K_N	Nernst distribution coefficient	-
z	Number of electrons	-

E_{Pulse}	Pulse potential	V
Q	Reaction quotient	-
E_{Step}	Step potential	V
T	Temperature	°C or K
t	Time	s
R	Universal gas constant	$\text{J mol}^{-1} \text{K}^{-1}$
T_0	VFT fitting parameter	K
A_{κ}	VFT fitting parameter electrical conductivity	-
B_{κ}	VFT fitting parameter electrical conductivity	-
A_{η}	VFT fitting parameter viscosity	-
B_{η}	VFT fitting parameter viscosity	-
η	Viscosity	Pa s
V	Volume	L

1. Introduction

Heavy metals embrace all metals in the periodic table of the chemical elements except for alkaline and earth alkaline elements. They can be found across earth's crust and to its inner core. Some are vital for the animate nature, others, and of course depending on the concentration, are toxic to organisms and are environmental hazards. Over the course of human history, anthropogenic activities are extracting elements from the soil to the surface, where they are processed to purified state, making value of their metallic properties. Corrosion of these materials leads to water dissolvable ionic species and finally to pollution of the environment. Due to their elemental nature, these pollutants are not bio-degradable and do not decay over time. Posing a threat to organisms even at low concentrations, regulations and measures have been put in place in order to limit the pollution and control the exposure. The World Health Organization (WHO) lists three heavy metals (Hg, Cd, Pb) among the "[ten] chemicals of public health concern".^[1] Mercury (Hg) is used in mining, illuminants and is emitted to the atmosphere by the combustion of coal. Cadmium (Cd) is used in batteries, corrosion protection and in pigments. Lead (Pb) is used in alloys, pigments, batteries and formally also in gasoline additives and water-piping, where it has been widely banned. The revised Drinking Water Directive, recently adopted by the European Parliament, targets a Pb-limit of $5 \mu\text{g L}^{-1}$ in tapped water within the next ten years.^[2]

Monitoring the concentrations in water and wastewater is commonly done via atomic absorption spectroscopy (AAS), inductively coupled plasma optical emission spectrometry (ICP OES), X-ray fluorescence and neutron activation analysis. All are well established standard analysis methods with low limits of detection (LOD).^[3,4] Depending on the exact method and device, femtomolar concentrations, few ng L^{-1} , can be quantified. However, there are drawbacks to these methods: they require trained personnel and laboratory environment for sample preparation plus the devices are costly, heavy in weight and use up a lot of space.^[4] This motivates the development of user-friendly, mobile and cheap techniques, delivering point-of-care (PoC) qualities.

Electrochemical devices may meet mentioned criteria. In numerous publications, researchers have demonstrated the feasibility of electrochemical detection of various heavy metals from sources such as food, soil, and aqueous phase. Multiple electrochemical methods have been developed.^[4] The underlying principle is the redox behaviour of the metals/metal ions. At different potentials redox reactions occur with currents related to the amount of the reactants. Computing the input signal and measuring the current and potential is done by galvanostats/potentiostats and computing. Due to the rapid evolution in computing power and electronic parts, more sophisticated methods are being developed and the technique is becoming less expensive.^[5,6]

Microfluidic devices make use of capillary forces for convection, use up little space and hence are suitable for PoC application. Next to traditional materials, paper can be utilized as an abundant, lightweight, biodegradable, and low-cost substrate. The technique has already been studied in electrochemical applications and proven to be beneficial to heavy metal ion detection in aqueous phase.^[7-9]

Today, electrochemical techniques are already applied for pH measurement, coulometric water titration, in gas sensors and can also be found in physiological function monitoring such as sensing glucose levels.^[10] For heavy metals, however, electrochemical sensors are not prevalent yet. While reported sensitivities are astonishingly high, sensors still lack in selectivity and stability. (Electro)chemical modifiers, membranes and coupling of different techniques are being investigated to counteract the interference of metal ions. Adopting principles from hydrometallurgy and water treatment, where metal ions ought to be selectively and efficiently extracted, might open up another promising route, that could simultaneously alleviate the requirements for the electrode materials.

The concept of utilizing ionic liquids for combined heavy metal ion extraction and subsequent electrochemical detection is investigated in the present study.

2. State of the Art

2.1. Electrochemical Heavy Metal Detection

Various analytes, e.g. organic molecules, gases, clinically relevant biomarkers, and ions, can be detected via a variety of electrochemical methods by measuring potentials, currents or frequency-dependent resistances. The term “sensor” in this context describes a device transforming a chemical, non-electric information into an electric signal in a quick manner.^[11] A sensor should be sensitive, selective and stable. Though sensors for a few analytes, such as pH meters and glucose monitors, are standardized, commercially available products, many more are subject to research, including heavy metal sensing. Lead (Pb) is a prominent representative for highly toxic heavy metals. Being exposed to lead ions is associated with severe risks to public health. Lead poisoning affects the development of brain and nervous system, reduces the intelligence quotient, alters social and learning behaviour and is linked to high blood pressure and damaging of the kidneys. It is estimated, that almost 1 million lives were lost due to lead exposure in 2019.^[12,13] It is hence frequently targeted as analyte in research on heavy metal sensing.

The property utilized for potential-controlled electrochemical heavy metal ion detection is the redox behaviour of the target analyte ion and the corresponding element at the interface of electrode and electrolyte. The potentials E , at which these electron transfers or redox reactions occur under standard conditions can be obtained from the list of standard electrode potentials (E^\ominus) and adapted using Nernst equation (Equation 1). The Nernst equation allows for calculating the potential in dependence of the temperature T and the activities of the redox couple a_{Red} and a_{Ox} . An extract of standard electrode potentials is given in Table 1. The current I over a certain time t (i.e. electric charge) is linked to the number of reactants via the Faraday constant (Equation 2) and the number of involved electrons, allowing for the determination of concentrations. However, in a real world scenario overpotentials and interferences, as well as the given conditions such as pH, temperature and the presence of chelating agents and adsorbents have to be taken into consideration.^[14]

$$E = E^\ominus - \frac{RT}{zF} \ln Q \quad \text{Equation 1}$$

$$Q = \frac{a_{\text{Red}}}{a_{\text{Ox}}}$$

$$F = N_A e \quad \text{Equation 2}$$

E electrochemical potential, E^\ominus at standard condition [V]

R universal gas constant [$\text{J mol}^{-1} \text{K}^{-1}$]

T temperature [K]

z number of electrons [-]

F Faraday constant [C mol^{-1}]

Q reaction quotient [-]

a activity [-]

N_A Avogadro constant [mol^{-1}]

e elementary charge [C]

Table 1 Extract of standard electrode potentials for some relevant reactions.^[15]

Ion	Half-cell reaction	E^{θ} vs SHE / V
Cd^{2+}	$\text{Cd}^{2+} + 2 e^{-} \rightleftharpoons \text{Cd}$	-0.403
Pb^{2+}	$\text{Pb}^{2+} + 2 e^{-} \rightleftharpoons \text{Pb}$	-0.126
Fe^{3+}	$\text{Fe}^{3+} + 3 e^{-} \rightleftharpoons \text{Fe}$	-0.037
H^{+}	$2 \text{H}^{+} + 2 e^{-} \rightleftharpoons \text{H}_2 (\text{g})$	0
Bi^{3+}	$\text{Bi}^{3+} + 3 e^{-} \rightleftharpoons \text{Bi}$	0.308
Cu^{2+}	$\text{Cu}^{2+} + 2 e^{-} \rightleftharpoons \text{Cu}$	0.342
Hg^{2+}	$\text{Hg}^{2+} + 2 e^{-} \rightleftharpoons \text{Hg} (\text{l})$	0.851

At standard conditions, Pb occurs as oxidized, divalent ions and a negative, cathodic potential relative to the standard hydrogen electrode is required to drive the reaction in favour of the reduction to the elemental, metallic state. Due to the challenges mentioned above and the expectably low concentrations of these ions might not be readily detectable by commonly applied methods in electrochemistry, such as linear sweep voltammetry (LSV) or cyclic voltammetry (CV), and more sophisticated methods have been developed. One of the most sensitive, fastest, versatile, and also most commonly applied method in heavy metal sensing purportedly is the square wave anodic stripping voltammetry (SWASV). Though, other methods such as anodic stripping (AS) in combination with the cognate differential pulse voltammetry (DPV) can also be found.^[4-7,14,16,17]

2.1.1. Square Wave Anodic Stripping Voltammetry

The square wave anodic stripping voltammetry (SWASV, for the sake of simplicity SWV in the following) is an electrochemical method comprising two consecutive steps. In the first step a constant cathodic potential is applied over a certain time period, corresponding to a chronoamperometry (CA), though here the resulting current is of little interest. During the CA the target metal ion, for example $\text{Pb}^{2+}(\text{aq})$, is reduced at the electrode surface to the elemental, metallic state, $\text{Pb}^0(\text{s})$. This pre-concentration of the analyte at the electrode can be affected by the time and the potential set for the CA and corresponds to an electrodeposition.^[7] Increasing the amount of electrodeposited metal can be achieved by either elongating the deposition time, allowing for more ions being transferred to the electrode surface, or by increasing the mass transport rate. The potential that can be applied at the electrode is limited by the hydrogen evolution reaction. Concomitant bubble formation alters the accessible surface area and proton depletion leads to increased pH, which facilitates hydroxide formation, withdrawing analyte from being detected. In the stripping step subsequent to the CA, the actual sensing is taking place. The electrode potential is inverted and over time changes into an anodic potential. Oxidizing the previously reduced metal back to its ionic state results in a peak of anodic current. Theoretically, the peak position can be assigned to a redox couple by applying Nernst equation. Via a calibration curve, the peak heights or peak areas can be assigned to the metal ion concentration, valid for this specific set of parameters. In contrast to a linear sweep of the potential (LSV), the input signal of the square wave voltammetry (SWV) follows a more complex form. The SWV is a superposition of a staircase and a pulse waveform. The current response by the system is taken at the end of each pulse with the pulsed potential E_{Pulse} , both in forward (anodic) and reverse (cathodic) direction, both within the period τ , the inverse of the frequency f . Subtraction of forward (F) and reverse (R) currents at each potential step E_{Step} leads to $\Delta I(\text{F-R})$, a peak-shaped voltammogram, when the total potential range spans over the redox potential of an analyte. The shape of resulting peaks is generally symmetrical.^[5,6,14,16] An exemplary SWV input waveform and a system response curve are depicted in Figure 1.

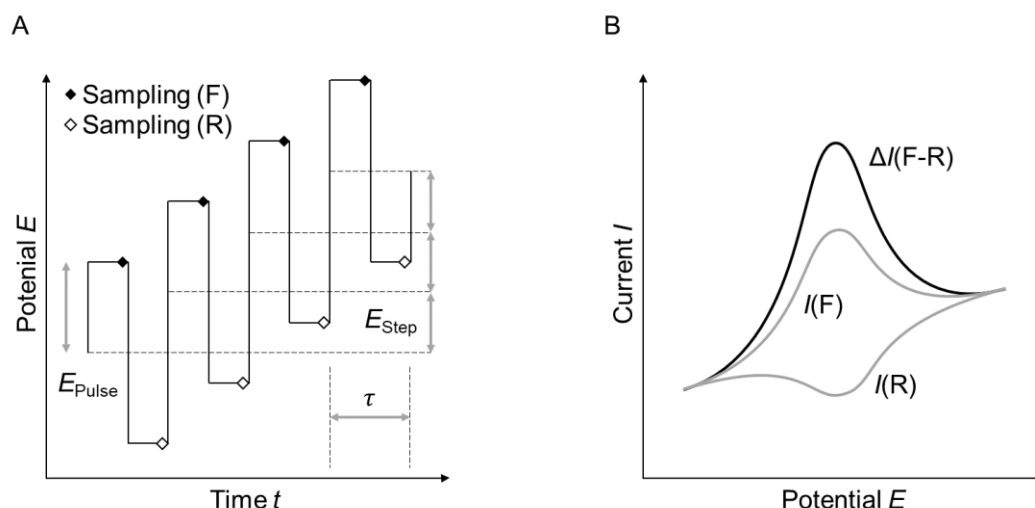


Figure 1: A: SWV input signal. If following up a chronoamperometric step of cathodic potential, this represents the stripping/detection step, and the method is referred to as SWV. B: Generic system response curve to a SWV input signal. Forward (F) and reverse (R) currents are subtracted and $\Delta I(F-R)$ is plotted at the according potential step. Shown curves represent the course of discrete data points.

Compared to other electrochemical techniques, SWV is fast, suppresses background currents and is highly sensitive. During a measurement, there is no renewal of the diffusion layer at the electrode. The high sensitivity is caused by the inverted direction of the reaction by the reversed pulse. The product of the forward pulse does not (fully) diffuse into the electrolyte but is (partially) returned to its initial state by the reverse pulse and can again be converted with the next forward pulse, until the redox potential of the analyte is surpassed. Multiplying E_{Step} and f determines the scan rate, allowing for estimation of the total duration for the scan of a certain potential window.^[5,16] The range of possible values for SWV parameters and their combination is infinite but this not rendered by the literature for heavy metal detection. A study on the influence of the frequency is included in one work, describing an increasing and broadening of stripping peaks from 5 to 50 Hz.^[18] Besides, a comprehensive sensitivity analysis seems to be lacking. Typical parameter settings used in for the stripping step in SWV Pb^{2+} detection are listed in Table 2.

Table 2 Typical values for SWV parameter settings in heavy metal detection.^[7,9,19–24]

Parameter	Value	Unit
E_{Step}	4-10	mV
E_{Pulse}	20-25	mV
f	15-25	Hz

Physical and chemical parameters of the environment of a sample may impact and impede the electrochemical sensing of heavy metals and need especially taken care of for the application in a real-world scenario. This includes the pH of a sample, sample conductivity, ions such as chlorine and bicarbonates, temperature and other heavy metal ions such as Cu.^[21] Latter two influences will be addressed in the following.

Temperature Influence

Controlled conditions prevalent in a laboratory environment do not represent actual field conditions. Temperature, however, is a critical parameter to be controlled especially in a potential real world sensing application. Changes in the temperature affect SWV in multiple ways. The viscosity of the electrolyte decreases, analyte diffusion and the electrical conductivity of the electrolyte increase and redox potentials change according to Nernst equation.^[14] RAHM et al. studied the influence of several parameters reflecting changes environmental conditions on the SWV detection of Pb²⁺. A drastic change in peak height could be observed with altering temperatures of the samples. Increasing the temperature from 20 °C to 40 °C led to a threefold increased signal. The same trend was found for real world samples. The authors hence suggest to adapt the conditions for calibration to the intended application.^[21]

Temperature can also be employed to induce forced convection of the electrolyte. A temperature gradient can thereby increase the mass transfer facilitate the deposition of analyte in the pre-concentration step.^[14] Forced convection can of course also be implemented via stirring, with a huge potential of increasing the stripping peak currents.^[20] Temperature is here regarded as a disruptive factor. Even though temperatures for the electrochemical experiments are often, though not always stated, a best-practice protocol or standardized field-experiment stress tests do not seem to exist.

Metal Ion Interference

A major challenge in electrochemical heavy metal detection is the interference of other metals contained in a real-world sample. Adjacent stripping signals of different metals might overlap, complicating the assignment to the metals as well as changing the shape of the peak and the stripping behaviour, compared to single metal detection. Intermetallic Cu-Zn formation at the electrode surface for example increases the signal assigned to Cu stripping, due to the similar potentials. This type of interaction can also be employed to bind otherwise interfering metals, as for instance Ga leads to Ga-Cu formation, enabling Zn detection in a Cu containing sample. In the same manner, Bi forms an intermetallic compound as shown for Cd and thallium (Tl) containing samples. Stripping potential of Cd was shifted to more negative potentials and thereby the signal from was separated from Tl stripping. Two signals, that otherwise would be difficult to assign.^[14]

The interference of Cu²⁺ is a severe challenge in Pb²⁺ SWV detection. Cu has a more noble character and electrodeposits at lower cathodic potentials compared to Pb. With increasing Cu

concentration, Cu stripping peaks are superimposing Pb peaks and both peaks become less separable. Eventually, no signal can be assigned to Pb stripping. In real world samples the influence, however, was shown to have counterintuitively smaller impact, possibly due to other, overlaying and opposing interactions within these samples.^[21] The presence of Fe and Cd furthermore impedes the stripping signal assignment in Pb^{2+} SWV detection.^[7,14]

Excluding some metals and thereby reducing the number of metals at the electrode reduces potential interference and increases selectivity and reliability of a sensor. This can be achieved via preceding steps featuring ion exchange resins and complexation. The elimination of Cu^{2+} for instance can be achieved by the addition of ferrocyanide. This complexes Cu^{2+} and prevents the ions from being electrodeposited on the electrode's surface.^[14,22] In addition to physical modifications of the electrodes or samples, learning algorithms were also shown to be a useful tool in determining the actual concentration of an analyte. Support vector regression (SVR) in combination with SWV was trained to derive Pb concentrations from signals in SWV of Pb^{2+} and Cu^{2+} containing samples. The relationship was found to be non-linear, stressing the complexity of the issue.^[22]

2.1.2. Electrode Materials

In the field of electrochemical heavy metal ion detection research is mainly focused on the development of novel electrode materials aiming for higher sensitivities, viz. lower LODs for the target analytes. A common approach is the utilization of a modifier, an electrocatalyst, that is opening up a new route for the electron transfer to and from the analyte. Formerly, Hg based electrodes were most commonly used in heavy metal sensing devices, delivering exceptional heavy metal detection performance. However, this approach somewhat contradicts the original motivation of this very discipline. Hg has been substituted by electrodes containing Bi, starting with WANG et al. introducing Bi-film electrodes in the year 2000 for the first time. Bi was then becoming one of the most dominant modifiers in this field. Along with its low toxicity, environmental friendliness, and the label “green element”, even wearable applications for heavy metal monitoring with Bi electrodes were proposed. During the deposition step, reduced metals form intermetallic compounds with Bi on the electrode surface, facilitating the deposition of analyte metals. Obtained peak heights are increased and stripping signals are usually well defined. Bi in this context was investigated in combination with different substrates, metal and carbon based, as well as together with other additives, such as Nafion[®], a PTFE derived polymer. The electrode modification with Bi can be conducted both in and ex situ. Therefore, a Bi source is either added to the analyte containing electrolyte buffer solution and is electrodeposited in the same step as the analyte, or Bi is brought onto the electrode before being used for heavy metal ion detection.^[25–28]

Another development of electrodes for heavy metal detection is directly motivated by the requirement of its disposability and large-scale production. In contrast to expensive and possibly toxic metals, carbon-based materials are used as electrically conductive and modifiable electrode materials. A range of carbon materials from carbon black to graphite, carbon nanotubes and graphene have been investigated.^[29–33] These materials can be casted as pastes or drop coated from inks, mixtures of dispersed electrode precursor materials, that solidify by evaporation of the solvent.^[7,31] A promising fabrication technique for cheap and reproducible preparation of disposable electrodes is screen printing. Obtained screen printed electrodes (SPE) are hence also popular in heavy metal detection and are demonstrated to provide WHO compliant LODs in real world samples.^[29,30,32–34] In carbon pastes as well as drop coated and SPEs, binders are incorporated. Nafion[®] is widely utilized in electrochemistry and is well known for its application as membrane separating the half-cells in proton exchange membrane fuel cells (PEMFC). The backbone of this polymer consists of fluorinated carbon chains, decorated with perfluorinated branches ending with sulfonic acid groups, conferring the cation exchange properties. As a dispersed polymer it serves as binder in mentioned electrode preparation.^[20,31,32,35] With the added functionality Nafion[®] also has a positive impact on the detection of heavy metals. In their work, XIE et al. demonstrate step by step, how the respective addition of Bi, carbon black and Nafion[®] on a glassy carbon substrate result in increased signals in combined Cd²⁺ and Pb²⁺ DPASV detection.^[31]

A prominent approach for electrochemical ion detections is the application of ion selective electrode (ISE), foremost known from pH electrodes and by analogy to Nafion[®] in PEMFC.^[10] The actual electrode in such a configuration is separated from the electrolyte by a membrane. Selective ionophores carry ions through the membrane material to the electrochemically

active surface of the electrode, allowing for their detection. For Pb^{2+} this carrier function can be provided by crown ethers, calixarenes, their derivatives, amides, and thioamides. However, membranes with these ionophores may still be permeable for other ions, reducing the overall sensing selectivity. It is concluded that the selectivity of ionophores towards Pb^{2+} needs to be increased to unfold the potential of electrochemical detection.^[36,37]

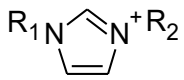
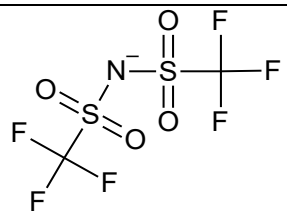
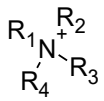
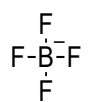
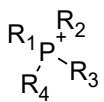

To selectively increase the concentration of a metal of interest on the surface of the electrode, chemical modifications can be introduced at the electrode. The analyte is attracted to the surface by the presence of chelating groups, increasing the local concentration. This technique is known as adsorptive stripping voltammetry (AdSV). ALSHAWI et al. prepared a Pt electrode with nitrilotriacetic acid as chelating molecule attached to a polymer, immobilized on the electrode surface and report LODs of 1.73, 2.33, and 1.99 $\mu\text{g L}^{-1}$ for combined Hg^{2+} , Pb^{2+} , and Zn^{2+} detection. Still, the presence of Cu and Co ions interfered by increasing the peak currents, whereas Ni ions decreased peak currents of the three analytes.^[38] In similar fashion, 5-chloro-7-iodo-8-hydroxyquinoline was employed as adsorbent. The LODs in combined detection were 0.1 $\mu\text{g L}^{-1}$ (Pb^{2+}) and 0.06 $\mu\text{g L}^{-1}$ (Cd^{2+} and Zn^{2+}). The addition of Cu^{2+} competes for the complexing sites and therefore decreases peak currents.^[39] JOSÉ et al. combine aspects of multiple approaches by modifying a glassy carbon electrode with a Hg film, Nafion[®] and the nucleobase guanine as adsorptive agent for Pb^{2+} and Cd^{2+} detection (LODs: 0.26 and 0.25 $\mu\text{g L}^{-1}$).^[18]

Other studies include the introduction of highly elaborated compounds such as graphene, graphene oxide, fluorinated graphene, gold nanoparticles and gold nano-cages for highly sensitive sensing.^[20,23,32,40,41] These materials and approaches clearly demonstrate the capabilities of electrochemical heavy metal detection with LODs far below WHO guidelines. However, they also feature complicated electrode preparation and high-tech materials, that will have to be proved to prevail. Despite these achievements in the development of highly sensitive electrode materials, though, also pristine technical grade graphite foil was shown to be a suitable electrode material. In their work, the researchers SHEN et al. designed a 3D-cell configuration with graphite foil WE, CE and RE, sandwiching a paper channel for electrolyte transport. LODs were 1.2 $\mu\text{g L}^{-1}$ and 1.8 $\mu\text{g L}^{-1}$ in simultaneous Cd^{2+} and Pb^{2+} detection via SWV. The sensing was further demonstrated to be feasible in spiked mineral water. In stability tests it was found that the modification with Bi_2O_3 indeed increases the sensing performance, though it is prone to the exposure to air and the performance decreases over time. The unmodified electrode in contrast remained stable.^[7] Stability is a crucial property for a reliable sensor in real-world application. The introduction of channels for passive electrolyte transport in microfluidic devices will be addressed in chapter 2.3.

2.1.3. Ionic Liquids in Electrochemical Heavy Metal Sensing

Ionic liquids (ILs) are salts with melting points below 100 °C – a class of substances that solely consist of ions and that can be subordinated to molten salts. The number of conceivable, simple, primary ion combinations is estimated to be > 1 Mio.^[42] One of the earliest mentions of a substance with the corresponding characteristic is ethylammonium nitrate [EtNH₃][NO₃] in 1914 with a melting point of 13-14 °C.^[43,44] The publication of origin is on molecular size and electrical conductivity of molten salts and written by WALDEN, who is also the eponym of the Walden plot and the Walden rule.^[43,45] Numerous compounds have been reported ever since, that can be further subdivided into room temperature (RT)ILs, protic (P)ILs, task specific (TS)ILs, etc.. Some of their physico-chemical characteristics can be attributed to the vast majority of ILs, though outlying examples can be found within the sheer number of compounds. A selection of chemical structures of cations and anions that can typically be found in ionic liquids and which are also mentioned in the following chapters, is shown in Table 3.

Table 3: Chemical structures of cations and anions typically found in ILs.
R=alkyl chain

Cations	Anions
 1-R ₁ -3-R ₂ -imidazolium	 Bis(trifluoromethane)sulfonimide
 R ₁ R ₂ R ₃ R ₄ -ammonium	 Tetrafluoroborate
 R ₁ R ₂ R ₃ R ₄ -phosponium	 Hexafluorophosphate
	Cl ⁻ Chloride

ILs are typically non-volatile, showing a neglectable vapour pressure. Mainly due to the concomitant low discharge into the atmosphere and non-flammability compared to volatile organic compounds (VOCs), that are usually used in chemical industry, ILs are labelled “green solvents”.^[46,47] In 2006 EARLE et al. surprisingly demonstrated the distillation and thermal separation of several ILs.^[48] This report is asterisking a core characteristic of ILs and at the

same time opens a new research field for the application of this class of substances, according to WASSERSCHIED.^[49]

ILs generally offer a wide liquid range, though with relatively high viscosities. Due to their ionic nature, ILs inherently feature an electrical conductivity with a wide electrochemical stability window.^[50] In contact with water different ILs show diverse behaviours, ranging from hydrolysis of aluminium chloride based ILs to high hydrophobicity of ILs with long alkyl chains or fluorinated anions such as bis(trifluoromethanesulfonyl)imide [NTf₂] and bis(pentafluoroethanesulfonyl)imide [BETI].^[51] The properties of an IL generally depend on the combination of the anion and cation and their chemical nature. Desired properties can be tuned by the choice of the ions and, especially in the case of comprising organic molecules, the addition of side chains and functional groups. Due to their low vapour pressure, ILs can be purified from water and other solvents via rotary evaporation. Entirely removing all residues, however, requires a lot of effort and remaining impurities impact physico-chemical properties, such as density, viscosity and electrochemical stability. The generally large electrochemical stability windows allow for studying the redox behaviour of compounds that would not be accessible within the electrochemical stability window of other electrolytes, such as water, where they would be superimposed by decomposition currents.^[52-56]

Due to these interesting and tailorable properties of ILs, they are also investigated in electrochemistry in general and in electrochemical detection in specific. A major group of analytes are gases and bio-organic compounds. However, ILs are also reported in connection with electrochemical heavy metal detection. Herein the IL may serve as replacement of insulating mineral oil and functioning as a binder in the fabrication of carbon pastes.^[57] The incorporation of ILs in electrode materials was moreover shown to be beneficial to the sensing performance.

KHANI et al. compared carbon pastes of multi walled carbon nanotubes with paraffin oil and the IL [BMIm][BF₄] as binder. In potentiometric monitoring of Hg²⁺ LODs could be improved by two orders of magnitude by the substitution of paraffin oil by the IL. The authors state three arguments for this observation: firstly, [BMIm][BF₄] has a higher dielectric constant and transport of analyte ions should be more mobile; secondly, conductivity increases, improving the dynamic working range; and thirdly, added 1-(2-ethoxyphenyl)-3-(3-nitrophenyl)triazene is soluble in [BMIm][BF₄], increasing the mobility of the ionophore.^[58]

In CV experiments with K₃[Fe(CN)₆] it was shown that the addition of the similar IL 1-butyl-2,3-dimethylimidazolium tetrafluoroborate [BMMIm][BF₄] leads to higher and more well-defined peaks as with graphene and graphene/Nafion[®] modified SPEs. Nafion[®] and IL combined further increase peak height and sharpness. In SWV detection of Zn²⁺, Cd²⁺ and Pb²⁺ this modification increased peak heights and the response could be further improved by the addition of Bi. Peak currents were found to be sensitive to the concentration of the compounds including the IL with an optimum at 5 wt-%, with approximately 5 times lower currents for 0.05 wt-% and 50 wt-%.^[32] Similar CV experiments did not reveal improvements by graphene oxide and [BMMIm][BF₄] modification of a glassy carbon electrode. Peak currents and sharpness, however, increased when graphene oxide and the IL were added to gold nanoparticles. This combination was also shown to increase the electroactive surface

area, which is attributed to a synergistic effect of the gold nanoparticles and the graphene oxide/IL film. This trend could also be transferred to DPV detection of Hg^{2+} .^[40]

PANDEY et al. modified graphene oxide electrodes with the IL [BMIm][PF₆] and Nafion® and without any addition of metal-based modifiers. LODs were determined to be 0.33 ppb for Cd^{2+} and 0.42 ppb for Pb^{2+} by the 3-sigma method. These results are stated to be comparable with Bi modified electrodes and tested for long term stability, where it retained 96 % of the response after 15 days at 5 °C. However, interference of other metal ions was still severe, with over 21 % larger Pb peak currents in the presence of Cu^{2+} (100-fold concentration) but dropping to <-1 % at the 5-fold concentration. Unfortunately, the influence of the IL itself is not further examined.^[20]

2.1.4. Ionic Liquids as Electrolytes

State-of-the art electrolytes used for heavy metal ion detection in aqueous media are acetate buffer solutions (0.1 M) with a pH around 4.5. The pH here is a key parameter. In a field sample, heavy metals can be found in the form of hydrated ions, complexed by compounds, adsorbed to solid matter, minerals, oxides, and hydroxides that might all be present in the sample. The form of the metal is sensitive to the pH of the solution and so is the resulting peak current of a ASV experiment. With decreasing pH, a greater amount of a metal is present in ionic form and the stripping peak intensifies.^[14] An increasing pH decreases peak heights in SWV Pb²⁺ detection and therefore leads to underestimation the lead concentration compared to more acidic samples. The influence seems less severe though in real world samples with more alkaline pH of 7 to 9.^[21] A suitable pH range might be derived from the Pourbaix diagram. In these types of diagrams, the thermodynamically favoured form and oxidation state of a metal is plotted in dependence of the pH and the applied potential. It should be noted that the positions of phase boundaries within the diagram change with temperature, concentration, and the presence of ligands. During an electrochemical measurement the local pH close to the electrode surface is additionally subject to fluctuations, when for instance the hydrogen evolution reaction (HER) consumes H⁺ during a cathodic deposition step and the pH consequently increases. An increased pH in turn facilitates the formation of insoluble hydroxides. This motivates for the utilization of a buffered electrolyte.^[14] Additionally, the electrical conductivity of a sample has to be considered, since SWV peak heights are sensitive to its change. For SWV Pb²⁺ detection in aqueous samples increased conductivities are desired for obtaining high peaks, as demonstrated by RAHM et al. for Pb²⁺ detection.^[21]

Being feasible in aqueous solutions is an ecologically desirable benefit of electrochemical methods. Nevertheless, this benefit also limits the technique to mild conditions. Molten salts and solid-state electrolytes on the other hand expand the applicability of electrochemistry to higher temperatures and beyond the electrochemical stability window of water. Additionally, also ionic liquids can be applied for the function of an electrolyte, addressing the potential drawbacks of aqueous electrolytes. ILs are already being utilized in various electrochemical applications.^[50,59] Their electrolyte properties and application in heavy metal ion sensing will be introduced in this chapter.

Electrolyte Properties of ILs

For comparison and classification of ILs in their function as electrolyte, the Walden plot can be constructed. It shows the relation between molar conductivity Λ_m and the fluidity η^{-1} , the inverse of the viscosity η (Figure 2).

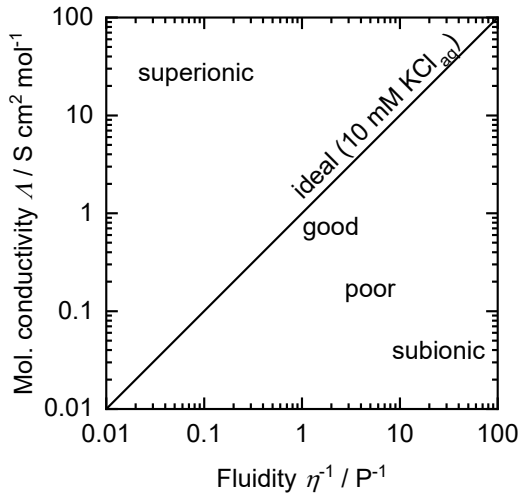


Figure 2: Walden plot including the ideal KCl_{aq} line of unit slope and Angell's classification for the ionicity of electrolytes.

For an ideal ionic state, the ionicity can be determined as a function of temperature T following the Nernst-Einstein equation (Equation 3).^[60,61] It describes Λ_m for known self-diffusion coefficients $Diff$, with the electronic charge e , Avogadro's number N_A and Boltzmann's constant k_B . According to the Stokes-Einstein equation $Diff$ of spherical species with the radius r is temperature and viscosity dependent (Equation 4).

$$\Lambda_m = \frac{e^2 N_A}{k_B T} Diff \quad \text{Equation 3}$$

$$Diff = \frac{k_B T}{6\pi r \cdot \eta} \quad \text{Equation 4}$$

Λ_m molar conductivity [$\text{S m}^2 \text{mol}^{-1}$]
 e elementary charge [C]
 N_A Avogadro constant [mol^{-1}]
 k_B Boltzmann constant [J K^{-1}]
 T temperature [K]
 $Diff$ self-diffusion coefficient [$\text{m}^2 \text{s}^{-1}$]
 r radius [m]
 η dynamic viscosity [Pa s]

Even though $Diff$ is not always easily accessible, a reciprocal dependency of Λ_m and η is obtained by combination of Equation 3 and Equation 4.^[62] Walden's rule predicts a linear dependency for a data set of Λ_m and η^{-1} at different temperatures in a double logarithmic plot (Equation 5).^[63] Both physico-chemical properties are experimentally easily measurable. The position and the course of the data sets are compared to the 'ideal' case of a 10 mM KCl

aqueous solution, existing of fully dissociated ions, a line of unit slope. The deviation from the ideal ionic state can be quantified.^[60]

$$\frac{\Lambda_m(T_1)}{\Lambda_m(T_2)} = \frac{\eta(T_2)}{\eta(T_1)} \quad \text{Equation 5}$$

Λ_m molar conductivity [$\text{S m}^2 \text{mol}^{-1}$]

T temperature [K]

η dynamic viscosity [Pa s]

Electrolytes can according to Angell's classification be labelled as 'good', 'poor', 'subionic' or 'superionic', depending on the deviation to the KCl_{aq} line.^[62] Originally, the Walden rule was applied to electrolytes in the form of diluted ions. However, it is also applicable to concentrated electrolytes and is popular in the characterization of ILs.^[61] Both the Walden plot and Angell's classification are widely used for IL comparison and ionicity determination. 'Poor' ILs are electrolytes with high fluidity (low viscosity), though its ions do not contribute to the conductivity as expected by the Nernst-Einstein equation, for instance due to ion pairing. Yet also 'superionic' materials were shown to exist as polymers containing ions, forming conductive gels and rubbers. Thereby ionic motion can practically be decoupled from segmental motion.^[64] Within the Walden plot substances usually move to the upper right direction, with increasing temperatures, since viscosities decrease and conductivities increase.

In order to include a new electrolyte in this diagram, its density ρ , electrical conductivity κ and viscosity η need to be known. For pure ILs Λ_m can then be calculated from the molar mass M and ρ (Equation 6). If the ILs are not in pure state and contain water, their concentration c can be calculated with respect to the water content $w_{\text{H}_2\text{O}}$ (Equation 7).

$$\Lambda_m = \kappa \cdot \frac{M}{\rho} \quad \text{Equation 6}$$

$$c(T) = \frac{\rho(T)}{M} \cdot (1 - w_{\text{H}_2\text{O}}) \quad \text{Equation 7}$$

Λ_m molar conductivity [$\text{S m}^2 \text{mol}^{-1}$]

κ electrical conductivity [S m^{-1}]

M molecular mass [g mol^{-1}]

ρ density [g cm^3]

c concentration [mol L^{-1}]

$w_{\text{H}_2\text{O}}$ mass fraction [g g^{-1}]

The densities of ILs usually range between 1.12 g cm^{-3} and 2.4 g cm^{-3} .^[65] Upon increasing temperatures, densities decrease and the volume expansion generally follows an exponential expression. For small temperature ranges the change can be linearly regressed. This correlation was shown for a variety of ILs.^[55]

An increasing temperature T decreases η while κ increases. For the interpolation of the non-linear temperature dependence of both η and κ the Vogel-Fulcher-Tammann (VFT) equation, with the fitting parameters A, B and T_0 can be employed (Equation 8 and Equation 9).^[66]

$$\ln(\eta) = A_\eta + \frac{B_\eta}{T - T_{0,\eta}} \quad \text{Equation 8}$$

$$\ln(\kappa) = A_\kappa + \frac{B_\kappa}{T - T_{0,\kappa}} \quad \text{Equation 9}$$

η dynamic viscosity [Pa s]
 A fitting parameter
 B fitting parameter
 T temperature [K]
 T_0 fitting parameter [K]
 κ electrical conductivity [S m⁻¹]

Formerly, this equation was established for describing the temperature dependent viscosity of molten glass and polymers but was shown to also be applicable to ILs.^[50] Parameters A and B allow for fitting to the experimental data, while $T_{0,\eta}$ and $T_{0,\kappa}$ were found to be similar for a variety of ILs (originally derived from ca. 300 data points of 15 ILs) and its optimum is determined to 165.06 K.^[66]

Ionic Liquids as Electrolytes in Heavy Metal Detection

In addition to the application in electrode preparation and modification, ILs can also serve as electrolyte in a heavy metal sensor, albeit this approach is rarely documented. Pb²⁺ was directly detected in a microcell with a boron doped diamond (BDD) electrode in the RTIL butyl-1-methylpyrrolidinium bis(trifluoromethanesulfonyl)imide [MPyl][NTf₂] spiked with the complexing agent trioctylphosphine oxide (TOPO). The analyte was prior extracted from aqueous 0.1 M citrate buffer solution. This extraction step comprised 15 repetitions of 1 min vortexing / 1 min decanting and centrifuging. The LOD is stated with 0.3 $\mu\text{g L}^{-1}$ (0.3 ppb), referring to a concentration of 0.033 $\mu\text{g L}^{-1}$ in the original aqueous phase with DPASV. Deposition conditions were -1 V (vs. BDD pseudo reference electrode) for 20 s, and $E_{\text{Pulse}} = 10$ mV for 0.07 s, $E_{\text{Step}} = 50$ mV with a scan rate of 50 mV s⁻¹ for stripping.^[67]

The IL betainium bis(trifluoromethylsulfonyl)imide [HBet][NTf₂] was used as electrolyte in its super cooled state by LU et al. on a 2-dimensional electrode arrangement. Particulates of heavy metals oxides such as PbO, CdO and CuO were dissolved directly in the IL layer that was coated on the indium tin oxide electrode. For PbO a LOD of 0.34 ng L⁻¹ is stated in the presence of Bi₂O₃. Applied method was a SWV with 120 s deposition time at -1.1 V (vs. ITO pseudo-RE), $E_{\text{Pulse}} = 25$ mV and $f = 25$ H (E_{Step} is not stated). 1-butyl-3-methylimidazolium hexafluorophosphate [BMIm][PF₆] and 1-butyl-3-methylimidazolium tetrafluoroborate [BMIm][BF₄] were utilized in the same manner, though no stripping signal could be detected.^[19] Apart from this article, this very compound is almost exclusively mentioned in

publications on the hydrometallurgical challenge of metal recovery, the dissolution of metal oxides and the extraction of metal ions from aqueous phase.

2.2. Extraction of Heavy Metal Ions

Extraction is a physical separation process, where a substance is transferred from a carrying matrix to an extractor. All combinations of matter of states are conceivable and are distinguished in nomenclature by subsequently naming the state of the carrying matrix and the extractor. In industry extraction processes are preferred over rectification, when the separation factor for thermal separation is small, the substance of interest is not volatile, unstable under the higher temperatures that are required for other separation processes such as rectification, or extraction simply offers the economically most favourable route. Examples are the processing of metal salts or pharmaceuticals and the separation of aromatics from aliphates. An important characteristic of an extraction process is, that the extracted substance is then envired in a different matrix and not necessarily in a purified state and further downstream processing might be necessary. However, enrichment and purification of the carrying matrix can be attained by the selection of a suitable extractor and the technical process implementation.^[68]

Thermodynamically, extraction is limited by the distribution at equilibrium of the concentrations of the substrate in both of the phases, carrying matrix and the extractor. The distribution of a substance in two non-miscible solvents is described by Nernst's distribution law (Equation 10), with the distribution coefficient K_N and the concentration c in the phases A and B.

$$K_N = \frac{c_A}{c_B} \quad \text{Equation 10}$$

K_N Nernst distribution coefficient [-]
 c concentration [mol L⁻¹]
indices A, B: phases A, B

This equation is only valid for small concentrations. More accurately and especially for higher concentrations it needs to be replaced by activities of the species in the solvent. It can be read as a case of the law of mass action. The nature and combination of the solvents, temperature, and the behaviour of the substance influence K_N . Kinetically, extraction is limited by the mass transport within each phase and the transfer at the phase boundary. A large exchange area at the phase boundary is thus accelerating the approximation of the equilibrium concentrations. Technically this large surface area is attained by energy input and instrumentation intensive operations such as stirring or vibrating for liquids and bubbling through or spraying into, in case of mixtures of gases and liquids. Certain criteria, that potential solvents are required to meet for the application in industrial scale extractions are immiscibility, low volatility, non-toxicity, availability, and low costs.

In many point-of-care analysis applications extraction plays an important role, when for instance a sample is collected with a swab from a surface of a food production line or from pharyngeal cavity for antigen or pathogen detection. To transfer the samples, the swabs are immersed in an extraction buffer that also functions as the running buffer in a subsequent lateral flow test.

The extraction of metal ions is considered with diverse motives. A general interest, driven by the protection of environment and health, is the reduction of metal ions from wastewater streams. Heavy metals are utilized in various applications, such as pigments, alloys and batteries. Lead, moreover, was found in water piping and gasoline until recently. In contrast to organic compounds, heavy metals do not decay over time, once emitted to the environment, due to their elemental nature. In order to reduce the emission of heavy metals to the environment, the technical possibilities of their extraction from waste and water streams, next to precipitation, adsorption, floatation and filtration, are investigated. Ion exchangers, a liquid-solid extraction or solid-phase extraction, are commonly used for the reduction of metal ion concentrations in an aqueous solution in exchange with a different ion. Acidic functional groups are presented on the surface of a resin. The same principles of high affinity towards the targeted substance, however, apply to liquid-liquid extraction.^[69]

Another driving force for metal extraction stems from the interest of the recovery of metals, in particular rare earth metals. Due to their limited abundancy on earth's crust in combination with some unique properties for technical applications, they are of high economic value.

Two parameters frequently used for describing the extraction of heavy metal ions are the extraction efficiency %*E* (Equation 11) and the distribution ratio *D* (Equation 12).

$$\%E = \frac{\text{amount of the extracted substance}}{\text{total amount of the substance in the system}} \cdot 100 \% \quad \text{Equation 11}$$

$$D = \frac{c_A}{c_B} \quad \text{Equation 12}$$

%*E* extraction efficiency [%]

D distribution coefficient [-]

c concentration [mol L⁻¹], [mg g⁻¹]

index A, B: phases A, B

%*E* is prominent in hydrometallurgy and is synonymously termed recovery. The amounts of solvent and changes due to reciprocal miscibility are not accounted for. *D* corresponds to Nernst's distribution coefficient *K_N* and is defined identically. It quantifies the difference in concentrations and hence includes the solvents. Units of the concentrations may vary, e.g. mol L⁻¹ or mg g⁻¹.

2.2.1. Ionic Liquids in Metal Ion Extraction

The substitution of traditional organic solvents by ILs and especially RTILs is discussed intensively in the strive for environmentally friendly and green chemistry. One of the highlighted disciplines are separation processes. Numerous scientific articles have been published in this field, proposing diverse materials and promising green solutions. Besides for the purification of wastewater streams from metal ions and metallurgy applications, ILs are also proven for extracting other classes of chemicals. ILs can be applied in the extraction of organic compounds such as amino acids and biofuels, as well as in gas separation, where prominently CO₂ can be selectively dissolved in [BMIm][PF₆].^[70,71]

Hydrophobic ILs, most certainly, seem to be promising candidates for solvent extraction, either as solvents spiked with extractants or functioning as extractants themselves. The documentation of extractions is thereby not limited to certain metals and rather reaches all over the periodic table of elements.^[70,72-75]

Ionic Liquids as Solvents in Extraction Systems

In analogy to common extraction systems, extracting agents can also be added to ILs. In this case the IL replaces the utilization of VOCs. Potential threats due to high vapour pressure and flammability of VOCs can be diminished. A variety of the chelating compounds are known for both specific and less specific heavy metal ion complexation from techniques like precipitation, UV-Vis spectroscopy and chelation therapy in the treatment of heavy metal poisoning. Typical representatives are crown-ethers, dimercaprol, 2,3-dimercaptosuccinic acid, 2,3-dimercapto-propane sulfonate, octyl(phenyl)-N,N-diisobutyl carbamoylmethyl phosphine oxide, ethylenediaminetetraacetic acid and dithizone.^[76,77] Latter is an hydrophobic, organic substance that is used as extractant in the spectrometric quantification of metal ions via extraction to chlorinated organic solvents.^[78,79]

The extraction capabilities of the hydrophobic metal chelator dithizone in combination with various ILs like 1-butyl-3-methylimidazolium hexafluorophosphate [BMIm][PF₆] were investigated and show high extraction efficiencies. WEI et al. studied this combination for the extraction of Ag, Cu, Pb, Zn and Cd ions and could achieve extraction efficiencies up to 98.4 % and could show a strong dependency of the pH. The pH dependency can be employed for separating the different metal ions in the extraction process, allowing for selective extractions and the pre-concentration of metal ions. The underlying mechanism was traced back to the pH dependent water solubility and dissociation equilibrium of dithizone and the formation constant and hydrophobicity of the metal dithizonate complex, illustrated in Figure 3.^[80]

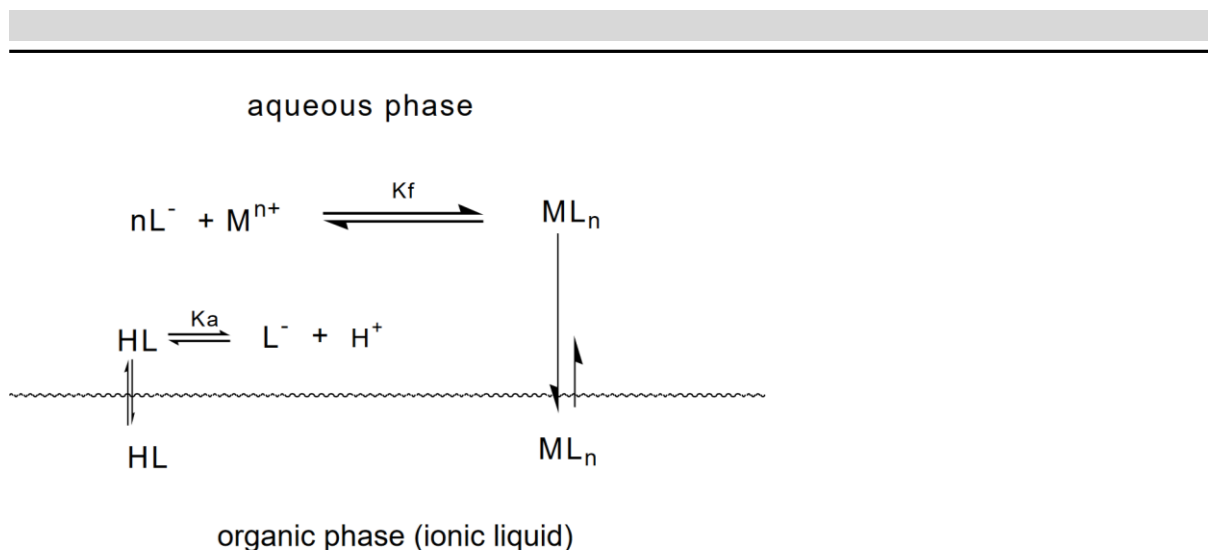


Figure 3: Phase boundary of an aqueous and an dithizone-IL phase and dissociation and extraction equilibria proposed with the metal ion M^{m+} and the dithizonate ligand L. Reprinted from *Analytica Chimica Acta* 488, G.-T. Wei et al., Room temperature ionic liquid as a novel medium for liquid/liquid extraction of metal ions, 183–192, Copyright (2003), with permission from Elsevier.^[80]

The same chelator was studied also in combination with a variety of imidazolium based ILs, revealing an influence of the chain length and the anion ($[NTf_2]$ and $[PF_6]$) in the extraction of Ag^+ . Longer alkyl chains thus tend to limit the extraction, while $[NTf_2]$ anions promote the extraction. Latter effect might be caused by the hydrophobicity of ILs with $[NTf_2]$ anions. The influence of the solvent however, depends heavily on the nature of the metal ion and the pH, as already discussed.^[72] The studies further proof the superiority of IL over chloroform as choice of solvent and the feasibility of acidic stripping for the purpose of recycling.

Ionic Liquids as Extractants in Extraction Systems

Several ILs reportedly provide extraction properties with high extraction efficiencies without the addition of chelators. Depending both on the nature of the metal and on the combination of the IL's anion and cation, extraction efficiency can be shifted from no detectable extraction to close to almost complete recovery. High selectivity towards one or a group of metal ions is possible. ILs carrying the functional, metal complexing group within their chemical structure are often referred to as task specific (TS)ILs. These ILs are designed for the extraction of particular metal ions and may contain carboxylic or (thio)urea derivatives, similar to those found in aforesaid, typical metal ion chelators. The TSIL accordingly combines the role of the solvent and the functional groups of an extracting agent. Back extraction or stripping of the metal ions for the purpose of reuse, usually by the addition of acidic aqueous phase, generally is reported to be feasible, if mentioned.

In multiple works, non-fluorinated, hydrophobic ILs from derivatives other amines with functionalized anions (carboxylic acids, dicyanamide, chlorosalicylate and saccharinate) for the extraction of highly toxic heavy metal ions are synthesized. LEYMA et al. studied

thiosalicylate anions paired with tetraalkyl phosphonium and ammonium cations and their extraction capabilities of Cd^{2+} , Cu^{2+} and Zn^{2+} . Depending on the time, the metal ion, the cation and the hydrocarbon rest at the thio-group, they yielded extraction efficiencies of up to 98.7 %. Interestingly, they also found differences of the efficiencies of up to 55 % for the same IL and different metal ions. They further emphasize the ability of fine tuning the extraction properties of ILs by their modification. Despite the existence of cheaper methods, studied ILs and their syntheses are described to be simple, cheap, highly pure and follow a sustainable standard strategy.^[81] A similar TSIL tri(n-butyl)(-ethoxy-2-oxotetraalkyl)ammonium chlorosalicylate $[\text{BuNC}_2\text{OC}_4][\text{ClSal}]$ was synthesized and shown to extract a series of heavy metal ions with differing distribution ratios: Cu^{2+} (1301.4) > Pb^{2+} (735.6) > Cd^{2+} (439.6) > Ni^{2+} (40.0) > Co^{2+} (29.7), resulting in a selectivity factor of up to 44 ($D_{\text{Cu}}/D_{\text{Co}}$). However, the authors remark the solubility of this TSIL. They conclude the compound with a longer alkyl chain to be more suitable as a starting point for more eco-compatible processes, despite its lower extraction efficiency.^[82]

Trioctyl/hexyl-methylammonium and mono and dicarboxylic acids were found to remove the divalent heavy metals ions Cu^{2+} , Ni^{2+} , Co^{2+} , Pb^{2+} and Zn^{2+} from aqueous media by up to 99.9 %.^[83]

Among the reported systems, some are ready for application scale, like the quaternary alkyl ammonium chloride (Aliquat 336[®]) and trihexyl(tetradecyl)phosphonium chloride (Cyphos[®] IL 101) and modifications based on these chemicals. Aliquat 336[®] and Cyphos[®] IL 101 are commercially available. Both ILs are less dense than water, non-fluorinated and gain their water-immiscibility from long alkyl chains. The IL phase hence floats on the aqueous phase in contrast to most ILs. In proposed approaches the two ILs and their derivatives are often, though not exclusively, diluted in VOCs such as kerosene, toluene, and chloroform. Due to their long alkyl chains, the obtained undiluted compounds are highly viscous.^[81,84–88]

In other works, the functional groups are part of the cation. An advantage of placing the complexing group within the cation is the possibility of utilizing fluorinated anions such as $[\text{PF}_6]$ and $[\text{NTf}_2]$. ILs of these anions tend to be highly hydrophobic. In their work, VISSER et al. synthesized imidazolium-based cations with thioether, thiourea and urea derivatives located in the side chains. The cations were combined with anions such as $[\text{PF}_6]$. The extraction of Hg^{2+} and Cd^{2+} was demonstrated and the selectivity could be tuned by the choice of the functional group and the pH of the carrier phase. They achieved distribution ratios as high as 710 for Hg^{2+} , even with diluted task specific ILs. Cd^{2+} could generally be extracted, though with lower distribution ratios compared to Hg^{2+} .^[89]

Imidazolium based ILs, that do not feature metal ion complexing groups within the chemical structure by design, and in the absence of a chelating substance, to some extent also show extraction capabilities. While $[\text{BMIm}][\text{PF}_6]$, $[\text{BMIm}][\text{NTf}_2]$ and $[\text{OMIm}][\text{NTf}_2]$ extract Cd^{2+} and Fe^{3+} by around 20 to 25 % (%E) and no Zn^{2+} , $[\text{OMIm}][\text{BF}_4]$ completely extracts Zn^{2+} and Cd^{2+} , though no Fe^{3+} from 1 M hydrochloric acid solution. The researchers state the possibility of selective separation by the choice of the IL.^[87]

2.2.2. Homogeneous Liquid-Liquid Extraction

Generally suffering from high viscosity, generating a large liquid-liquid interface to perform efficient extraction and to encounter the slow mass transfer is challenging when handling ILs and other viscous liquids.^[80,81,90] In order to decrease the viscosity and thus increase mass transfer, the temperature can be increased. However, this also increases the instrumental expenses and generally increases the reciprocal miscibility of solvents.

Some IL-water mixtures show a temperature induced single phase generation and separation. The temperature above which the phase boundary disappears, and reforms when the temperature drops below, is referred to as the upper critical solution temperature (UCST, Figure 4).^[91] This thermomorphic behaviour of a mixture can be applied in the extraction of metal ions from aqueous phase. The extraction rate limitation by a limited exchange surface area of the phases is bypassed. Stirring and the equipment for stirring are rendered unnecessary, which could be advantageous for mobile point of care devices.

This technique is referred to as homogeneous liquid-liquid extraction (HLLE) in literature. At least two such compounds are reported, betainium bis(trifluoromethylsulfonyl)imide [HBet][NTf₂], and choline bis(trifluoromethylsulfonyl)imide [Chol][NTf₂], with UCSTs of 55.5 °C and 72.1 °C, respectively.^[92,93]

Besides the UCST also LCST (lower critical solution temperature) systems of ILs and water are described in literature. These mixtures are completely miscible below a certain temperature and separate when the temperature is exceeded.^[94]

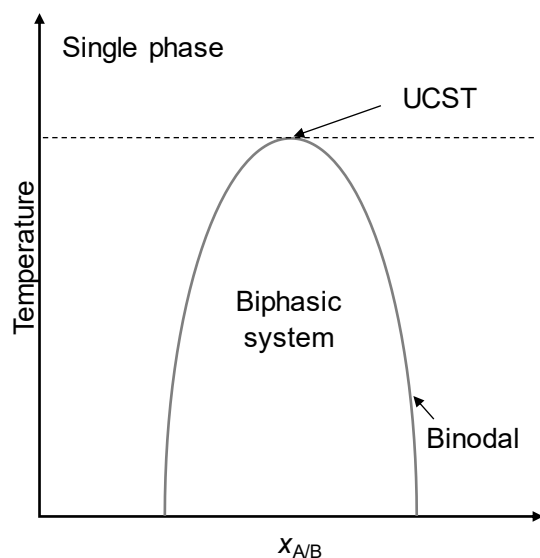


Figure 4: Thermomorphic phase behaviour of a mixture of the generic substances A and B with an UCST.

NOCKEMANN et al. intensively studied the thermomorphic phase behaviour of both of the substances in mixtures with water and already introduced the idea of an application in hydrometallurgy. [HBet][NTf₂] was shown to selectively dissolve heavy metal oxides. While oxides of U⁶⁺, Zn²⁺, Cd²⁺, Hg²⁺, Ni²⁺, Cu²⁺, Pd²⁺, Pb²⁺, Mn²⁺ and Ag²⁺ are soluble, Fe³⁺, Mg²⁺, Co oxides, Al oxides and Si oxides are poorly soluble or not soluble at all.^[92] This list was later extended by RICHTER and RUCK, who investigated 30 metal oxides and their dissolution in dry [HBet][NTf₂]. They further suggest a reaction scheme for the dissolution of divalent metal oxides and the metal complexation, reproduced in Figure 5.^[95]

The selectivity of the dissolution of metal oxides was taken advantage of by FAN et al. in the separation of fission products, proposing an approach for the recycling of the valuable spent nuclear fuels.^[96]

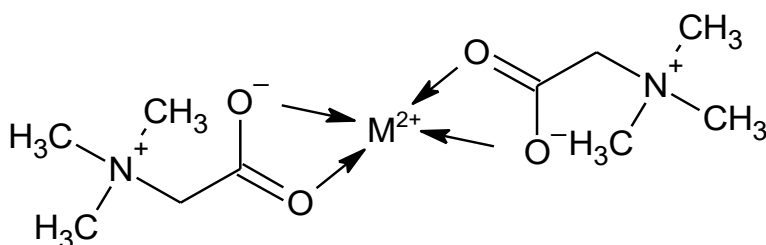


Figure 5: Scheme of the complexation of a M²⁺ metal ion by two zwitterionic betaine molecules.^[95]

The research was further intensified towards HLLC and dominantly rare-earth metal recovery. The extractions of U⁶⁺, Nd³⁺, Sc³⁺, In³⁺, La³⁺, Pr³⁺, Nd³⁺, Dy³⁺, Ho³⁺, Er³⁺, Ga³⁺, Eu³⁺, Ru³⁺, Rh³⁺, Pd³⁺ and Tl³⁺, as well as Mn²⁺, Ni²⁺, Cu²⁺, Zn²⁺ and Ag⁺ are reported.^[90,97-102] The extraction step follows a simple procedure of heating above the UCST, short shaking to ensure single phase generation and subsequent phase separation and settling during cooling.

HOOGERSTRAETE et al., who compared the distribution of a number of metal ions, obtained higher extraction efficiencies when zwitterionic betaine was added to the mixture of water and [HBet][NTf₂]. Thereby also the UCST is lowered by around 10 °C for the addition of 10 wt-% zwitterionic betaine (20 wt-% when referred to the organic phase only). As long as the temperature drops below the UCST, the extraction efficiencies do not change significantly. Additionally, it was shown, that the time the solution is kept above the UCST does not influence the extraction efficiency. This proves the robustness of the extraction procedure exploiting the thermomorphic phase behaviour.^[90,98]

Metal ion extraction from aqueous betaine solution (13 wt-%) reveals distribution ratios over a span of 4 orders of magnitude (Figure 6). While Sc³⁺, Ga³⁺, and In³⁺ from the according [NTf₂] salts could be extracted with distribution ratios of ≥100, Ag⁺, Mn²⁺, Ni²⁺ and Zn²⁺ were extracted with distribution ratios of ≤1. This demonstrates the potential of the enrichment of some heavy metal ions in the organic phase over others. For Cu²⁺, Y³⁺, Dy³⁺, Er³⁺, Ho³⁺, La³⁺, Pr³⁺ and Nd³⁺ the distribution ratios were found to be around 10 and within

a narrow deviation, implying, that these ions could not be separated in the same manner and their concentration ratios would rather be upheld during the extraction process.^[90]

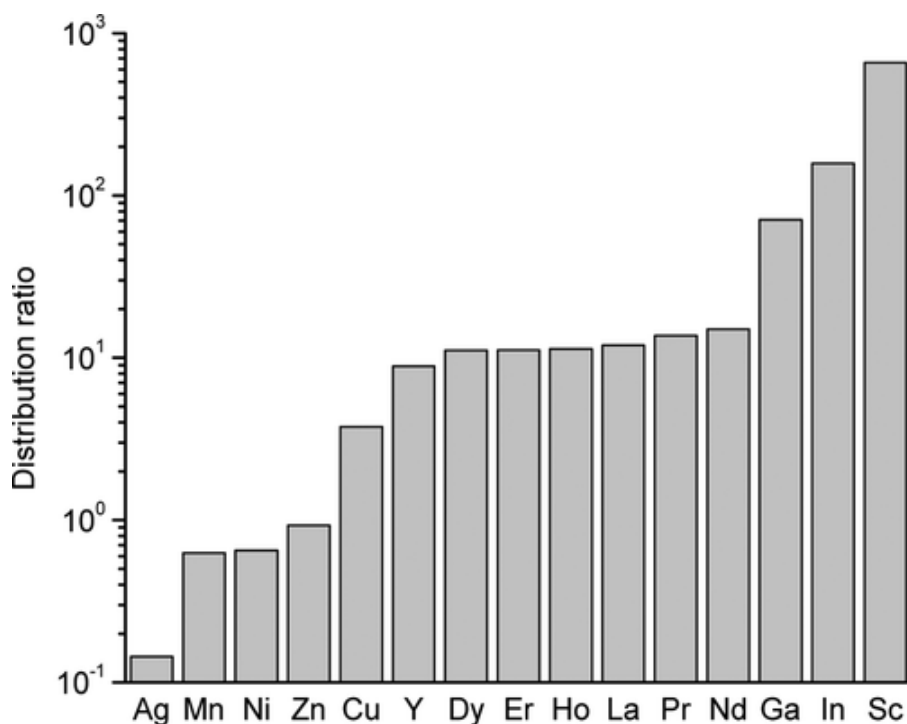


Figure 6: Distribution ratios of metal ions after HLLC from $m_{aq}:m_{IL}$ of 1:1. Aqueous phase contains 13 wt-% zwitterionic betaine and a metal concentration of ca. 1000 mg kg⁻¹. Reprinted with permission from *J. Phys. Chem. Lett.* 2013, 4, 10, 1659–1663. Copyright 2013 American Chemical Society.^[90]

A pH dependency is also reported for this system. While for a low pH of 0.1 almost no extraction could be observed, extraction efficiencies of 11.6 % (La³⁺) to 82.9 % (Sc³⁺) at pH 3.1 could be achieved.^[99] The selectivity of the extraction process can hence be further tuned. Acidic stripping for recycling of the IL is reported to be feasible and moreover offers another step for selective extraction, as shown for the leaching of Sc³⁺. The metal ion of interest could here be separated from a spiked leaching solution by the stepwise addition of hydrochloric acid.^[98,103]

Even though [HBet][NTf₂] can be labeled hydrophobic, it is also partially miscible with water also below the UCST. It takes up about 12 wt-% water at room temperature and dissolves to the aqueous phase by 15 wt-%.^[90] The reciprocal miscibility of the IL and the aqueous phase and its dependency of pH and zwitterionic betaine concentration was studied by VOLIA et al. by employing deuterium chloride, Karl Fischer titration and quantitative nuclear magnetic resonance spectroscopy. A lower pH accordingly decreases the solubility of the IL's anion and increases the solubility of the IL's cation in water. It was shown, that controlling the pH helps avoiding loss of IL due to the reciprocal miscibility. The addition of betaine is assumed to bind water and promoting water transfer from the IL phase. The solubility of water in the IL phase is not affected by the addition of 15 % (weight per volume) zwitterionic betaine and was

found to be 13.8 ± 0.5 wt-% and 13.9 ± 0.5 wt-%, respectively. The zwitterionic betaine is found in both phases.^[104] The addition of metal ions leads to a lower UCST. For a mobile application and the reduction of the required energy input, this would be beneficial, even though the UCST of 35 °C was found for a high metal loading of 3.5 wt-% Nd³⁺.^[105] An overview of properties of [HBet][NTf₂] and its water saturated state is compiled in Table 4.

Table 4: Properties of [HBet][NTf₂] and its water saturated state. *) Literal quote.

Property	Value	Unit	Ref.
<i>M</i>	398.3	g mol ⁻¹	
H ₂ O sat. (RT)	12 – 13.8±0.5	wt-%	[90,104]
Solubility in H ₂ O (RT)	14 – 15	wt-%	[90,99]
UCST with H ₂ O	55.5	°C	[92]
Density ρ (water sat.)	1.439±0.014	g cm ⁻³	[104]
Viscosity η (water sat., 25 °C)	around* 30	cP	[99]
pH (water sat.)	1.42±0.05	-	[104]

Another IL showing thermomorphic phase behaviour is [Chol][NTf₂]. This IL differs from [HBet][NTf₂] in the nature of the functional group, carrying a hydroxyl group instead of a carboxylic group. It does not allow for heavy metal ion extraction by itself, though the addition of hexafluoroacetylacetonate, a well-known, chelating metal ion ligand, as extractant enables Nd³⁺ extraction.^[106] Exploiting the UCST for extraction is hence also transferable to more systems and extraction tasks.

2.3. Microfluidic Devices

At larger scale, transport of liquids requires pumping, adding an extra apparatus with a periphery of energy supply and maintenance. For small volumes and in channels of 10^{-4} to 10^{-5} m, capillary forces can be employed for liquid transport, arousing interest in the research and development of chemical and biochemical sensors. In addition to channels for transportation, operations such as valves, mixers and pumps have been presented and subsumed under the term lab-on-a-chip. WHITESIDES, a pioneer in the field of microfluidic devices, even ponders a revolutionary impact of this technology in the future.^[107] He and his co-workers also presented the first microfluidic paper-based analytical device (μ PAD).^[108] The developed device uses cellulose paper as substrate. Compared to other materials and their processing, such as glass and polymers, paper materials are abundant, lightweight, biodegradable and low-cost. They intrinsically feature a hydrophilic, porous structure and their processing is well established. For sophisticated designs of paper channels and integrated systems techniques like wax-printing, deposition of polymers, cutting and stacking of the paper is possible. Paper-based sensors are subject to research, however, a range of products is also commercially available.^[8,109,110]

The capillary flow of a fluid in a paper material is described by the Lucas-Washburn equation (Equation 13) and depends in addition to the time on the properties of the liquid such as viscosity, the surface tension and the contact angle with the paper fibres, as well as the pore diameter of the paper.^[111,112]

$$l = \sqrt{\frac{\sigma \cdot t \cdot d \cdot \cos(\theta)}{4 \eta}}$$

Equation 13

l distance covered by fluid [m]
 σ liquid-air surface tension [N m^{-1}]
 t time [s]
 d average pore diameter of the paper material [m]
 θ liquid fibre contact angle
 η viscosity of the liquid [Pa s]

The flow velocity of a fluid with fixed σ can accordingly be increased by larger pore diameters in the solid phase, small θ viz. high ‘philicity’ of liquid and fibre, and lower η of the liquid.

2.3.1. Flow Channels in Electrochemical Heavy Metal Sensing Devices

Microfluidic paper-based electrochemical devices (μ PEDs) combine the benefits of a paper material for analyte transport and electrochemical analysis and are also investigated for heavy metal detection. NIE et al. demonstrated the feasibility for the detection of Pb^{2+} . They could show, that introducing a flow of the aqueous electrolyte at the electrode via a paper-based channel massively increases the Pb stripping current in SWV. They estimate a factor of 2.5

lower LODs over 'bulk' systems with stirring for convection. The sensor features a Bi-modified SPE and provides a LOD of 1 ppb ($\mu\text{g L}^{-1}$) for Pb^{2+} .^[9] This study is backed by SHI et al. in the combined detection of Pb^{2+} and Cd^{2+} in a very similar set-up, using commercial Whatman[®] filter paper No.1.^[24] MEDINA-SÁNCHEZ et al. added another functionality of sample filtering to a disposable μPED and achieve LODs of 7 and 11 ppb for Pb^{2+} and Cd^{2+} , respectively.^[113]

The electrode configuration in all of the mentioned set-ups is arranged in a two-dimensional plane. SHEN et al. rearranged the electrodes and presented a three-dimensional configuration so that working and counter electrode are facing each other. The electrodes are solely separated by the fluid carrying paper strip. Obtained peak currents were much higher than in the tested 2D configuration. The researchers explain that this might be caused by the smaller ohmic losses, a higher current efficiency in the pre-concentration step and an overall more efficient electric field. Again, they could show the beneficial contribution of the flow of electrolyte by a paper-based microfluidic channel.^[7]

Microfluidic electrochemical heavy metal detection devices are typically a set-up of three electrodes, identically to bulk cells: the working electrode (WE), the auxiliary or counter electrode (CE) completing the electric circuit and the reference electrode (RE) for controlled potential. Since customary RE might not fit within small sensor designs and do not necessarily meet disposability criteria, pseudo or quasi RE are commonly resorted to. The materials can vary from Ag wire, Ag/AgCl and graphite pastes to ITO, BDD and graphite foil.^[7,19,24,41,67] Even though the occurring reaction might be unknown, these qRE allow for potential control and comparison within the according systems.

2.3.2. Paper Materials and Ionic Liquids

Ionic liquids have been investigated in the processing of biomass, biopolymers and paper materials. Some ILs are able to dissolve biocompounds such as lignin and cellulose, and need consequently be excluded from possible application in a μPED , where the structural integrity shall be preserved.^[114,115] The dissolution capabilities are mainly attributed to the anion of the IL. WANG et al. concluded the capabilities to follow acetate > chloride > formate > dicyanamid > $[\text{NTf}_2]$ by reviewing different dissolution testings.^[116] In the cited publication, cellulose dissolution with $[\text{NTf}_2]$ containing ILs at 110 °C was found to be low or below or not detectable. This is explained by the low solubility in this IL.^[117] The role of the cation remains unclear. $[\text{EMIm}]$ acetate and tetrakis(hydroxymethyl)phosphonium chloride were found to be suitable ILs for the extraction of cellulose and hemicellulose from papermill wastewater and kraft paper pulp, respectively.^[118,119] Despite their lower ion mobility, ILs can be applied in paper-based batteries and supercapacitors, counteracting drying out due to evaporation.^[120,121] A paper-based gas sensor was demonstrated without the use of a membrane. The device features a RTIL soaked filter paper with screen-printed WE, RE and CE and detects 1-butanethiol vapours.^[122] A field to be studied remains to be the application of ILs as medium in microfluidic channels, due the high viscosity of this type of fluids, possibly limiting the flow velocity.

3. Objective and Scope

The subject of heavy metal ion detection motivates the development of sensitive, reliable, cheap, and disposable point-of-care solutions. Electrochemical approaches present promising, electrode materials and integrated microfluidic sensors. A major challenge remains to alleviate the influence of interfering factors such as of other heavy metal ions. Coincidentally in hydrometallurgy, ionic liquids are being investigated for the selective recovery of heavy metal ions of economic value.

The objective of this work is the proof of concept of the combination of these applications by an IL. A liquid-liquid extraction of heavy metal ion with its subsequent electrochemical detection in the extractor phase will be examined. This entails a number of requirements on the IL. It should be immiscible with water and feature extraction capabilities, provide electrolyte qualities, as well as being paper compatible. Lead ions (Pb^{2+}) shall serve as a model analyte for extraction and electrochemical detection.

[HBet][NTf₂] is selected as a potentially suitable candidate, that features thermomorphic mixing behaviour with water. To the date of writing this work, no report on the extraction of Pb^{2+} with [HBet][NTf₂] could be cited. Except from one publication, no detection of heavy metal ions directly in an IL phase is documented.^[67] Its physico-chemical properties are characterized and compared with other ILs. The characterization of the ILs is based on their viscosity, electrical conductivity, and pH. Additionally, the water content after contact with an aqueous phase as well as the influence on the properties shall be included.

The following two, overarching research questions can be formulated:

1. Can [HBet][NTf₂] combine temperature induced liquid-liquid extraction of Pb^{2+} from aqueous phase and the subsequent electrochemical Pb^{2+} detection?
2. Can this concept be transferred to a paper-based microfluidic sensor?

For electrochemical detection, a disposable and easy to prepare working electrode are resorted to. Standard modifications of the working electrodes for Pb^{2+} detection shall be investigated. Square wave anodic stripping voltammetry (SWV) as highly sensitive and popular detection method is chosen. SWV parameters adopted from aqueous systems will need to be adopted to the system. Due to the anticipated lower conductivities in IL electrolytes, a small-volume cell will need to be realized, reducing the electrode distance, and counteracting high ohmic losses. Besides electrode modifications the influence of temperature and addition of zwitterionic betaine as extracting agent on the detection performance shall be studied.

The insights from experiments in small bulk setups shall be transferred to a 3D paper-based cell design and an outlook on the application of the IL in a microfluidic sensor shall be provided. The preparation of the paper materials and the experiments on the microfluidic behaviour is not conducted by the author. Paper materials are selected in collaboration with the Macromolecular and Paper Chemistry department of the Ernst-Berl-Institut at TU Darmstadt.

4. Experimental Setup, Materials and Methods

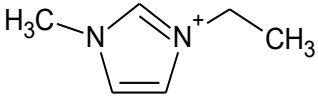
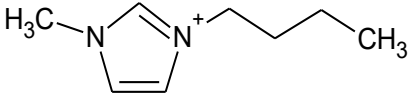
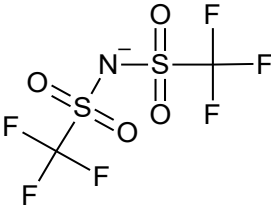
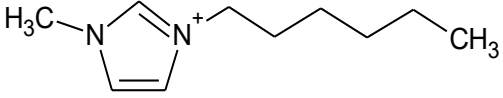
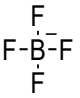
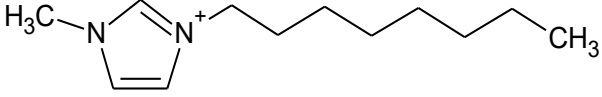
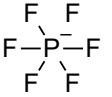
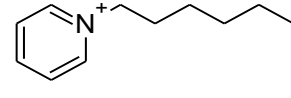
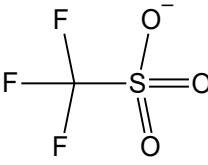
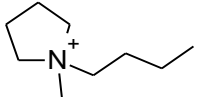
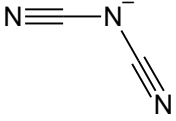
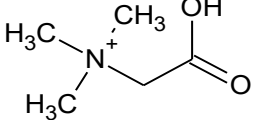
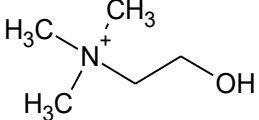
4.1. Physico-chemical Properties of ILs

Out of the enormous number of ILs a selection of a few ILs was picked for the identification of a suitable substance, as well as the verification of the results and for the classification within this class of substances. In Table 5 listed ILs were used in this work. The abbreviations for cations and anions correspond to common nomenclatures, though they do not follow IUPAC recommendations and differing nomenclatures may be found in literature. Structural formulas are given in Table 6.

Table 5 ILs used in this work, including nomenclature and their molar mass. Note: Letter 'H' in [HBet] stands for a proton, while in [HMIm] and [HPy] it abbreviates the hexyl chain.

Abbreviation	Cation	Anion	$M / \text{g mol}^{-1}$
[EMIm][NTf ₂]	1-Methyl-3-Ethyl-imidazolium	Bis(trifluormethane) sulfonimide	391.31
[BMIm][NTf ₂]	1-Methyl-3-Butyl-imidazolium	Bis(trifluormethane) sulfonimide	419.37
[HMIm][NTf ₂]	1-Methyl-3-Hexyl-imidazolium	Bis(trifluormethane) sulfonimide	447.42
[OMIm][BF ₄]	1-Methyl-3-Octyl-imidazolium	Tetrafluoroborate	282.13
[OMIm][PF ₆]	1-Methyl-3-Octyl-imidazolium	Hexafluorophosphate	340.29
[BMIm][OTf]	1-Methyl-3-Butyl-imidazolium	Trifluoromethanesulfonate	288.29
[BMIm][DCA]	1-Methyl-3-Butyl-imidazolium	Dicyanide	205.26
[HPy][NTf ₂]	<i>N</i> -Hexyl-pyridinium	Bis(trifluormethane) sulfonimide	444.41
[BMPyl][NTf ₂]	1-Methyl-1-Butyl-pyrrolidinium	Bis(trifluormethane) sulfonimide	422.41
[HBet][NTf ₂]	Protonated <i>N,N,N</i> -trimethylglycine (Betainium)	Bis(trifluormethane) sulfonimide	398.30
[Chol][NTf ₂]	2-Hydroxy- <i>N,N,N</i> -trimethylethan-1-aminium (Choline)	Bis(trifluormethane) sulfonimide	368.32

Table 6 Chemical structures of the anion and cations of the ILs used in this work.

Cations	Anions
 <p>1-Methyl-3-Ethyl-imidazolium</p>	
 <p>1-Methyl-3-Butyl-imidazolium</p>	 <p>Bis(trifluoromethane)sulfonimide</p>
 <p>1-Methyl-3-Hexyl-imidazolium</p>	 <p>Tetrafluoroborate</p>
 <p>1-Methyl-3-Octyl-imidazolium</p>	 <p>Hexafluorophosphate</p>
 <p>N-Hexyl-pyridinium</p>	 <p>Trifluoromethanesulfonate</p>
 <p>1-Methyl-1-Butyl-pyrrolidinium</p>	 <p>Dicyanide</p>
 <p>Protonated N,N,N-trimethylglycine (Betainium)</p>	
 <p>2-Hydroxy-N,N,N-trimethylethan-1-aminium (Choline)</p>	

4.1.1. Setting the Water Content

Physico-chemical properties of ILs can depend heavily on the water content. Due to the underlying aim of this work, ILs have been in contact to water and their properties might have been affected. For studying the water influence on the properties of the different ILs, four stages were defined:

1. Pristine: Samples of the ILs were taken from the container as obtained by the manufacturer, without any further treatment.
2. Dried: The IL samples were dried in a rotary evaporator over night at 40 °C and 10 mbar.
3. Moist: The ILs were stored over saturated, aqueous magnesium nitrate solution for two weeks, providing a relative humidity of 51 %.
4. Wet: For water saturation the ILs were mixed with an equal volume of purified water (1.1 μS cm⁻¹, VWR Chemicals). The mixtures were occasionally shaken intensively over a period of one week.

After reaching the defined stage, sample containers (snap-on lid glass tubes) were closed with a lid and stored at room temperature until further use.

4.1.2. Karl Fischer Titration

The water content in the ILs at the different stages was measured by Karl Fischer titration, using a Metrohm 720 KFS Titrino and Karl-Fischer-Rot[®] hydroqant 5 (Carl Roth) and HYDRANAL[™]-Methanol dry (Honeywell) as solvent. Determination of the titer was done by titrating a weighed amount of water. Water concentration of ILs was measured at least two times and arithmetically averaged. Water contents that are obtained as mass fractions $w_{\text{H}_2\text{O}}$ can be converted to molar fractions $x_{\text{H}_2\text{O}}$ by the following equation. Due to the large differences in molecular masses of ILs and water, this leads to much higher values.

$$x_{\text{H}_2\text{O}} = \frac{\frac{w_{\text{H}_2\text{O}}}{M_{\text{H}_2\text{O}}}}{\frac{w_{\text{H}_2\text{O}}}{M_{\text{H}_2\text{O}}} + \frac{1 - w_{\text{H}_2\text{O}}}{M_{\text{IL}}}} \quad \text{Equation 14}$$

$x_{\text{H}_2\text{O}}$ molar fraction [mol-%]

$w_{\text{H}_2\text{O}}$ mass fraction [wt-%]

M molar mass [g mol⁻¹]

4.1.3. Density

The density of liquids in this work was measured using a glass pycnometer (ca 10 mL) in tempered water bath. The volume is calibrated with purified water. The temperature was varied from 30 to 70 °C in steps of 10 °C. For validation and literature comparison the more

intensively studied 1-butyl-3-methylimidazolium bis(trifluoromethylsulfonyl)imide (IoLiTec Ionic Liquids Technologies GmbH) was measured alongside [HBet][NTf₂].

4.1.4. Viscosity

A spindle type viscometer DV-II+ by Brookfield was used for viscometry. According to the expected viscosities the spindle model S87 was installed. At least 5 mL of liquid is filled to ensure volume independence of the measurement. The sample container was tempered by a cryostat. A temperature range from 15 to 70 °C was adjustable. The sample container is open to the atmosphere.

4.1.5. Electrical Conductivity

Potentiostatic Electrochemical Impedance Spectroscopy (PEIS) was applied for the determination of the electrolyte's resistance. The measurements were conducted in a conductivity measurement cell Philips PW 9512/01, consisting of two parallel, plane platinum electrodes. A detailed description of electrochemical equipment and experimental set-ups can be found in chapter 4.3.2.

4.1.6. Walden Plot and Vogel-Fulcher-Tammann Equation

The Walden plot was constructed using the measured water content (at RT), density, electrical conductivity, and viscosity at different temperatures between 20 and 70 °C. The data sets were interpolated by linear regression (density) and Vogel-Fulcher-Tammann (VFT) equation (electrical conductivity and viscosity). Applied equations are addressed in chapter 2.1.4. Parameters A_η , A_κ , B_η and B_κ for the VFT fit are the results of minimal standard derivations to the experimental data. All calculations were run in Microsoft Excel 2016. Plots were produced with OriginLab OriginPro 2021 and 2022.

$$\text{Walden eq.} \quad \frac{\Lambda_m(T_1)}{\Lambda_m(T_2)} = \frac{\eta(T_2)}{\eta(T_1)} \quad \text{Equation 5}$$

$$\Lambda_m = \kappa \cdot \frac{M}{\rho} \quad \text{Equation 6}$$

$$c(T) = \frac{\rho(T)}{M} \cdot (1 - w_{\text{H}_2\text{O}}) \quad \text{Equation 7}$$

$$\text{VFT } \eta \quad \ln(\eta) = A_\eta + \frac{B_\eta}{T - T_{0,\eta}} \quad \text{Equation 8}$$

$$\text{VFT } \kappa \quad \ln(\kappa) = A_\kappa + \frac{B_\kappa}{T - T_{0,\kappa}} \quad \text{Equation 9}$$

A_m molar conductivity [$\text{S m}^2 \text{mol}^{-1}$]
 e elementary charge [C]
 N_A Avogadro constant [mol^{-1}]
 k_B Boltzmann constant [J K^{-1}]
 T temperature [K]
 D self-diffusion coefficient [$\text{m}^2 \text{s}^{-1}$]
 r radius [m]
 η dynamic viscosity [Pa s]
 M molecular mass [g mol^{-1}]
 ρ density [g cm^3]
 c concentration [mol L^{-1}]
 $w_{\text{H}_2\text{O}}$ mass fraction [g g^{-1}]
A fitting parameter
B fitting parameter

The temperature variation for the investigation of electrolyte parameters was only carried out for [HBet][NTf₂] and [BMIm][NTf₂]. Latter was included to verify the results by its comparison to the literature. Data for the verification of [BMIm][NTf₂] as well as the values for the constants $T_{0,\eta}$ and $T_{0,\kappa}$ (both 165.06 K) were gathered from reference.^[66,123]

4.1.7. pH Measurements

The potential of protons pH was measured by transferring a drop of the liquid of interest on a pH sensitive paper (VWR). The induced change of colouration was visually compared with the colour scale provided by the manufacturer. Hereby the pH could only be stated semi-quantitatively and an accuracy cannot be specified.

4.1.8. Thermogravimetric Analysis

[HBet][NTf₂] was thermogravimetrically analysed with a NIETZSCH STA 449 C Jupiter. For flushing and during the measurement a nitrogen stream of 88 mL min⁻¹ was passing through the chamber. The heat ramp is 2 K min⁻¹ and the plateau at 450 °C was held for 30 min before cooling to room temperature at 10 K min⁻¹. Alongside water saturated [HBet][NTf₂] also dry, pristine [HBet][NTf₂] and a water sample were analysed.

4.2. Homogeneous Liquid-Liquid Extraction

4.2.1. Water Saturation of [HBet][NTf₂]

At the beginning of this work, [HBet][NTf₂] was not commercially available. Its synthesis was achieved by an ion-exchange reaction of betaine hydrochloride and lithium (trifluoromethylsulfonyl)imide in water (1.1 $\mu\text{S cm}^{-1}$, VWR Chemicals). Following NOCKEMANN et al., equimolar amounts of both substances were weighed in, dissolved in water and stirred for at least 3 h. Subsequently, the aqueous phase was removed and the IL was washed with cold, purified water (1.1 $\mu\text{S cm}^{-1}$, VWR Chemicals) until no precipitate was observed with silver nitrate testing.^[92]

Since being commercially available, betaine bis(trifluoromethylsulfonyl)imide as ordered from the manufacturer IoLiTec Ionic Liquids Technologies GmbH and was mixed with purified water without any further purification. The mixture was left overnight for phase separation and reheating to room temperature. An aqueous phase completely covering the IL ensured saturation. For further utilization, the denser IL-phase was withdrawn from the lower phase. Both, self-prepared and purchased [HBet][NTf₂] showed identical behaviour in the following experiments and thus are neither differentiated nor indicated in the following. The saturation of choline bis(trifluoromethylsulfonyl)imide (IoLiTec Ionic Liquids Technologies GmbH) was executed in analogous manner.

4.2.2. Lead Ion Extraction

For the extraction of heavy metals from aqueous phase, lead solutions or dilution series were prepared by weighing in Pb(NO₃)₂ (Sigma-Aldrich) and dissolving in purified water (1.1 $\mu\text{S cm}^{-1}$, VWR Chemicals). The desired concentrations were obtained from the stock solution.

The extraction was performed by single phase generation of the aqueous lead solution and the water saturated IL. Latter was handled with a 1 mL mechanical single-channel pipette (VWR) and the mass was verified by weighing. The two-phase mixture was heated above its upper critical solution temperature (UCST) of 55.5 °C.^[92] Brief shaking results in a clear, single phase, which clouds when the temperature falls below the UCST. In order to ensure phase separation, the mixture was left for at least one hour at room temperature ere sampling.

If not otherwise stated, the extractions in this work were performed with a volume ratio of the initial volumes equal to one, verified by weighing, due to the challenges of handling the highly viscous ILs.

4.2.3. Determination of Lead in the Extraction Process

The concentration of lead in the IL-phase after the extraction was determined by inductively coupled plasma optical emission spectrometry (ICP-OES) externally at the State Materials Testing Institute Darmstadt (MPA) and the Department and Institute of Materials Science (IfW) with a Perkin Elmer Optima 2000DV. The analysed samples stemmed from extractions with higher starting concentrations (1 mg mL⁻¹), due to the high dilution required to obtain a single aqueous phase. After the extraction, a sample of the IL phase was taken and diluted with the ten- to twentyfold amount of 0.1 M HCl for complete dissolution. The concentration in the IL phase was calculated by the dilution factor. The same matrix of dissolved IL was used for the calibration of the ICP OES.

The extraction efficiency %*E* and the distribution coefficient *D* cannot directly be derived from the concentration of Pb²⁺ in the organic phase (water saturated IL). The composition of the the phases needs to be known and can be calculated by the following set of equations (Equation 17 to Equation 20).

$$\%E = \frac{\text{amount of the extracted substance}}{\text{total amount of the substance in the system}} \cdot 100 \% \quad \text{Equation 15}$$

$$D = \frac{c_{\text{org}}(\text{Pb}^{2+})}{c_{\text{aq}}(\text{Pb}^{2+})} \quad \text{Equation 16}$$

$$m_{\text{IL total}} = m_{\text{IL,org}} + m_{\text{IL,aq}} \quad \text{Equation 17}$$

$$m_{\text{H}_2\text{O total}} = m_{\text{H}_2\text{O,org}} + m_{\text{H}_2\text{O,aq}} \quad \text{Equation 18}$$

$$w_{\text{IL,aq}} = \frac{m_{\text{IL,aq}}}{m_{\text{IL,aq}} + m_{\text{H}_2\text{O,aq}}} \quad \text{Equation 19}$$

$$w_{\text{H}_2\text{O,org}} = \frac{m_{\text{H}_2\text{O,org}}}{m_{\text{H}_2\text{O,org}} + m_{\text{IL,org}}} \quad \text{Equation 20}$$

Solution
approach:

$$m_{\text{H}_2\text{O,org}} = \frac{w_{\text{H}_2\text{O,org}} \cdot m_{\text{IL total}} - \frac{w_{\text{H}_2\text{O,org}} \cdot w_{\text{IL,aq}} \cdot m_{\text{H}_2\text{O total}}}{(1 - w_{\text{IL,aq}})}}{1 - w_{\text{H}_2\text{O,org}} - \frac{w_{\text{IL,aq}} \cdot w_{\text{H}_2\text{O,org}}}{(1 - w_{\text{IL,aq}})}}$$

%*E* extraction efficiency [%]

D distribution coefficient [-]

c concentration [mol L⁻¹], [mg g⁻¹]

indices aq, org: aqueous phase, organic phase (water sat. IL) HLLE

*m*_{IL total} total mass of IL in both phases [g]

*m*_{IL,org} mass of IL in organic phase [g]

*m*_{IL,aq} mass of IL in aqueous phase [g]

*m*_{H₂O total} total mass of H₂O in both phases [g]

*m*_{H₂O,org} mass of H₂O in organic phase [g]

*m*_{H₂O,aq} mass of H₂O in aqueous phase [g]

*w*_{IL,aq} mass fraction of IL in aqueous phase [g g⁻¹]

*w*_{H₂O,org} mass fraction of H₂O in organic phase [g g⁻¹]

For ICP analysis higher concentrations were chosen compared to the extractions prior to electrochemical detection experiments. According to literature, the extraction efficiency of heavy metal ions could be higher for lower concentrations.^[87]

4.3. Electrochemical Methods

Electrochemical measurements in this work were carried out with two different potentiostats. An IVIUM Octostat 5000 was used for initial parameter studies. In all other experiments an AMETEK Parstat 4000, operated via AMETEK's VersaStudio software in various versions (2.54.2 and earlier), was used. No differences of the results could be noticed between the two devices and within a series of experiments the hardware was not changed.

4.3.1. Lead Detection with Square Wave Anodic Stripping Voltammetry

For the square wave anodic stripping voltammetry (SWASV), the techniques chronoamperometry (CA) and square wave voltammetry (SWV) were combined in one method. In the first step, the CA, the deposition potential E_{dep} and time t_{dep} are defined. In the second step, where the deposit is reoxidized and stripped from the electrode surface, the potentials E_{Start} , E_{End} , E_{Step} , E_{Pulse} and the frequency f can be set.

Prior to the CA, another CA step was implemented with a fixed oxidative potential, aiming for the same, controlled starting conditions of each experiment. The range of parameter setting for the detection method can be found in Table 7.

Table 7: CA and SWV parameter settings for the electrochemical detection of lead in water saturated [HBet][NTf₂].

Step	Parameter	Value	Unit
Cleaning (CA)	Potential	0.2	V vs. Ag-qRE
	Time	120	s
Deposition (CA)	Potential	-1	V vs. Ag-qRE
	Time	60-1200	s
Stripping (SWV)	Initial potential	-1	V vs. Ag-qRE
	Final potential	0.2	V vs. Ag-qRE
	Pulse height	25-200	mV vs. Ag-qRE
	Step height	5-40	mV vs. Ag-qRE
	Frequency	25-150	mV vs. Ag-qRE

Cell Design

The cells used for heavy metal detection in this work developed over time. Starting from a three-neck laboratory glass flask set-up, task specific electrochemical cells were designed using the CAD software Inventor Professional (2019 and earlier) by Autodesk and manufactured by the workshop of the department of chemistry at TU Darmstadt. The polymer polyether ether ketone (PEEK) was chosen as construction material, due to its chemical resistance and workability. Next to basic electrochemical cell requirements such as fixed and parallel electrode positioning, the design focused on a small electrolyte volume, due to the valuable material and the small volume remaining after the extraction step. Furthermore, the electrode distance was reduced in comparison with most commercially available cells, counteracting the electrolytes low electrical conductivities. An overview of the two cell designs can be found in Figure 7.

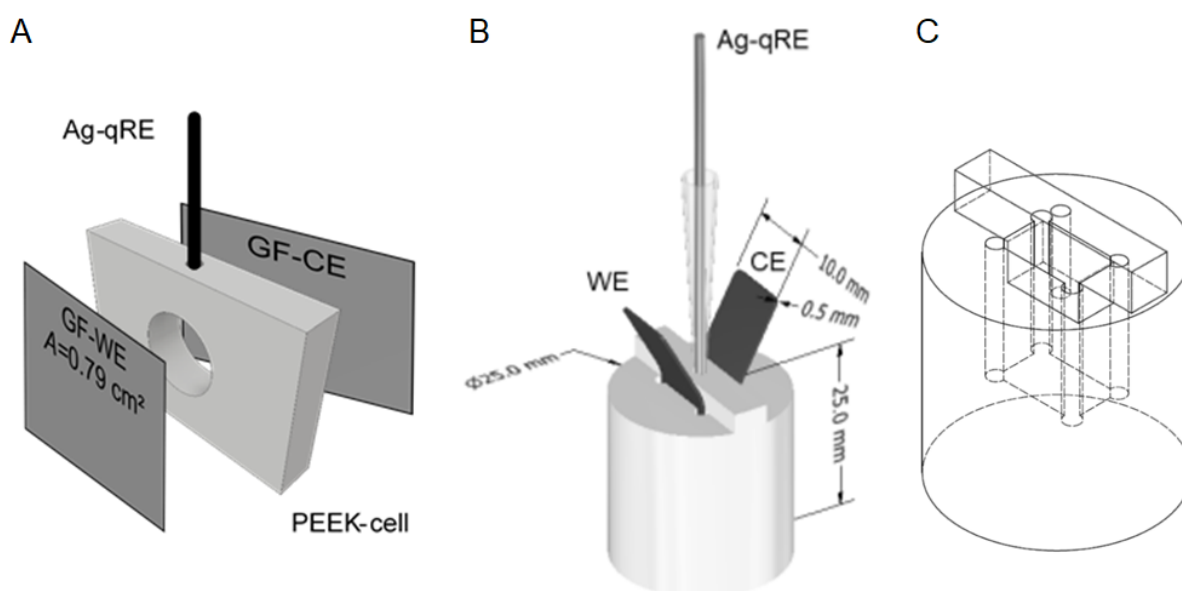


Figure 7 Images of the electrochemical cells used in this work. A) Cell used for initial parameter studies. B) Assembled heatable cell used for the majority of the presented studies. C) Transparent image showing the electrolyte chamber of the heatable cell.

Electrodes and Electrode Preparation

The electrochemical cells were operated as three electrode set-ups, featuring a working electrode (WE), a counter electrode (CE) and a reference electrode (RE). Technical grade graphite foil (GF) by SIGRAFLEX® (Typ NH) was used as WE and CE. The electrodes were brought into shape by die cutting in a press, to ensure reproducible areas and to avoid fraying of the edges. Prior to their application, the electrodes have been cleaned with a lint-free paper towel.

Pristine GF sheets were used as electrodes in all experiments, while additionally experiments with modified WE were performed. Therefore, the same GF sheets were drop coated with inks containing different compositions of carbon materials, a carbon black (CB, Vulcan XC-72, Cabot) or graphite powder (GP), Nafion® (5-wt% solution, Sigma Aldrich) and bismuth in ethanol. The procedure of the modifications is visualized in Figure 8. After drop coating the inks onto the electrode substrate, the electrodes were dried by evaporating the solvents, water, ethanol, and acetone, under argon gas at room temperature.

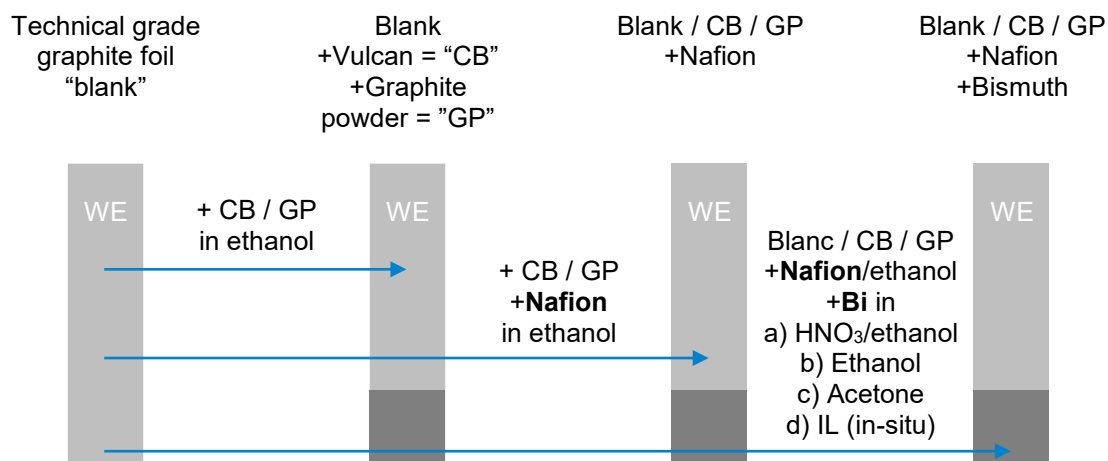


Figure 8: Overview of the different electrode modifications and the production thereof.

The amount of ink and its composition (ethanol and Nafion®-solution content) for carbon black and graphite powder are empirically evaluated according to the handling of the ink drops and the evaporation, leaving behind a film on the electrode surface. An equivalent final Bi content on the electrode is ensured. The addition to the IL can only be estimated.

Electrode Name	Ink composition				Coating V_{coating} μL^{-1}
	$c_{\text{Carbon Material}}$ mg $^{-1}$ mL	Ethanol V-% $^{-1}$	Nafion® (5 wt% sol.) V-% $^{-1}$	Bismuth (solution) V-% $^{-1}$	
Blank	0	0	0	0	0
Blank +Nafion	0	75	25	0	20
Blank +Nafion +Bi (HNO ₃)	0	73.75	25	1.25 200 mg mL $^{-1}$ Bi(NO ₃) ₃ *5H ₂ O in 15 V-% HNO ₃ (69%) 85 V-% ethanol	20
GP	GP 2.5	100	0	0	25

GP +Nafion	GP 2.5	83.33	16.67	0	25
GP +Nafion +Bi (HNO ₃)	GP 2.5	82.33	16.67	1 200 mg mL ⁻¹ Bi(NO ₃) ₃ *5H ₂ O in 15 V-% HNO ₃ (69%) 85 V-% ethanol	25
GP +Nafion +Bi (EtOH)	GP 2.5	73.33	16.67	10 20 mg mL ⁻¹ Ink Bi(NO ₃) ₃ *5H ₂ O in ethanol	25
GP +Nafion +Bi (Acetone)	GP 2.5	73.33	16.67	10 20 mg mL ⁻¹ Bi(NO ₃) ₃ *5H ₂ O in acetone	25
GP +Nafion +Bi (IL)	GP 2.5	83.33	16.67	0 4.6 mg mL ⁻¹ Bi(NO ₃) ₃ *5H ₂ O in water saturated [HBet][NTf ₂]	25
CB	CB 3.75	100	0	0	20
CB +Nafion	CB 3.75	75	25	0	20
CB +Nafion +Bi (HNO ₃)	CB 3.75	73.75	25	1.25 200 mg mL ⁻¹ Bi(NO ₃) ₃ *5H ₂ O in 15 V-% HNO ₃ (69%) 85 V-% ethanol	20
CB +Nafion +Bi (EtOH)	CB 3.75	62.5	25	12.5 20 mg mL ⁻¹ Ink Bi(NO ₃) ₃ *5H ₂ O in ethanol	20
CB +Nafion +Bi (Acetone)	CB 3.75	62.5	25	12.5 20 mg mL ⁻¹ Bi(NO ₃) ₃ *5H ₂ O in acetone	20
CB +Nafion +Bi (IL)	CB 3.75	75	25	0 4.6 mg mL ⁻¹ Bi(NO ₃) ₃ *5H ₂ O in water saturated [HBet][NTf ₂]	20

As RE silver wires with a diameter of 1 mm have been resorted to. Since the here occurring reaction is unknown, the RE must be described as a pseudo or quasi RE (qRE), in contrast to an actual RE. The qRE was immersed in the water saturated [HBet][NTf₂], which was used as electrolyte in all experiments, allowing for comparability within this set of experiments.

Evaluation

The datasets of potential and measured current were transferred from the VersaStudio software to Microsoft Excel. Here the baseline was manually created by choosing areas to the left and right of the peak. Three to five sets of values each were averaged, resulting in two points. A straight line through both points was drawn. This baseline was then subtracted from the measured data. The baseline corrected data points were being transferred to Origin for peak fitting and evaluation. “Gaussian” fit was chosen, and the target area narrowed to the width of the peak. The base parameter y_0 was set to 0. The current at maximum peak height was extracted. Plots were produced in Origin.

Limit of Detection

The 3- σ -method was applied for determining the limit of detection (LOD). The peak current in dependence of the Pb²⁺ concentration in the initial aqueous phase was linearly fitted and the standard deviation σ of Pb²⁺-free samples was determined. The theoretical concentration leading to a peak current as high the threefold of σ of a Pb²⁺-free sample was calculated using the linear function (calibration curve) and is referred to as LOD.

4.3.2. Resistance and Conductivity Determination

Potentiostatic Electrochemical Impedance Spectroscopy (PEIS) was applied for inspection of the set-up and the electrolyte resistance in the beginning of and in between detection measurements. It was also used for conductivity measurements of electrolytes in a conductivity measurement cell Philips PW 9512/01, consisting of two parallel, plane electrodes. The PEIS parameters are listed in Table 8.

Table 8: Parameter settings for PEIS.

Parameter	Value	Unit
Start frequency	10000	Hz
End frequency	1	Hz
Amplitude	10	mV
Potential	0	V vs. OCV
Points per decade	10	-

4.3.3. Electrochemical Stability

Cyclic Voltammetry (CV) was carried out in the heatable cell with graphite foil working and counter electrode to verify the electrochemical stability of the water saturated [HBet][NTf₂] electrolyte and the accessible window for the detection at a given temperature in the measurement set-up. The applied potential was IR-compensated post hoc, assuming the impedance $|Z|$ at 10 kHz in the PEIS to be the electrolyte's resistance. Parameters are listed in Table 9.

Table 9: Parameter settings for cyclic voltammetry.

Parameter	Value	Unit
Start potential	0	V vs. Ag-qRE
Cathodic Vertex	-1.5	V vs. Ag-qRE
Anodic vertex	1.5	V vs. Ag-qRE
Scan rate	0.1	V s ⁻¹
Number of cycles	3	-
IR-compensation		Post hoc

4.3.4. Introduction of a Paper Channel

The paper materials intended as microfluidic channel and spacer in between the electrodes were prepared by TIZIAN VENTER within the Laboratory of Macromolecular and Paper Chemistry, Ernst-Berl-Institut, Department of Chemistry, TU Darmstadt. Different materials in various thicknesses have been investigated for the transport qualities of ILs. The choice of the

paper material was made upon the performance in imbibing behaviour and flow velocity of ILs within the material. Respective experiments were carried out in collaboration with TIZIAN VENTER.

For the electrochemical measurements, experiments were conducted using water saturated [HBet][NTf₂] without the addition of zwitterionic betaine nor other additives. Unmodified technical grade graphite foil as WE and CE and a flattened silver wire with insulated rear or technical grade graphite foil as qRE were used. A 3D configuration with a stack of WE, a tailored paper sheet and CE was arranged. The geometrical surface area of the WE was limited to 1 cm². The presented data result from experiments without electrolyte flow. The Pb²⁺ spiked IL was pipetted on the paper sheet and the experiment was started when the section of the paper covered by the electrodes was fully soaked.

In addition to the paper based cell, a 3D printed spacer with a thickness of 1 mm was used analogously, due to reusability and development of a handling procedure.

In most of the experiments errors due to overloads were reported by the potentiostat that led to abortions of the experiments. In this context, also shorter experiments with a deposition time of 60 s were conducted. Furthermore linear scan voltammograms were applied for controlled initiation of the deposition of -1 V vs. Ag-qRE. However, the occurrence of abortions could not fully be comprehended. Some of these issues could later be traced back to a malfunction of the potentiostat's hardware.

5. Results and Discussion

5.1. Choice of the Ionic Liquid

Out of the enormous number of ILs, a suitable candidate needs to be identified, that shows analyte extraction capabilities, as well as electrolyte and paper imbining qualities. Physico-chemical properties, such as viscosity, electrical conductivity and pH are considered elementary in evaluating these qualities and are hence chosen for comparison, as illustrated in Figure 9.

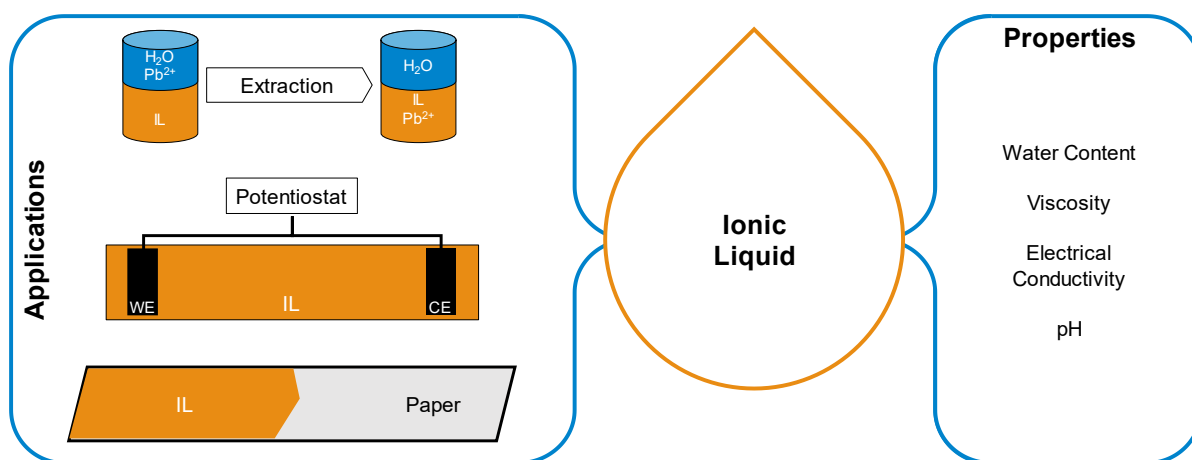


Figure 9: Separated applications defining the requirements to the IL and derived physico-chemical properties to be analysed for characterization, comparison and identification of a suitable IL.

An IL that is suitable to combine extraction from aqueous phase, serving as electrolyte in electrochemical detection and transport medium in a paper channel, preferably needs to feature low miscibility, low viscosity and high electrical conductivity and at least mild acidity.

Initially, ten ILs were characterized at the four defined stages of set water content – pristine, dried, moist and wet (cf. chapter 4.1). Due to the underlying aim of this work and the inevitable contact to a liquid water phase, the wet stage will be focussed on and compared to the pristine stage here. Results for other stages are attached in the appendix.

5.1.1. Water Content of Saturated ILs

After extraction from aqueous phase, the water content in the IL will have changed compared to their pristine stage. In order to further characterize the physico-chemical properties, the water content at the wet stage needs to be known. The water contents of the ILs are measured by Karl Fischer titration. Obtained mass contents of water are converted to molar contents (mol-%) by Equation 14, revealing the impact of the differences in molar masses of water compared to the investigated ILs. Samples taken from the container as received from the distributor (pristine) range below 0.06 wt-% or 1 mol-%, except for [OMIm][BF₄] (1.27 mol-%, see appendix). However, the contents increase after contact to liquid water. Figure 10 shows the molar water content of the wet stages of different ILs.

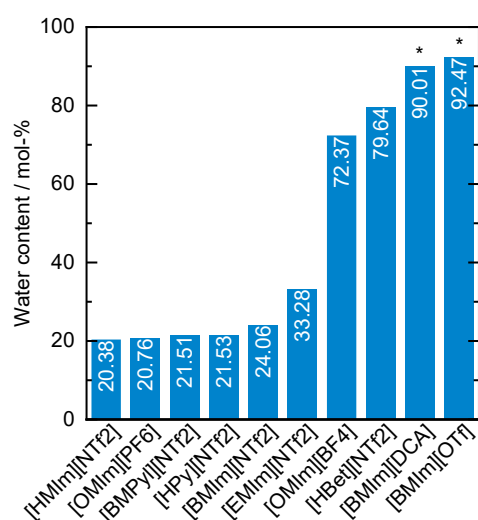


Figure 10: Molecular ratios of water in ILs converted from mass ratios obtained by Karl Fischer titration after contact to water ($V_{aq,ini}V_{org,ini}^{-1}=1$). Note: [DCA] and [OTf] containing ILs, indicated by *, are completely miscible with water.

As expected, ILs featuring [NTf₂] anions take up the smallest amount of water of around 20 mol-% (1-2 wt-%). Additionally, the trend of increasing hydrophobicity with longer alkyl chains at the imidazolium based ILs, [HMIm] < [BMIm] < [EMIm], can also be followed. The ILs with [OTf] and [DCA] anions are miscible with water. The shown data are results of complete miscibility of the aqueous phase and the IL phase, which are brought into contact initially ($V_{aq,ini}V_{org,ini}^{-1}=1$). Stated values for the two ILs thus can be regarded arbitrary. Due to the high miscibility, both ILs are ruled out for an extraction application.

ILs with reported intrinsic heavy metal extraction capabilities, [OMIm][BF₄] and [HBet][NTf₂] contain water up to 72 and 80 mol-% (14.33 and 15.03 wt-%) at the wet stage. They take up the highest amount of water within the non-miscible ILs. Even though they are hydrophobic and still form a two-phase system with water, their properties certainly are affected by contact

to water. For [HBet][NTf₂] a certain miscibility at room temperature is reported in the literature, that is in accordance with the results presented here.^[92] With a measured water content of 15 wt-%, four water molecules are present for every anion-cation-pair of the IL (=80 mol-%). Also, for the prominent hydrophobic imidazolium based ILs with [NTf₂] anions, the molar ratios of water jump above 20 mol-%. The difference in water content in pristine and wet stage hence impel a reassessment of the water influence on the physico-chemical properties of the IL phase. This will be addressed in the following chapter.

5.1.2. Physico-Chemical Properties after Water Exposure

Two physico-chemical properties of ILs influencing the electrolyte properties and imbibing qualities and that are affected by the water content are the viscosity η and the electrical conductivity κ . The inversely proportional dependency of κ on η can be traced in Figure 11 A and B. ILs are arranged by increasing value in the wet state (left to right) and follow reversed order regarding the two properties. Due to the arbitrariness of the water content of [BMIm][DCA] and [BMIm][OTf], both ILs can be excluded for the pursued application. Their measured properties align the trend of the water saturated ILs.

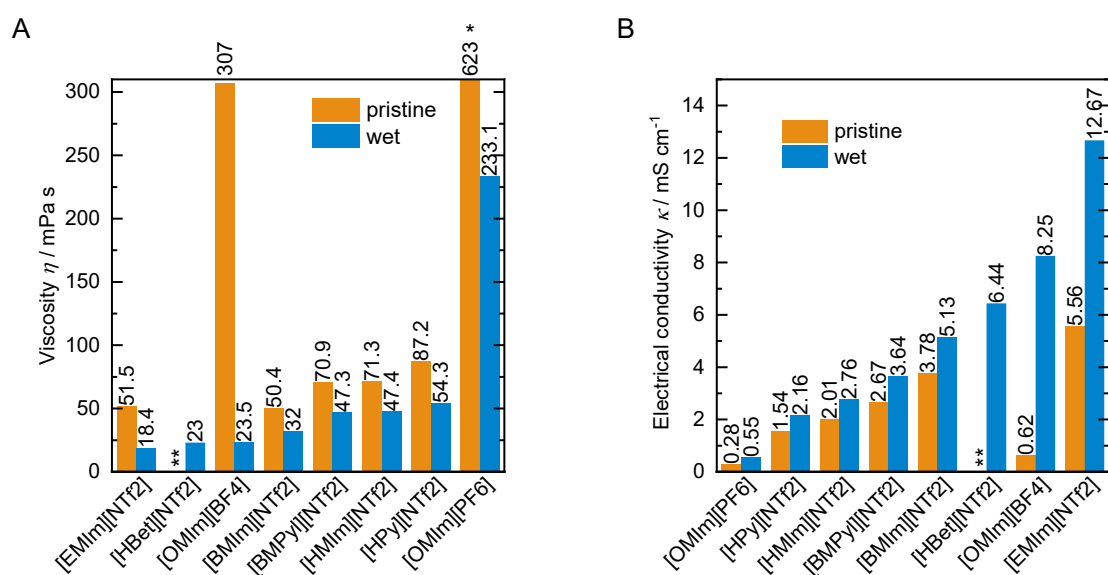


Figure 11: A: Viscosity of ILs in their pristine stage and after saturation with water. *) pristine [OMIm][PF₆] exceeds the limit of the displayed section; **) pristine [HBet][NTf₂] could not be measured. B: Electrical conductivity of ILs in their pristine stage and after saturation with water. **) pristine [HBet][NTf₂] could not be measured.

Generally, the viscosity decreases after contact to water, while the electrical conductivity increases. The smallest effects can be observed for the most hydrophobic ILs, featuring [NTf₂] anions. They show comparable changes in η and κ within the same range, corresponding to the low uptake of water. The strongest influence of exposure to water is measured for [OMIm][BF₄], that also shows the highest water uptake. No pristine state of pure [HBet][NTf₂] could be measured. At dry state it is a crystalline solid with a melting point of

57 °C.^[92] The super cooled state could not be maintained either throughout the measurements and only moist samples could be analysed. Its viscosity at wet stage can be compared with [OMIm][BF₄] with comparable water content and the more hydrophobic [EMIm][NTf₂]. Comparing the overall trends of η and κ for wet ILs aligns with theoretical considerations. A high viscosity is accompanied by a low electrical conductivity and vice versa.

In addition to the η and κ , the pH of the water saturated ILs were determined, utilizing a pH paper. Measurements were exclusively carried out for the wet stage of the ILs (Figure 12). [BMIm][DCA] and [BMIm][OTf] were left out of the figure, due to their complete miscibility with the aqueous phase.

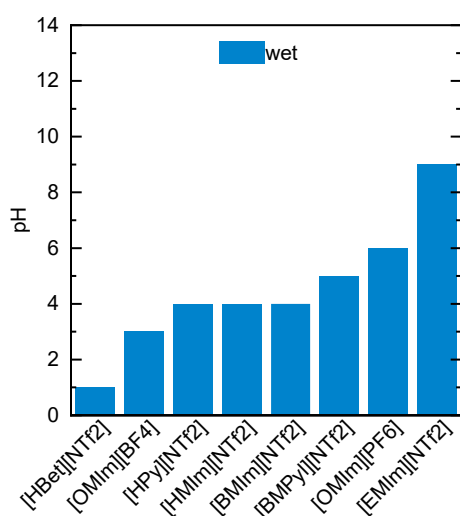


Figure 12: pH values of water saturated ILs.

Most of the studied [NTf₂] containing ILs are moderately acidic with pH values of around 4. Exceptions being the ILs with [HBet] and [EMIm] cations. The pH of [HBet][NTf₂] is the most acidic with pH=1 and is in consistence with the protonated carboxylic function in betaine cation of this IL. Given the accuracy of the visual determination of the pH, this is in good agreement with the literature (1.42±0.05).^[104] The second most acidic IL is [OMIm][BF₄] with a pH of around 3. Unexpectedly high is the pH of [EMIm][NTf₂] (pH=9).

At wet stage, the most acidic IL [HBet][NTf₂] has the lowest viscosity and comparably high electrical conductivity, after ruling out [EMIm][NTf₂] due to its high pH. Furthermore, this IL was already shown to be applicable as electrolyte in a heavy metal sensing application.^[19] It hence seems to be a suitable candidate for combining the three applications.

5.2. Homogeneous Liquid-Liquid Extraction of Lead Ions with [HBet][NTf₂]

5.2.1. Phase Behaviour

Among the screened ILs one compound is outstanding due to its exceptional properties: [HBet][NTf₂] shows a thermomorphic phase behaviour. At temperatures below the UCST its mixture with water is biphasic for a large mixing ratio. Heating above the UCST generates a single phase for all mixing ratios.^[92] For the extraction from aqueous phase in a mobile application, this is considered as a valuable asset, due to the avoidance of a mixing unit.

Homogeneous liquid-liquid extraction can be performed in accordance with descriptions in the literature. Both, self-synthesized and purchased substances could be used identically. The optical appearance of a sample during the heating and cooling/settling procedure is chronologically imaged in Figure 13. The extraction of the model analyte Pb²⁺ is investigated in the following chapter.

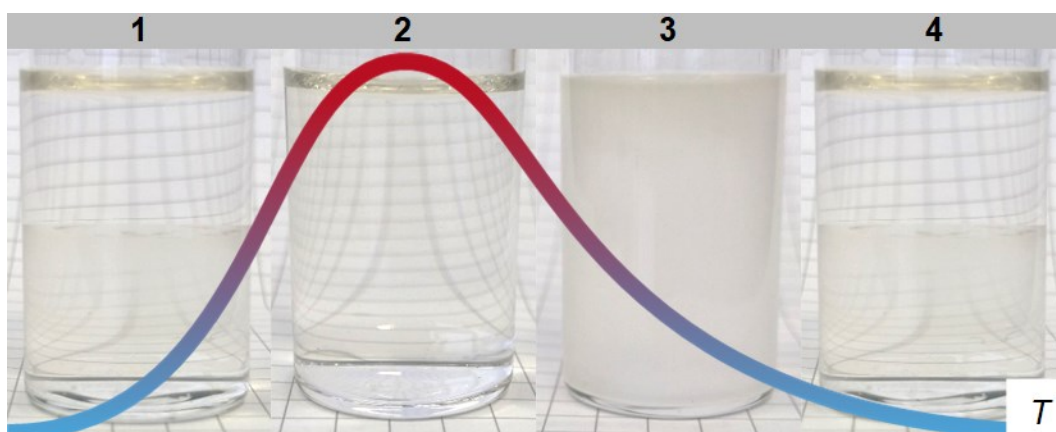


Figure 13: Temperature dependent phase behaviour of water saturated [HBet][NTf₂] with water in four stages: 1. Room temperature, two phases with a clear phase boundary; 2. Above the UCST a clear, single phase is stable; 3. During cooling below the UCST the solution clouds and the phases separate; 4. After settling the phase boundary is rebuilt.

5.2.2. Extraction Behaviour

Following the sufficiently documented process HLLLE, consisting of heating, cooling/settling and subsequent ICP-OES analysis, reveals the successful extraction of Pb²⁺ ions from aqueous media to the water saturated [HBet][NTf₂]. Due to the necessity of dilution for the quantification of Pb²⁺, the initial heavy metal ion concentration was set high with 1 mg mL⁻¹ in the aqueous phase. However, performed electrochemical measurements verify Pb²⁺ extraction, starting from lower concentrations.

High analyte concentrations in the extractor phase are favourable since they are easier to detect in subsequent quantification analysis. As plotted in Figure 14, the concentration of Pb^{2+} in the IL-phase $c_{\text{IL}}(\text{Pb}^{2+})$ can be enriched by increasing the volume ratio $V_{\text{aq,ini}}V_{\text{org,ini}}^{-1}$ at a constant initial Pb^{2+} -concentration in the aqueous phase $c_{\text{aq,ini}}(\text{Pb}^{2+})$. The concentration increases linearly from $c_{\text{IL}}(\text{Pb}^{2+})=0.33 \text{ mg mL}^{-1}$ ($V_{\text{aq,ini}}V_{\text{org,ini}}^{-1}=1.03$), one third of the initial concentration in the carrier, to 1.17 mg mL^{-1} ($V_{\text{aq,ini}}V_{\text{org,ini}}^{-1}=8.22$), which exceeds the initial concentration $c_{\text{aq,ini}}(\text{Pb}^{2+})=1 \text{ mg mL}^{-1}$. No organic phase could be obtained for experiments with volume ratios higher than 8.22. In between, the concentration can be linearly fitted by the function

$$c_{\text{IL}}(\text{Pb}^{2+}) = (0.11273 V_{\text{aq,ini}}V_{\text{org,ini}}^{-1} + 0.23031) c_{\text{aq,ini}}(\text{Pb}^{2+}).$$

The analyte can thus be extracted and, closer to the maximal possible volume ratio, even be concentrated in the organic phase.

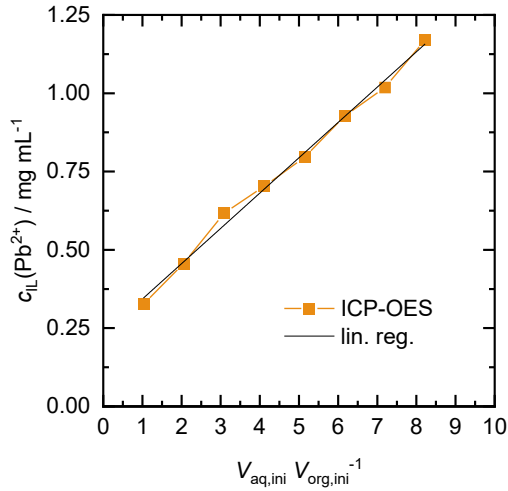


Figure 14: Pb^{2+} concentration found in the IL phase by ICP analysis after HLLC in dependence of the initial volume ratio of the carrier and extractor phase. The initial Pb^{2+} concentration in the aqueous phase was $c_{\text{aq,ini}}(\text{Pb}^{2+})=1 \text{ mg mL}^{-1}$.

The mass ratio of the phases w_{org} (water saturated $[\text{HBet}][\text{NTf}_2]$ phase) and w_{aq} (aqueous phase) left after HLLC, when the system has reached phase equilibrium, can be calculated with the reciprocal miscibilities of IL in the aqueous phase $w_{\text{IL,aq}}$ and of H_2O in the organic phase $w_{\text{H}_2\text{O,org}}$ as a function of the initial volume ratio $V_{\text{aq,ini}}V_{\text{org,ini}}^{-1}$. The system of equations is a set of four equations containing four variables (Equation 17 to Equation 20). Based on miscibilities from literature, two scenarios are calculated and plotted in Figure 15.^[90,99,104] The plots result from a combination of the lowest and highest values of miscibility reported. A no-miscibility-scenario is also included.

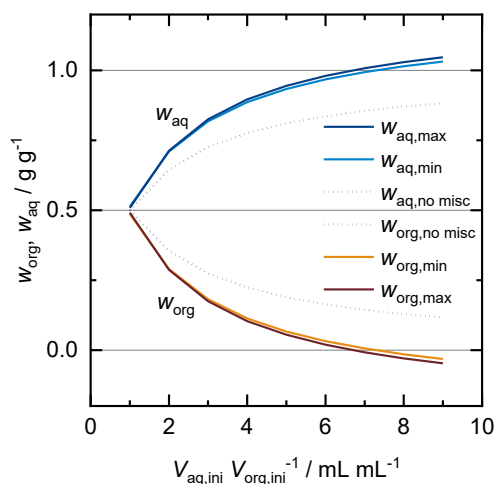


Figure 15: Calculated mass ratios of the remaining organic and aqueous phases after HLLE of water saturated [HBet][NTf₂] and water as function of the initial volume ratio. Values outside of $0 < w < 1$ are physically not plausible. At the corresponding volume ratios the system is single-phase.

Due to the reciprocal miscibility, the ratio of the masses of each phase after HLLE alters stronger than without miscibility and eventually exceed 1 and 0, respectively. Mixtures with mass ratios >1 and <0 are not physically plausible and the corresponding volume ratios exceed in these limits indicate a single-phase system. By plotting absolute masses of the organic and aqueous phase in dependence of $V_{aq,ini}V_{org,ini}^{-1}$, the amount of added H₂O to the fixed volume of IL can easily be calculated from linear regression (graph in the appendix). In both cases, the smallest values and the lowest values for reciprocal miscibility, a complete dissolution of the IL into the aqueous phase ($w_{org}=0$) will occur at a $V_{aq,ini}V_{org,ini}^{-1}$ of 7.33 and 6.67, respectively. That translates to volumes of 7.33 mL and 6.67 mL H₂O added to 1 mL of water saturated [HBet][NTf₂]. At that point, the system is single-phase. No organic phase can theoretically be obtained.

In this work, an organic phase could be sampled for ICP analysis at an initial $V_{aq,ini}V_{org,ini}^{-1}$ of up to 8.22 and the organic phase disappeared at $V_{aq,ini}V_{org,ini}^{-1}=9$. This is only possible if the IL solubility in H₂O is lower than 12.9 wt-% and the experimentally determined H₂O solubility in IL is 15 wt-%. Not included in this calculation are the real pH values of the aqueous phase. Plus, the influence of the Pb²⁺-salt is also excluded.

For this case (12.9 wt-% IL in aqueous phase and 15 wt-% H₂O in the organic phase) the distribution ratio D and the extraction efficiency $\%E$ can be calculated (Figure 16). Note that D in this calculation is based on mass-concentrations (mass of Pb²⁺ in mass of solvent). D , however, would be larger, if based on volume-concentrations, due to the high density of the organic phase (1.47 g mL⁻¹).

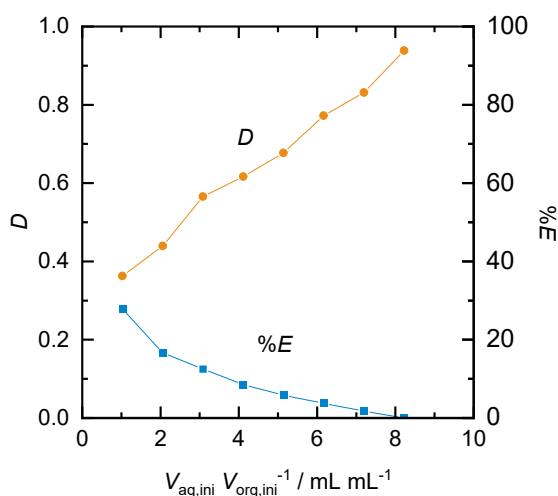


Figure 16: Distribution ratio D and extraction efficiency $\%E$ based on the calculated mass ratios, a [HBet][NTf₂] solubility in water of 12.9 wt-% and the measured Pb²⁺ concentration in the organic phase after HLE.

D increases linearly with the volume of added Pb²⁺-containing H₂O. The concentrations in each phase are in equilibrium, though the total concentration of Pb²⁺ in the entire system increases with lower IL fractions, diluting the total concentration. The actual trajectory follows the Pb²⁺ concentration as measured by ICP analysis in Figure 14. Due to the solubility of the IL in the aqueous phase, eventually the organic phase is dissolved completely. This is reflected in $\%E$, consequently becoming zero, when no extractor phase is left. The competing equilibria are hence the extraction of Pb²⁺ by the IL-dominated, organic extractor versus the dissolution of the IL by the aqueous carrier. For the application in trace analysis, increasing $V_{aq,ini}V_{org,ini}^{-1}$ can be employed in order to enrich the analyte concentration in the extractor above the initial concentration. A decrease in recoveries ($\%E$) is not of concern since the downstream step of electrochemical detection is concentration sensitive.

5.2.3. Effect of the Addition of Zwitterionic Betaine

The addition of an extractor, a metal ion chelating agent with high affinity to the extractor phase in the chelating form, is used for extraction applications and discussed in literature to tune the extraction capabilities of ILs. HOOGERSTRAETE et al. added zwitterionic betaine to water saturated [HBet][NTf₂].^[90] Here, this approach is also applied for the extraction of Pb²⁺. As shown in Figure 17 the concentration of Pb²⁺ in the organic phase can be increased from 0.22 mg g⁻¹ to 0.55 mg mL⁻¹ at a $V_{aq,ini}V_{org,ini}^{-1} = 1.03$ when 10 wt-% and 20 wt-% zwitterionic betaine (per mass of water saturated IL) are added to the 1.43 g IL and 1 mL water containing 1 mg mL Pb²⁺. It is assumed, that the density of the organic phase does not

change with the addition of zwitterionic betaine. This corresponds to an enhancement of +150 % compared to the additive-free experiment with [HBet][NTf₂].

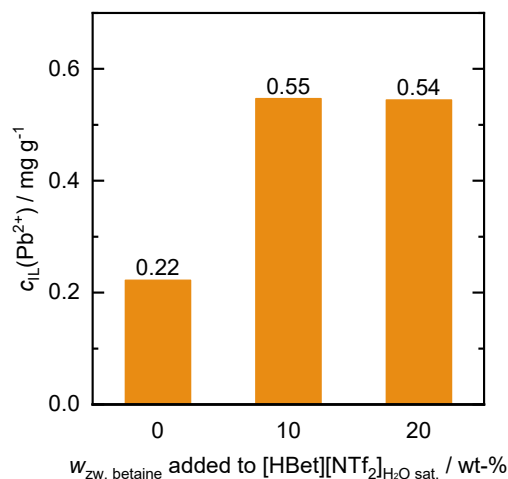


Figure 17: Pb^{2+} concentration found in the IL phase by ICP analysis after HLE in dependence of [HBet][NTf₂] and the addition of zwitterionic betaine. Note: the concentrations are referred to the mass of the organic phase (IL).

Assuming 12.9 wt-% loss of IL into the aqueous phase as previously calculated for the additive free experiments, and the same density of the IL phase as without additional betaine, %*E* and *D* can be estimated. The highest Pb^{2+} extraction yielded in this work is %*E*=68.1 % and *D*=2.02 for the addition of 10 wt-% zwitterionic betaine per mass of water saturated IL. Comparing to other ions, this result would rank Pb^{2+} between Zn^{2+} (*D*≈1) and Cu^{2+} (*D*≈4), extracted in similar fashion.^[90] HOOGERSTRAETE et al. mixed equal masses of water saturated [Hbet][NTf₂] and water, equal to a volume ratio of 1.47, and report *D*<1 for the extraction of lanthanide ions. For Nd^{3+} bis-(trifluoromethylsulfonyl)imide salts they could increase %*E* from around 30 % (no additive) to almost complete extraction by the addition of zwitterionic betaine as extractant. The highest extraction of 99 % was yielded when *n*(betaine)/*n*(Nd³⁺) was 200, translating into the addition of 200 mg g⁻¹ aqueous starting solution.^[90]

The 10 wt-% of zwitterionic betaine added in this work translates to 143 mg zwitterionic betaine per 1 g aqueous starting solution. Thereby, the total amount of zwitterionic betaine, either originating from is [HBet][NTf₂] or the additive, is increased by around 30 %. However, the distribution of the added zwitterionic betaine after HLE has not been studied in this work and is ignored for this calculation. VOLIA et al., who investigated the effect of betaine on this system, found that betaine is transferred to the IL phase and reduces the loss of H[NTf₂] into the aqueous phase. The solubility of H₂O in the IL phase is not affected and added zwitterionic betaine was found in both phases.^[104] It is concluded, that the phase behaviour is not drastically changed by the presence of the additive. From the perspective of

extraction performance, the addition of zwitterionic betaine, hence, seems beneficial. D can be enhanced by a factor of over 2, compared to the $V_{\text{aq,ini}}V_{\text{org,ini}}^{-1}$ of 8 in absence of an additive and due to the preservation of the IL phase $\%E$ is also increased.

5.3. Temperature Influence on Electrolyte Properties of [HBet][NTf₂]

After homogeneous liquid-liquid extraction of Pb²⁺ from aqueous phase by water saturated [HBet][NTf₂], the wet IL serves as electrolyte in heavy metal detection. Since temperature control is key for the temperature induced extraction it suggests itself to also employ heat for decreasing viscosity and increasing electrical conductivity. The classification within the Walden-plot can also be realized in this context. This has not been reported in literature up to writing this work. Shown results refer to wet [HBet][NTf₂], which is saturated with water at room temperature. [BMIm][NTf₂] is measured alongside for comparison and validation. “dry” implicates, that this IL was not deliberately saturated with water prior but taken as received from the supplier. Evaporation of water and a concomitant change in properties was tried to prevent by sealing to the atmosphere, where possible and minimizing the exposure time to heat.

5.3.1. Viscosity

The temperature dependent viscosity of ILs was assessed with a spindle viscometer. The experimentally determined results are compared in Figure 18 with a dataset from literature for 1-butyl-3-methylimidazolium bis(trifluoromethylsulfonyl)imide [BMIm][NTf₂] (unfilled circles). They show a very good agreement for the overall values as also temperature trend for experimental values for [BMIm][NTf₂] (blue triangles). Minor deviation may be caused by differences in water contents of the ILs. Since the spindle viscometer is an unsealed construction, open to the atmosphere, and therefore slow evaporation of water during the experiments cannot completely be excluded. This looms larger for higher temperatures.

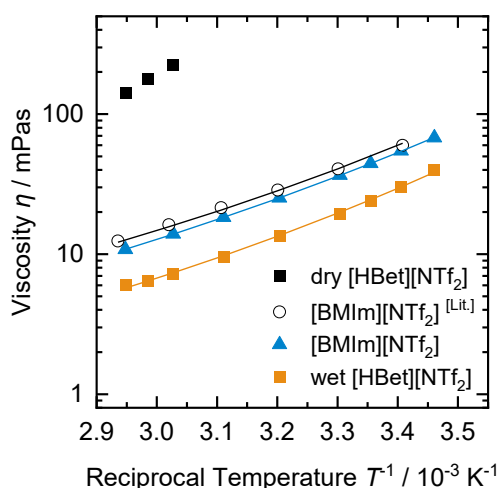


Figure 18: Viscosity-temperature diagram of dry and water saturated [HBet][NTf₂], [BMIm][NTf₂] and comparison to a dataset from literature “[Lit.]”.^[123] Experimental data (symbols) are fitted by Vogel-Fulcher-Tammann equation (lines).

After validation, temperature dependent viscosity of the IL [HBet][NTf₂] (orange squares), which is employed for extraction and sensing within this study, was characterized. More exactly, a mixture of [HBet][NTf₂] and water resulting from saturation with water at room temperature ($w(\text{H}_2\text{O})=0.15 \text{ g g}^{-1}$) was employed to study the temperature influence on viscosity. This concentration of water represents the maximum amount where still a single-phase behavior throughout the whole studied temperature range (20 to 70 °C) can be ensured. The viscosity of wet [HBet][NTf₂] is consistently lower than of [BMIm][NTf₂] throughout the entire temperature range. The trends of both ILs run parallel to each other with increasing viscosity with increasing T . VFT parameter can be adjusted to fit the experimental data by the values given in Table 10.

Table 10: VFT parameters for viscosity resulting from experimental data for [BMIm][NTf₂] and [HBet][NTf₂] as well as for a dataset from literature.^[123]

VFT	A_η	B_η / K	$T_{0,\eta} / \text{K}$
dry [BMIm][NTf ₂]	-2.1430	789.55	165.06
[BMIm][NTf ₂] ^[Lit.]	-1.9143	775.19	165.06
wet [HBet][NTf ₂]	-2.9456	817.05	165.06

For comparison, the viscosity of dry [HBet][NTf₂] was measured above its melting point (black squares). They are about one order magnitude higher as compared to wet, water saturated [HBet][NTf₂]. This indicates the benefit of a certain water content in the IL, while still retaining its hydrophobicity for easy phase separation in the extraction. Besides the contribution to the electrical conductivity, a low viscosity is favourable for the application in a microfluidic device.

5.3.2. Electrical Conductivity

The electrical conductivity is obtained from PEIS experiments in a conductivity cell. To validate the self-build heating setup for electrical conductivity measurements for higher temperatures, the temperature dependent conductivity of the more intensively studied IL 1-butyl-3-methylimidazolium bis(trifluoromethylsulfonyl)imide [BMIm][NTf₂] was determined alongside and compared to a dataset from literature. Experimental data of wet, room temperature water saturated [HBet][NTf₂] ($w(\text{H}_2\text{O})=0.15 \text{ g g}^{-1}$, orange squares) and [BMIm][NTf₂] (blue triangles) are plotted in Figure 19 together with their VFT fits and the dataset from literature (unfilled circles).^[123]

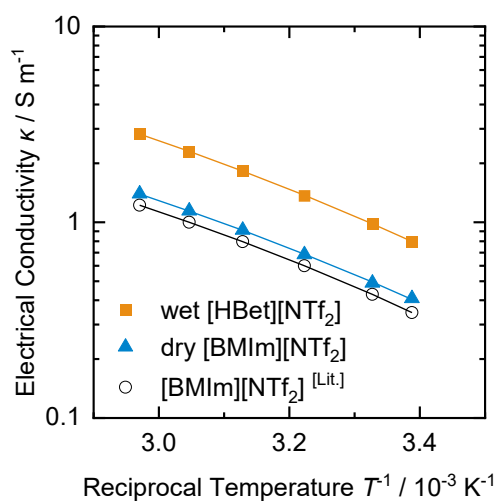


Figure 19: Electrical conductivity-temperature diagram of water saturated [HBet][NTf₂], [BMIm][NTf₂] and comparison to a dataset from literature“[Lit.]”,^[123] Experimental data (symbols) are fitted by Vogel-Fulcher-Tammann equation (lines).

The experimental data align well with the data set from literature, validating the measurement setup. The difference might be attributed to different water contents. The electrical conductivity of all liquids tested follow the same trend and run parallel in this plot. Their electrical conductivity increases with increasing temperature. The electrical conductivity of wet [HBet][NTf₂] is higher than that of [BMIm][NTf₂].

Experimental data can be fitted by Vogel-Fulcher-Tammann equation in the same manner as for viscosities. Found VFT parameters are listed in Table 11. For fitting the data set of [BMIm][NTf₂] from literature also literature VFT parameter were resorted to for electrical conductivity.

Table 11: VFT parameters for electrical conductivity resulting from experimental data for [BMIm][NTf₂] and [HBet][NTf₂] as well as for a dataset from literature.^[123]

VFT	A_{κ}	B_{κ} / K	$T_{0,\kappa} / K$
dry [BMIm][NTf ₂]	4.2222	-667.43	165.06
[BMIm][NTf ₂] ^[Lit.]	3.7612	-565	178
wet [HBet][NTf ₂]	5.000	-679.92	165.06

5.3.3. Walden Plot

Based on the temperature dependent viscosity and electrical conductivity, the classification of the IL can be performed. For the inclusion into the Walden plot, the conductivity needs to be transferred into the molar conductivity. Densities for water saturated [HBet][NTf₂] (orange squares) and dry [BMIm][NTf₂] (blue triangles) are therefore measured in dependence of the temperature and linearly regressed (Figure 20 A). For comparison, data from literature are plotted alongside in the Walden plot in Figure 20 B.^[123]

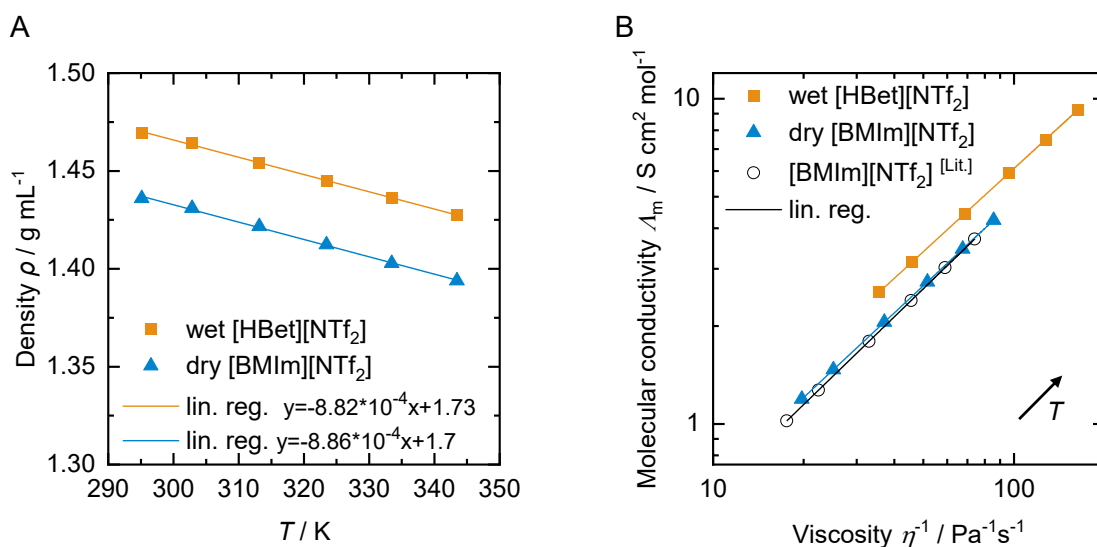


Figure 20: A: Density-temperature diagram for water saturated [HBet][NTf₂] and dry [BMIm][NTf₂] with linear regressions (lines) for the preparation of the Walden plot (B), where also data from literature are plotted “[Lit.]”.^[123] Note the double logarithmic scales of the Walden plot.

The regressions of the data in the Walden plot validates the linear dependency of $\log \Lambda_m$ and $\log \eta^{-1}$ with high coefficients of determination of $R^2 \geq 0.9998$ for the ILs.

$$\text{wet [HBet][NTf}_2\text{]} \quad \log \Lambda_m = 0.849 \log \eta^{-1} - 0.912 \quad R^2=0.9999$$

$$\text{dry [BMIm][NTf}_2\text{]} \quad \log \Lambda_m = 0.863 \log \eta^{-1} - 1.041 \quad R^2=0.9998$$

$$\text{[BMIm][NTf}_2\text{]}^{\text{[Lit.]}} \quad \log \Lambda_m = 0.896 \log \eta^{-1} - 1.105 \quad R^2=1$$

As expected from the isolated consideration of the temperature influence on viscosity and electrical conductivity, the trends run parallel. The plots of experimental [BMIm][NTf₂] and literature data set (unfilled circles) seem to correlate well. In contrast to the ideal case of diluted aqueous KCl solution, the slope of the investigated ILs is lower than 1. Meaning, that with increasing temperature, ions within the IL contribute less to its electrical conductivity. For the experimental data this might be facilitated by the evaporation of water. That higher Λ_m and η^{-1} are reached already at lower T in experimental [BMIm][NTf₂] might also be a

consequence of impurities and water in the pristine IL. All data points range below the ideal line (angle bisector). According to Angell's classification they are allocated within the regime of 'good' to 'poor' electrolytes. Here, water saturated [HBet][NTf₂] shows the highest Λ_m and η^{-1} at all temperatures and hence exhibits the more favourable electrolyte properties. Compared to [BMIm][NTf₂], the molar conductivity of [HBet][NTf₂] is higher or differently expressed, the ions contribute more to the electrical conductivity. Major difference in nature of the cations [BMIm]⁺ and [HBet]⁺ is the functional carboxylic group for the betaine. Despite the direct molecular difference, also the lower water content for [BMIm][NTf₂] might play a role, as water could help reducing the ion pairing.

Consequently, an elevation in temperature and thus decrease of viscosity can be employed to decrease solution resistance losses within the IL during electrochemical sensing.

Water Influence on the Electrical Conductivity

The electrical conductivity of [HBet][NTf₂] was furthermore studied in dependence of the water content. Water interaction with [HBet][NTf₂] at room temperature changes its aggregate condition from dry, solid state to wet, liquid state. Arbitrary homogeneous single-phase water-IL-compositions can hence only be reached above the UCST. Below UCST, two phases and a phase boundary form. A temperature of 70 °C is set for the investigation of the influence of the water content. No drying nor purification step of the IL was carried out and the IL was used as obtained from the manufacturer. Water is added to dry IL up to a weight fraction of 0.25 g g⁻¹. Obtained electrical conductivities are plotted in Figure 21.

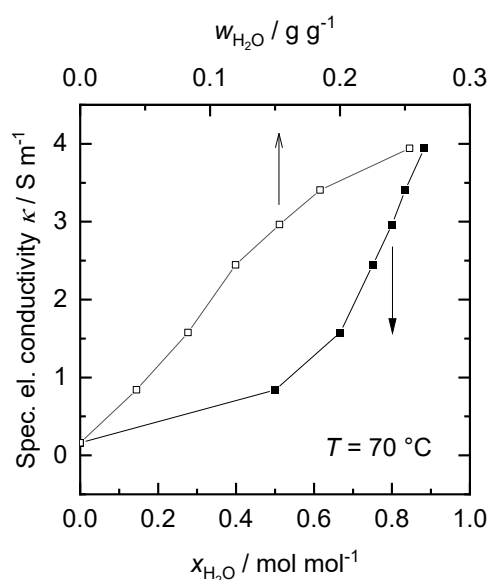


Figure 21: Electrical conductivity in dependence of the water fraction in [HBet][NTf₂] at 70 °C. Note: bottom axis shows molecular ratios (filled squares).

The plot for mass fractions of water (unfilled squares) implies an increase of the electrical conductivity with the addition of water. The incline can be linearly approximated when referring to the mass fraction (upper abscissa). It was found that the electrical conductivity increases drastically from dry state (no added water) to $w(\text{H}_2\text{O}) = 0.25 \text{ g g}^{-1}$. It needs to be noted, that due to the 20-fold difference in molecular mass of the two compounds of $M(\text{H}_2\text{O}) = 18 \text{ g mol}^{-1}$ and $M([\text{HBet}][\text{NTf}_2]) = 398 \text{ g mol}^{-1}$, respectively, at a water mass fraction of 0.15 g g^{-1} only every fifth molecule is $[\text{HBet}][\text{NTf}_2]$. Taking the differences of mass fractions into account, reveals a steeper slope around the water content at saturation at room temperature ($x(\text{H}_2\text{O}) = 0.8 \text{ mol mol}^{-1}$). It can be concluded that water management, especially at higher temperatures, plays an important role in electrochemical application of $[\text{HBet}][\text{NTf}_2]$. A certain water content, however, is favourable for facilitating higher electrical conductivity and lower viscosity. Especially since interaction with water enables a liquid state of $[\text{HBet}][\text{NTf}_2]$ at room temperature in the first place.

5.3.4. Electrochemical and Thermal Stability

ILs are known for their wide electrochemical window and liquid range. Nevertheless, this electrochemical stability window is influenced by the purity and surrounding conditions. Employing graphite foil as WE and CE, similar to the later electrochemical sensing device, the electrochemical stability $[\text{HBet}][\text{NTf}_2]$, saturated with water at room temperature, is studied from 25 to 56 °C. Additionally, from the iR -drop correction, the temperature dependent cell resistance results. As shown before, with increasing temperature, the electrolyte conductivity increases and therefore the cell resistance drops (Figure 19).

In Figure 22 A cyclic voltammograms of water saturated $[\text{HBet}][\text{NTf}_2]$ at graphite foil electrodes are given for the studied temperatures of 25 to 56 °C. While currents above +1 V increase with the temperature, the onset of anodic currents at +1 V vs. Ag-qRE does not change. The onset of cathodic currents at around -1.2 V vs. Ag-qRE at 25 °C shift to less negative potentials with increasing temperatures, narrowing the accessible window for electro deposition slightly. Nevertheless, as the deposition of lead takes place approximately at -1 V vs. Ag-qRE and the stripping occurs at -0.7 V vs. Ag-qRE, the electrochemical detection should also be possible at the elevated temperatures. Around these potentials, no faradaic currents can be observed. The cathodic peak at around +0.8 V vs Ag-qRE cannot be assigned. For the highest temperature of 56 °C the resistance increases again, which might be caused by the evaporation of water, which was shown to also have a strong influence on the electrical conductivity (Figure 21). The electrochemical stability window for water saturated $[\text{HBet}][\text{NTf}_2]$ has a width of around 2.2 V.

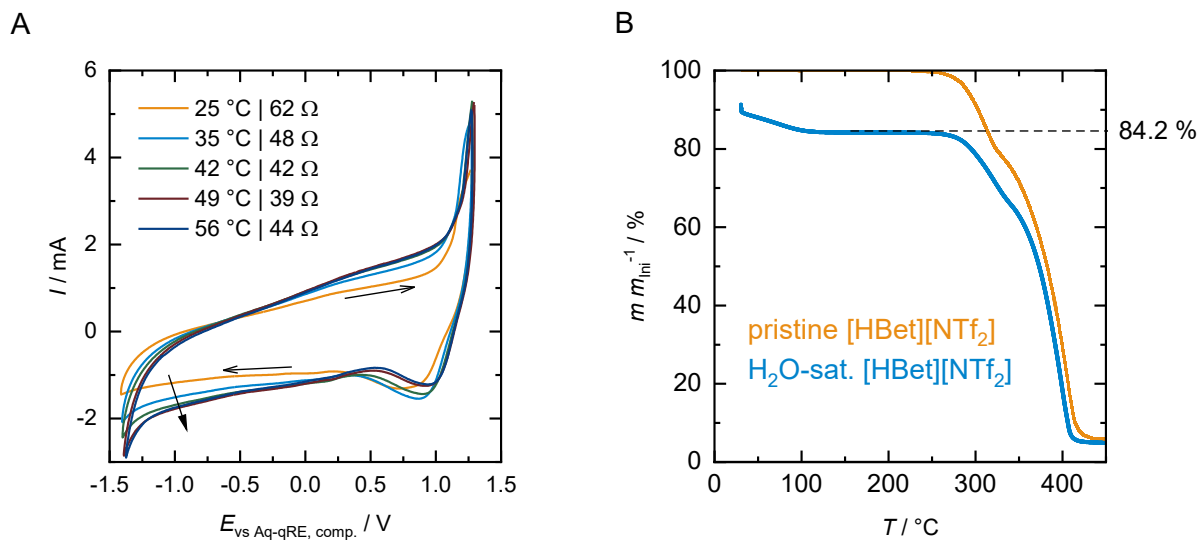


Figure 22: A: Cyclic voltammograms for determination of the electrochemical stability window of water saturated [HBet][NTf₂] at graphite foil electrodes and a scan rate of 100 mV S⁻¹. B: Mass curves of thermogravimetric analysis of water saturated and dry, crystalline [HBet][NTf₂] under N₂ gas flow of 88 mL min⁻¹ and a T ramp of 2 K min⁻¹.

The thermal stability of water saturated [HBet][NTf₂] is investigated via thermogravimetric analysis (Figure 22 B). By comparing water saturated [HBet][NTf₂] (blue graph) and crystalline [HBet][NTf₂] as received from the supplier (orange graph), the water content can be determined to 15.8 wt-%. This result is in accordance with Karl Fischer titration (15.03 wt-%). Most of the contained water is evaporated during the preparation phase of the measurement under N₂ gas flow. This is reflected by the onset at around 90 wt-% (blue graph). Remaining water evaporates before 100 °C is reached and the remaining mass hence declines. From there, mass losses of both samples behave similar. The samples evaporate and possibly decompose, starting at 250 °C.

5.4. Electrochemical Heavy Metal Ion Detection

Electrochemical Pb^{2+} detection in water saturated $[\text{HBet}][\text{NTf}_2]$ is performed with the SWV method. Prior to the electrochemical detection in water saturated $[\text{HBet}][\text{NTf}_2]$, Pb^{2+} was extracted from aqueous phase by homogeneous liquid-liquid extraction. Concentration stated in the following correspond to the Pb^{2+} concentration in aqueous phase, that was set before the extraction, $c_{\text{aq,ini}}(\text{Pb}^{2+})$, as schematically illustrated in Figure 23.

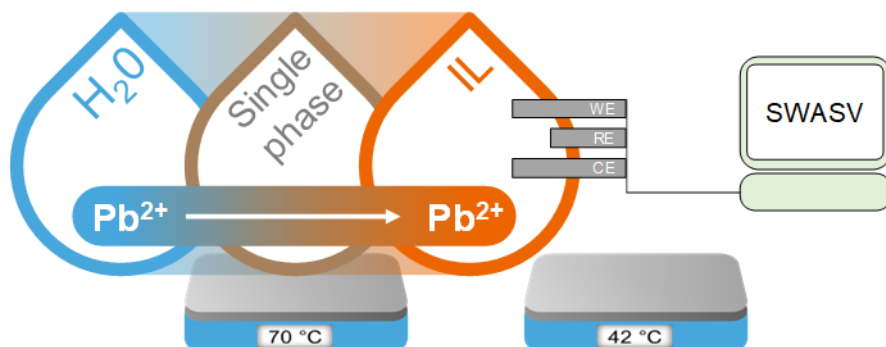


Figure 23: Schematic illustration of the homogeneous liquid-liquid extraction of Pb^{2+} from aqueous to IL phase and the subsequent electrochemical detection in the IL.

In order to achieve low LODs, intensive stripping peaks are desired. Therefore, the influence of SWV method parameters, temperature, extracting additives and electrode modification is studied within this work. Adding an extracting agent is aiming for a higher analyte concentration in the electrolyte but might also interact with the sensing.

5.4.1. Adaptation of SWV Parameters

Stripping Parameters

While SWV Pb^{2+} detection in aqueous electrolyte is well reported, there are hardly any reports on studying the employment of ionic liquids, that are accompanied by higher viscosities and lower electrical conductivities compared to aqueous electrolytes. Consequently, parameter settings that established for aqueous systems (cf. Table 2) might not be suitable in the new environment and need to be adjusted for high stripping peak currents. In a sensitivity study, suitable parameter settings for the stripping step shall be found. Alongside a frequency variation, a variation of E_{Step} and E_{Pulse} is carried out. The ratio of $E_{\text{Pulse}}/E_{\text{Step}}$ is kept at 5, as usually applied in literature. Baseline corrected SWV current response curves (ΔI_{corr}) of lead stripping in water saturated $[\text{HBet}][\text{NTf}_2]$ with constant $c_{\text{aq,ini}}(\text{Pb}^{2+}) = 100$ ppm are plotted in Figure 24.

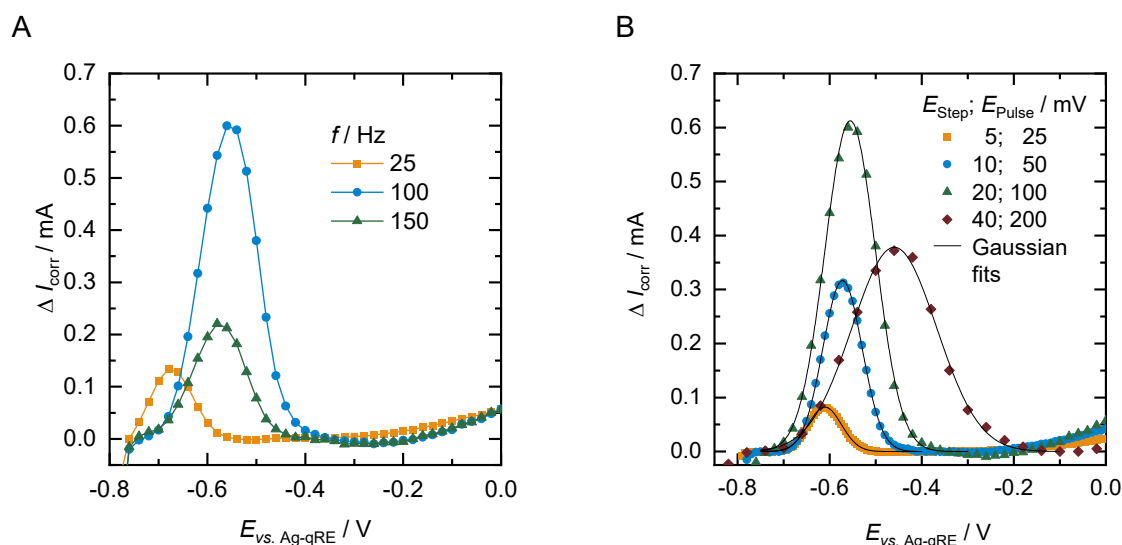


Figure 24: Baseline corrected SWV current response curves (ΔI_{corr}) of Pb^{2+} detection in water saturated [HBet][NTf₂] with constant $c_{\text{aq,ini}}(\text{Pb}^{2+})=100$ ppm and $E_{\text{Dep}}=-0.8$ V vs. Ag-qRE for 300 s at room temperature. A: Variation of the frequency f with E_{Step} and E_{Pulse} of 20 and 100 mV. Coloured lines for optical guidance. B: Variation of E_{Step} and E_{Pulse} at constant $f=100$ Hz. Note: stripping in this experiment -0.9 V vs. Ag-qRE for “40; 200” Data baseline corrected. Black lines represent gaussian fits.

To identify more suitable parameters for the IL as electrolyte, first, the influence of the frequency at fixed E_{Step} and E_{Pulse} of 20 and 100 mV was studied. Figure 24 A shows the strong influence and improvement and that a maximum peak height results for $f=100$ Hz. For aqueous electrolytes, an increasing and broadening of stripping peaks from 5 to 50 Hz was already described.^[18] The reduction of peak height for higher f in this study is unclear. Subsequently, the potential width for E_{Step} and E_{Pulse} were varied. Figure 24 B shows that lowering E_{Step} and E_{Pulse} increases the data point density within the peak strongly. Nevertheless, the intensity is reduced in parallel and sensitivity is lowered. Increasing both potentials results in a maximum peak current for $E_{\text{Step}}=20$ and $E_{\text{Pulse}}=100$ mV, which reduces with higher potentials again as also a leads to broadening of the peak and further reduced data point density.

This behaviour might be explained by the redox processes of the analyte species (Pb^{2+} and Pb) at the electrode surface. A high E_{Pulse} covers a larger portion of the potential range, determined by the scan rate ($E_{\text{Step}} \cdot f$) and that leads to re-oxidation but is reported at a lower potential in the response curve within the plot. In combination with a suitable f and E_{Step} this potential range is scanned often, taking advantage of this method of re-oxidation and re-reduction. For high sensitivities, high peak currents are desired. A widening of the peak might intensify interference with stripping signals of other metal ions. For the simultaneous detection of several analytes high E_{Step} and E_{Pulse} can hence be problematic. In this approach, however, potential metal ion interference shall be reduced by the ideally selective analyte extraction step prior to the detection.

The identified parameters result in intensive peak heights but relatively sparse data. E.g. in the stripping process from -1 to +0.2 mV vs. Ag-qRE the data density in total is reduced to 61 $\Delta I(F-R)$ -values, while only approximately 15 data points build the Pb stripping peak. Especially for lower concentrations, and hence smaller peaks, identifying the maximum peak current accurately could thus be challenging. Fitting the peaks, offers an elegant way to still extract a solid peak height value as raw data and fitted peaks (black lines) given in Figure 24 B demonstrate.

As suitable stripping parameters, $E_{\text{Step}}=20$ mV, $E_{\text{Pulse}}=100$ mV and $f=100$ Hz, were set for following experiments. However, besides the electrolyte also changes in the electrode material the seems to influence the optimum of the settings, as addressed in chapter 5.4.3.

Deposition Time and Electrode Surface Area

In addition to the stripping parameters, also an investigation of the deposition time t_{dep} and the accessible geometrical surface area A_{geo} of the working electrode was conducted. Within the preceding deposition step, Pb^{2+} is reduced and Pb^0 accumulates on the electrode surface, increasing the amount of detectable analyte for detection during the stripping step. Thus, through the accumulation time t_{dep} , the intensity of the current peaks during the SWV stripping step can be increased, as long as a saturation or total depletion can be excluded.

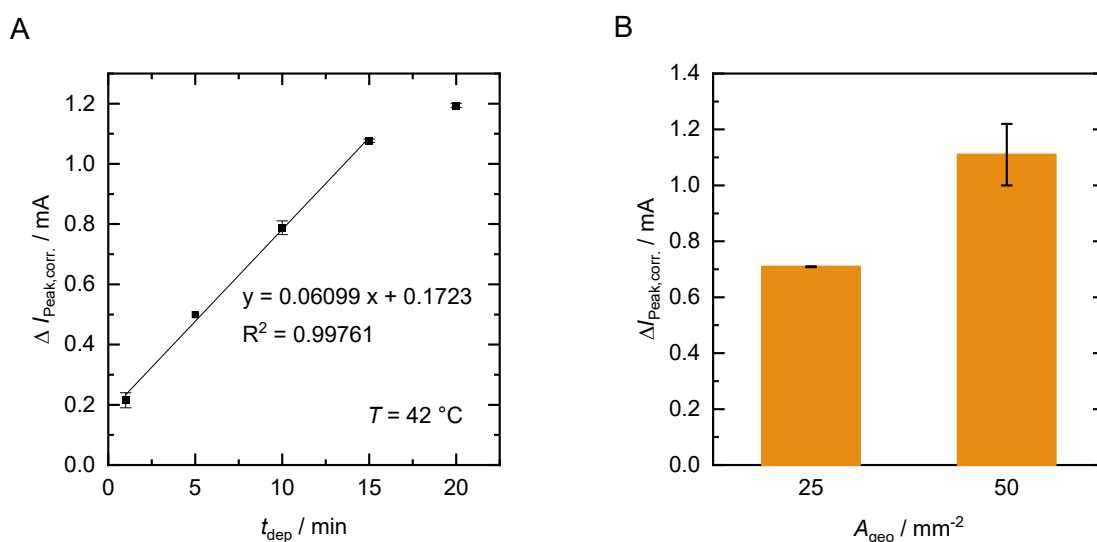


Figure 25: Peak intensities of the SWV current response in Pb^{2+} detection with $E_{\text{dep}}=-1$ V vs Ag-qRE and $c_{\text{aq,ini}}(\text{Pb}^{2+})=10$ ppm as function of (A) the deposition time t_{dep} at $T=42 \text{ }^\circ\text{C}$, ($E_{\text{Step}}=20$ mV, $E_{\text{Pulse}}=100$ mV, $f=100$ Hz) and (B) the accessible geometrical surface area A_{geo} of the working electrode ($E_{\text{Step}}=30$ mV, $E_{\text{Pulse}}=150$ mV, $f=50$ Hz).

Figure 25 A shows the influence variation of the deposition time t_{dep} from 1 min to 20 min at $42 \text{ }^\circ\text{C}$ for $c_{\text{aq,ini}}(\text{Pb}^{2+})=10$ ppm at deposition potentials of $E_{\text{dep}}=-1$ V vs Ag-qRE. As expected, the peak intensity increases with elongation of the deposition time and can be linearly approximated in the range of 1 to 15 min. It is unclear, whether the slight decrease at 20 min

is a first sign for saturation. For most experiments in this work, a t_{dep} of 10 min is set as a compromise of duration of an experiment and stripping peak intensities.

Figure 25 B shows the peak intensities of SWV Pb^{2+} detection in water saturated [HBet][NTf₂] for two different geometrical areas of accessible electrode surface A_{geo} , 25 and 50 mm². The restriction of the area is achieved by application of Kapton[®] adhesive tape. Increasing the surface area of the electrode, that is in direct contact to the analyte containing electrolyte increases the currents of the stripping signal. The increase does not double according to the doubling of the area. This might be attributed to the edges of the electrodes, that restrict the area at three of the four sides. These edges are also in contact to the electrolyte and might be more active for electrodeposition of the analyte as they exhibit edges and corners of graphite, where deposition might take place.^[7]

5.4.2. Temperature Influence on the Sensing Performance

Electrical conductivity is a key factor affecting SWV peak heights.^[21] For the IL employed in this work, the electrical conductivity can be increased by elevating the temperature of the water saturated [HBet][NTf₂] electrolyte (c.f. chapter 5.3.2).

Applying the identified SWV parameter for detection in this IL, the influence on temperature on the electrochemical detection of a constant Pb^{2+} concentration of $c_{\text{aq,ini}}(\text{Pb}^{2+})=5$ ppm was studied. Figure 26 A shows the resulting peak heights. The peak intensities increase linearly with the temperature elevation. Within the temperature range from 27 to 56 °C the intensity is nearly tripled, which can be directly employed to increase the sensitivity. Figure 26 B shows the temperature influence for a broad range of Pb^{2+} concentrations from $c_{\text{aq,ini}}(\text{Pb}^{2+})=1$ to 50 ppm.

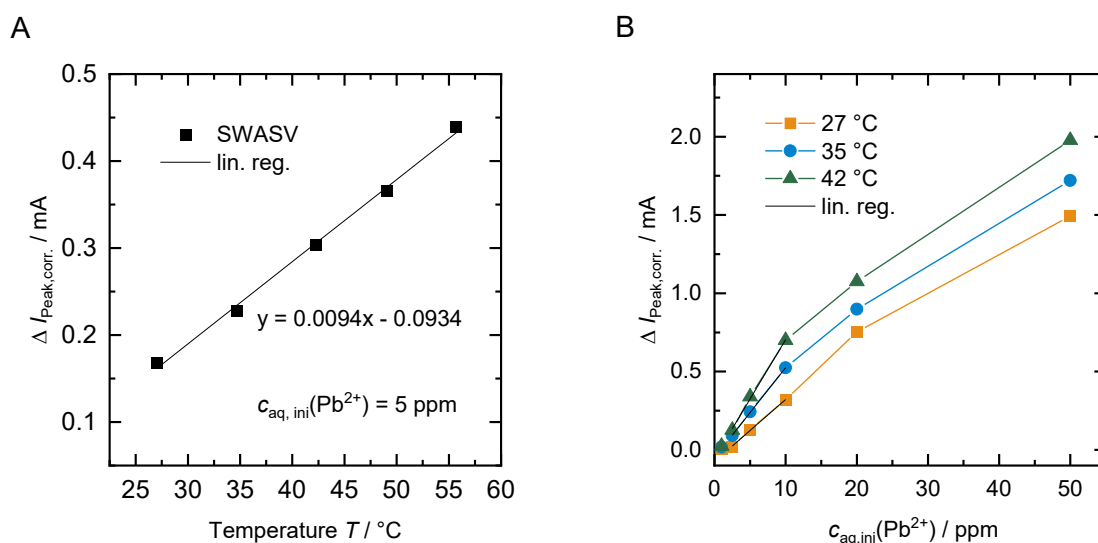


Figure 26: A: Peak intensities of the SWV baseline corrected and Gaussian fitted current response (ΔI_{corr}) as function of the temperature for a fixed concentration of $c_{\text{aq,ini}}(\text{Pb}^{2+})=5$ ppm. B: Variation of $c_{\text{aq,ini}}(\text{Pb}^{2+})$ and the resulting SWV peak intensities at different temperatures. Coloured lines are added for optical guidance; black lines are linear regressions. ($E_{\text{Step}}=20$ mV, $E_{\text{Pulse}}=100$ mV, $f=100$ Hz)

It gets obvious, that a linear range for obtained stripping peak currents to Pb^{2+} concentration in aqueous phase is limited to the lower region with a steeper slope and curves flatten with increasing $c_{aq,ini}(Pb^{2+})$. By fitting the linear range from $c_{aq,ini}(Pb^{2+})=2.5$ to 10 ppm, however, LODs can be derived for the different temperatures utilizing the 3σ -method (Table 12). The temperature does not seem to have an influence on the standard deviation σ . Increasing the temperature by 15 °C thus improves the LOD by a factor of around 2.5 from 2.29 to 0.9 ppm. This demonstrates the potential of employing elevated temperatures when using ILs for electrochemical sensing.

Table 12: Linear regressions for the linear ranges for the variation of $c_{aq,ini}(Pb^{2+})$ at different temperatures and derived limits of detection (LOD) via the 3σ -method.

SWV Temperature	27 °C	35 °C	42 °C
Linear range / ppm	2.5-10	2.5-10	2.5-10
Linear fit equation	$y=0.0397x-0.0745$	$y=0.0575x-0.0496$	$y=0.0759x-0.0542$
R^2	0.9985	0.9997	0.9983
Std. deviation (σ) / mA	0.0055	0.0072	0.0053
3σ / mA	0.0165	0.0216	0.0159
LOD / ppm	2.29	1.24	0.92

For temperatures above 42 °C, the influence of water evaporation was found to be more difficult to handle and reproducibility became problematic. With the improvement in LOD with elevation of temperature, 42 °C was chosen as suitable SWV sensing temperature in this study.

5.4.3. Electrode Modification

For SWV heavy metal ion detection in aqueous phase, promising electrode modifications are presented in literature as discussed in chapter 2.1.2. Here, prominent modifications with Nafion[®] and bismuth, with and without additional carbon materials (carbon black CB and graphite powder GP) shall be investigated for potential application in [HBet][NTf₂] electrolyte for the detection of the model analyte Pb²⁺. The manufacturing procedure and ink compositions of the electrode modifications can be looked up in chapter 4.3.1. For this series of experiments $c_{\text{aq,ini}}(\text{Pb}^{2+})=50$ ppm, $V_{\text{aq,ini}}V_{\text{org,ini}}^{-1}=1$, $E_{\text{dep}}=-1$ V vs. Ag-qRE for $t_{\text{dep}}=120$ s and room temperature are set.

Modification with Nafion[®] and Bismuth

The results of the stepwise modification with Nafion[®] as well as Nafion[®] and bismuth, with and without graphite powder (GP), on the peak intensity are plotted in Figure 27.

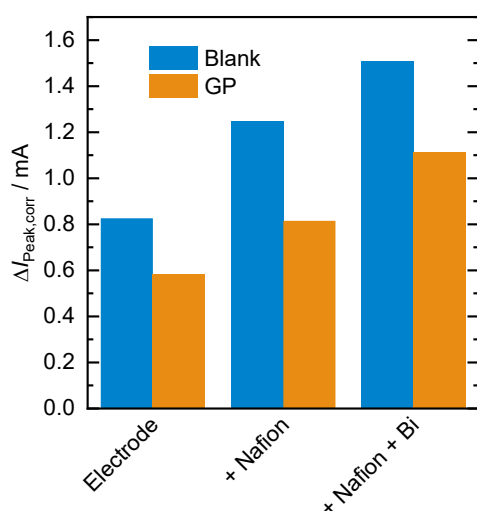


Figure 27: Peak intensities for stepwise modification with Nafion[®] and Bi, with and without graphite powder (GP) for SWV detection of Pb²⁺ in [HBet][NTf₂].
 $c_{\text{aq,ini}}(\text{Pb}^{2+})=50$ ppm, $V_{\text{aq,ini}}V_{\text{org,ini}}^{-1}=1$ $t_{\text{dep}}=120$ s,
 $E_{\text{Step}}=24$ mV, $E_{\text{Pulse}}=120$ mV, $f=120$ Hz, RT.

For blank electrodes, the modification with Nafion[®] increases the stripping peak current ΔI by 51 %. The intensity can further be increased by the addition of bismuth in the ink recipe. The intensities compared to using the blank electrode can in total be increased by 80 %. The same trend can be observed for electrode modifications with GP in the ink. Nafion[®] increases peak height by 41 %. Further addition of bismuth ads 93 % compared to only GP on the electrode. Comparing blank and GP modified electrodes reveals higher intensities for the blank graphite foil without GP for all further modifications. Nonetheless, the trends confirm the improved

sensing performance by the tested modifications. It is concluded that the modification by drop coating an ink containing Nafion[®] and bismuth is most suitable for the SWV detection of Pb²⁺ in water saturated [HBet][NTf₂]. The lower performance of the GP containing modification might be attributed to insufficient electrical contact of the carbon materials to the graphite foil electrode surface. This might cause a reduction of accessible surface area of the electrode as shown in Figure 25 B. For aqueous electrolyte, increased peak intensities are already reported in literature for the electrode modification with Nafion[®] and bismuth by ink drop coating in differential pulse anodic stripping voltammetric Pb²⁺ detection.^[31]

Influence of Carbon Materials

In addition to GP also carbon black (CB) was investigated as part of the modification as it is also applied in published works. In combination with Nafion[®] inverse trends are found for a sensitivity analysis of the stripping parameters E_{Step} , E_{Pulse} and f . Peak intensities for electrodes containing Nafion[®] and CB or GP for SWV Pb²⁺ detection are plotted in Figure 28.

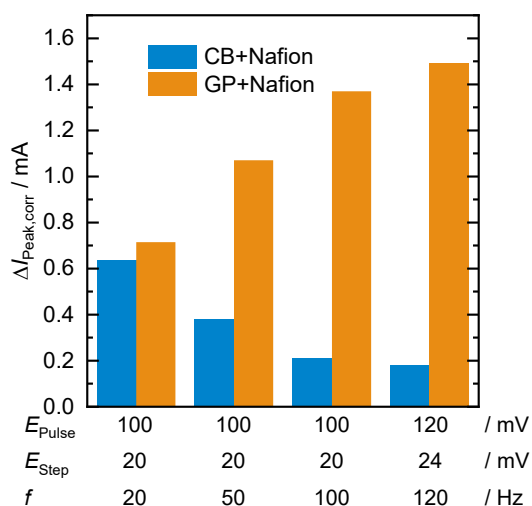


Figure 28: Peak intensities using GP, CB and Nafion[®] modified electrodes with different stripping parameter settings. $c_{aq,ini}(Pb^{2+})=50$ ppm, $V_{aq,ini}V_{org,ini}^{-1}=1$, $E_{dep}=-1$ V vs. Ag-qRE for $t_{dep}=120$ s, RT.

The peak intensities of experiments with GP+Nafion[®] samples increase with the frequency. This is in accordance with the findings presented in chapter 5.4.1. For electrodes drop coated by inks containing CP and Nafion[®] show an inverse trend. With increasing frequency, the according peak intensities decrease, and an optimum is expected for lower frequencies compared to GP electrodes and no addition of a carbon material.

It needs to be noted, that the impedance at 10 kHz, that is attributed to the electrolyte resistance, was notably lower for GP+Nafion[®] in this series experiments, with around

45 Ohms compared to ca. 70 Ohms in other experiments. This leads to the generally higher absolute intensities shown here. The trend in this parameter study, however, should not be affected. It is concluded that not only the nature of the electrolyte, but also the nature of the electrode material influences the optimal SWV parameter settings for Pb^{2+} detection.

Forms of Bismuth Modification

Bismuth added in different forms finally function as a modifier for the metal ion detection on the surface of an electrode. Within the ink, that is later drop coated (ex-situ), bismuth salts ($\text{Bi}(\text{NO}_3)_3 \cdot 5\text{H}_2\text{O}$) can be present in dissolved form or as dispersed solids. $\text{Bi}(\text{NO}_3)_3 \cdot 5\text{H}_2\text{O}$ in this series of experiments was either dissolved in nitric acidic ethanol (HNO_3) or dispersed in ethanol or acetone. A solubility of $\text{Bi}(\text{NO}_3)_3 \cdot 5\text{H}_2\text{O}$ in acetone is reported by the distributor, and could also be optically ascertained.^[124] In addition, the deposition of Bi on the electrode can take place from the electrolyte in the deposition step of the SWV (in-situ), when added to the IL. Resulting peak intensities are shown in Figure 29 for modified electrodes containing Nafion[®] and either CB or GP. The setting for the most intense peaks found in Figure 28 for CB and GP electrodes, respectively, are applied.

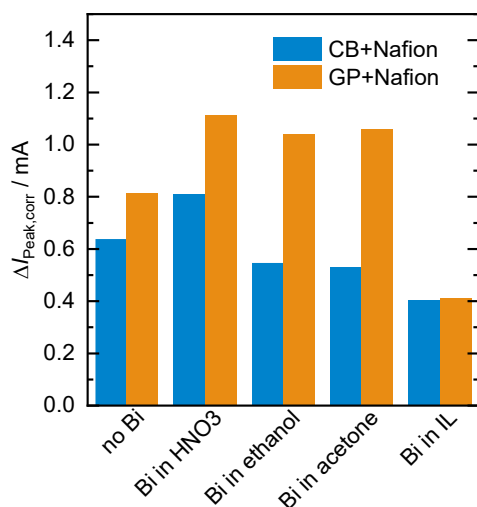


Figure 29: Peak intensities using GP/CB+Nafion modified electrodes with different presentation forms of Bi. $C_{\text{aq,ini}}(\text{Pb}^{2+})=50$ ppm, $V_{\text{aq,ini}}V_{\text{org,ini}}^{-1}=1$, $E_{\text{dep}}=-1$ V vs. Ag-qRE for $t_{\text{dep}}=120$ s, RT, GP: $E_{\text{Step}}=24$ mV, $E_{\text{Pulse}}=120$ mV, $f=120$ Hz, CB: $E_{\text{Step}}=20$ mV, $E_{\text{Pulse}}=100$ mV, $f=20$ Hz, RT.

The stripping peak intensities in SWV Pb^{2+} detection in water saturated $[\text{HBet}][\text{NTf}_2]$ with CB containing electrodes are consistently lower than with the GP electrodes. Similar trends, however, can be drawn for the different Bi presentation forms. The most intense peaks can be found, when Bi is dissolved in nitric acidic ethanol (HNO_3) and applied with the ink via drop coating. The peak heights increase by 27 % (CB) and 37 % (GP) compared to Bi-free

electrodes. The same peak heights are observed for the dispersion/dissolution in ethanol and acetone. While for the CB containing electrode peaks decrease by 14 and 17 %, for GP peaks increase by 28 and 30 % compared to the Bi-free electrodes. It can be concluded that the solvent does play a minor role, though the contribution of Bi increases, when dissolved by the help of an acid. It is likely, that nitric acid evaporates in the drying process. Remaining acid could have an influence of the pH during the electrodeposition and stripping of the analyte. However, this has not been investigated here. In contrast to the other presentation forms, a reduction in peak intensities can be recorded for the in-situ presentation of Bi in the IL electrolyte. For all other forms, the electrode modification with Bi (and Nafion®) via drop coating is found to be beneficial for SWV detection of Pb^{2+} in [HBet][NTf₂]. The addition of a carbon material comprising matrix does not increase peak intensities.

5.4.4. Influence of Extraction Additives on the Sensing Performance

In chapter 5.2.3 it was presented that adding zwitterionic betaine (zw.Bet) to the mixture of water and [HBet][NTf₂] before performing the homogeneous liquid-liquid extraction, increases the concentration of Pb^{2+} in the organic phase (water saturated [HBet][NTf₂]). This evaluation is based on ICP analysis. As this increase is linked to more intense peaks in the subsequent electrochemical detection, the influence of the additive on the SWV remains to be investigated. Therefore, 1, 5, 10 and 20 wt-% zw.Bet were added to the water saturated [HBet][NTf₂] before HLLLE with $V_{aq,ini}V_{org,ini}^{-1}=1$. Resulting peak intensities are plotted in Figure 30, together with the impedance $|Z|$ at 10 kHz, that is assigned to the electrolyte between WE and RE, as well as the pH of the IL phase after extraction.

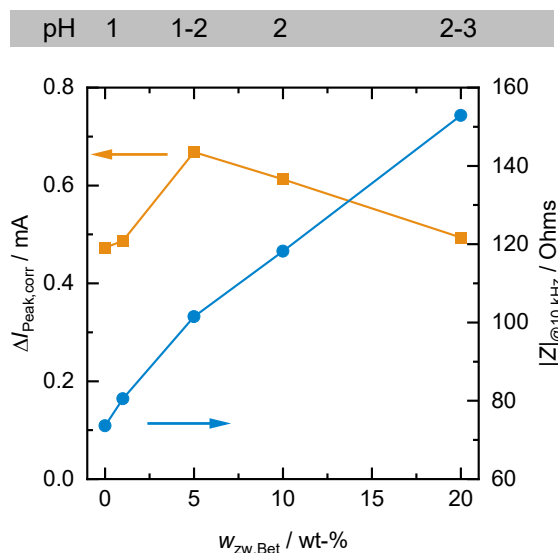


Figure 30: Peak intensities, impedance @10 kHz and pH of water saturated [HBet][NTf₂] after HLLLE in dependence of the addition of zwitterionic betaine. $C_{aq,ini}(Pb^{2+})=10 \text{ ppm}$, $V_{aq,ini}V_{org,ini}^{-1}=1$, $E_{dep}=-1 \text{ V vs. Ag-qRE}$ for $t_{dep}=600 \text{ s}$, $42 \text{ }^\circ\text{C}$, $E_{Step}=30 \text{ mV}$, $E_{Pulse}=150 \text{ mV}$, $f=30 \text{ Hz}$, blank WE.

With increasing mass fractions of zw.Bet peak heights of the SWV (orange squares) follow an optimum curve with a maximum for 5 wt-%. The increase in peak intensity here is +41 %. Further addition of zw.Bet lead to smaller increases of +30 % (10 wt-%) and 4 % (20 wt-%). If the addition of zw.Bet solely increases the concentration of Pb^{2+} in the organic phase, an increase of +150 % compared to additive-free could be expected for 10 and 20 wt-%, based on the increased extraction coefficients. However, the additive will distribute in the phases and hence be also present in the electrolyte. This is supported by the curve progression of the impedance at 10 kHz (blue circles), which in contrast to ΔI increases steadily, doubling from 74 Ohms (no zw.Bet added) to 153 Ohms (20 wt-%). $|Z|_{10\text{ kHz}}$ for 5 wt-% zw.Bet is 102 Ohms. The concentration for this composition is not known.

Beside the decreased conductivity, also the activity of protons in the electrolyte changes (grey textbox above the graph). The pH of the electrolyte increases from 1 (no zw.Bet added) to 2-3 (20 wt-%). At 5 wt-% zw.Bet the pH has slightly increased to 1-2. The same variation was carried out for the similar system, where $[\text{HBet}][\text{NTf}_2]$ was replaced by $[\text{Chol}][\text{NTf}_2]$ with a pH of 4-5. This IL barely shows extraction of Pb^{2+} by HLLC, but concentrations increase by a factor of 24, when 10 wt-% zw.Bet is added (cf. appendix). However, neither of the experiments with $[\text{Chol}][\text{NTf}_2]$ resulted in detectable stripping peaks. Although the SWV parameters have not been adjusted for the application of this electrolyte, it might be concluded, that an increasing pH might impede detectability of Pb^{2+} in the electrolyte.

5.4.5. Limit of Detection

In the preceding studies of the SWV in water saturated $[\text{HBet}][\text{NTf}_2]$, series of experiments were conducted mainly isolated from findings of other studies, in order to reduce complexity of the preparation and reduce sources of error. For the evaluation of the capabilities of the presented proof of concept of HLLC and subsequent SWV in a miniaturized electrochemical cell, findings were combined and a corresponding LOD determined. Therefore, the following parameter were set:

1. The extraction was performed with an initial volume ratio $V_{\text{aq,ini}}V_{\text{org,ini}}^{-1}=5$, instead of 1 as for most experiments. The best result was found at higher ratios, but due to the loss of organic phase, this seemed reasonable with respect to practicability.
2. Zwitterionic betaine was added with a mass fraction of 5 wt-%, based on the mass of the organic phase before HLLC.
3. The WE was modified with Nafion[®] and bismuth that was dissolved in nitric acidic ethanol.
4. The temperature during SWV was set to 42 °C in the electrolyte.
5. The chronoamperometry for electrodeposition was carried out at -1 V vs. Ag-qRE for 600 s (no changes).

6. Stripping parameters were set to $E_{\text{Step}}=30$ mV, $E_{\text{Pulse}}=150$ mV and $f=30$ Hz.

The resulting peak intensities are plotted for different concentrations of Pb^{2+} in the initial aqueous phase $c_{\text{aq,ini}}(\text{Pb}^{2+})$ from 0.1 ppm to 20 ppm in Figure 31.

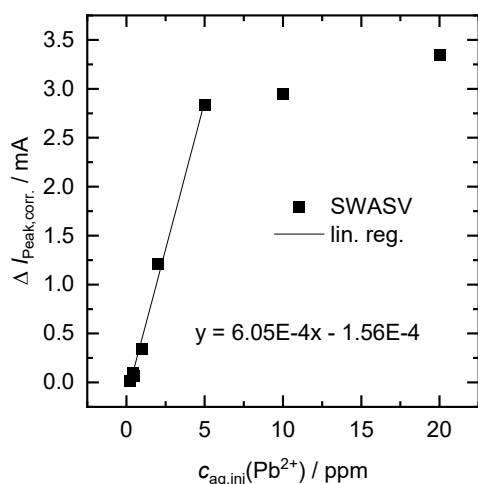


Figure 31: Variation of $c_{\text{aq,ini}}(\text{Pb}^{2+})$ for constant $V_{\text{aq,ini}}V_{\text{org,ini}}^{-1}=5$, 5 wt-% zW,Bet, $E_{\text{dep}}=-1$ V vs. Ag-qRE for $t_{\text{dep}}=600$ s, 42 °C, $E_{\text{Step}}=30$ mV, $E_{\text{Pulse}}=150$ mV, $f=30$ Hz, Nafion® and Bi modified WE.

The progression of the curve flattens with increasing $c_{\text{aq,ini}}(\text{Pb}^{2+})$, with a stronger change around 5 ppm. A concentration of 10 ppm in this series of experiments results in a peak intensity of $3 \mu\text{A}$. Without any electrode modification and an initial volume ratio $V_{\text{aq,ini}}V_{\text{org,ini}}^{-1}=1$ and identical settings for the remaining parameters, the peak intensity is $0.67 \mu\text{A}$ (cf. Figure 30). This equates to an increase by a factor of 4.5 in peak intensity. For the linear range of concentrations $c_{\text{aq,ini}}(\text{Pb}^{2+}) \leq 5$ ppm peak intensities are linearly fitted (black line). Combined with the standard deviation σ of $8.44 \mu\text{A}$ for samples with a Pb^{2+} concentration of 0, a LOD of 0.03 ppm (30 ppb) can be calculated according to the 3σ -method. Compared to the LOD with pristine graphite foil, no additive and $V_{\text{aq,ini}}V_{\text{org,ini}}^{-1}=1$ in chapter 5.4.2, 76 times lower concentrations can be detected. However, an improvement of at least one magnitude of order lower LOD remains to be achieved in order to meet WHO recommendations.

5.4.6. Integration of a Paper Channel

The feasibility of a combined temperature induced extraction and subsequent electrochemical detection and the possibilities of improvements by various techniques have been discussed in the previous chapters. In the following, the feasibility of the introduction of a paper channel shall be studied, towards the development of an integrated microfluidic sensing device. Besides the microfluidic properties added by the porous material, it also functions as a spacer between the electrodes. This miniaturization lowers the electrode distances and reduces the required electrolyte volume.

Selection of the Paper Material

The paper material was selected based on the flow velocity of water saturated [HBet][NTf₂] in a horizontal configuration. Figure 32 shows the distances of different paper materials, with and without glass fibres, covered after different time stamps. These experiments were conducted by Tizian Venter at the Laboratory of Macromolecular and Paper Chemistry, Ernst-Berl-Institut, Department of Chemistry, TU Darmstadt.

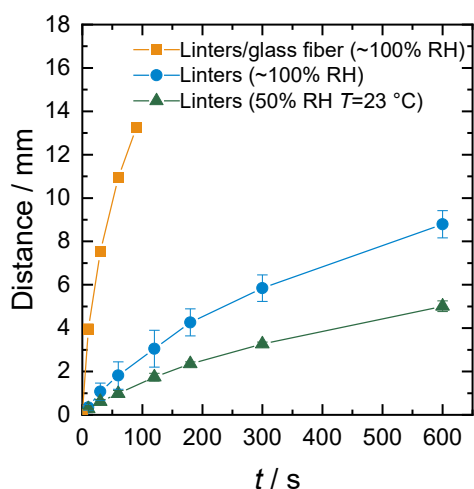


Figure 32: Flow velocities for water sat. [HBet][NTf₂] in paper sheets of different fibres (horizontal configuration) and at different conditions (RH=relative humidity).

All plotted curves flatten with increasing time. This shape complies with the square root function of the Lucas-Washburn equation (Equation 13). The decrease in flow velocity could furthermore be intensified by the loss of water in the IL over time, increasing its viscosity. The effect can be mitigated by increasing the relative humidity (RH), supporting this assumption. In comparison to paper materials without glass fibre, here the flow was found to be significantly faster. Water saturated [HBet][NTf₂] covers a distance of 1 cm in about 1 min in

linters/glass fibre, whereas without the addition of glass fibres, this distance couldn't be covered in over 10 min.

Lead Detection in Channel Cells

As paper material for electrochemical channel cells, a mixture of eucalyptus and glass fibres was used (ca. 100 μm thickness). It was placed in a 3D arrangement between WE and CE/RE. Unmodified graphite foil was used as WE. The homogeneous liquid-liquid extraction was performed with $c_{\text{aq,ini}}(\text{Pb}^{2+}) = 10$ ppm and $V_{\text{aq,ini}}V_{\text{org,ini}}^{-1} = 1$, without the addition of zwitterionic betaine. For reasons of handling and avoidance of short circuit currents, a 3D printed spacer with a thickness of 1 mm and 200 μm pores in every direction, was also included in this study, in parallel to the paper channel experiments. The configurations and settings for this series of experiments are listed in Table 13. Alongside, data of the bulk cell experiments that are utilized and discussed the previous chapters, are given for comparison.

Table 13: Configurations and settings for comparison of bulk and channel cells. *) Distance between WE and RE. Data, that deviate in the according row is highlighted in bold font.

Parameter	Bulk cell		Channel cell	
	42 °C	optimized	3D printed	Paper
Electrolyte volume / mL	0.5	0.5	0.25	0.1
Electrode distance* / mm	2	2	1	0.1
WE A_{geo} / cm^2	0.5	0.5	1	1
WE modification	-	Nafion® + Bi	-	-
$V_{\text{aq,ini}}V_{\text{org,ini}}^{-1}$	1	5	1	1
Extraction additive	-	5 wt-% zw.Bet	-	-
RE	Ag wire	Ag wire	Ag wire	Graphite foil
T / °C	42	42	RT	RT
E_{dep} / V vs. Ag-qRE	-1	-1	-1	-1
t_{dep} / s	600	600	600	60
E_{Step} / V	20	30	100	100
E_{Pulse} / V	100	150	20	20
f / Hz	100	30	100	100
Electrolyte flow	-	-	-	-

Initially, experiments were conducted without electrolyte flow. The Pb^{2+} containing, water saturated [HBet][NTf₂] was pipetted onto the channel material after HLL. The SWV procedure was started, when electrolyte was fully imbibed into the channel material.

Obtained current response curves are plotted in Figure 33 A. In both curves from cells, featuring a 3D printed channel or a paper channel, a Pb^{2+} stripping peak is observable, seemingly being superimposed by a change in current. Compared to the 3D printed channel (orange) and also bulk cell experiments, the position of the peak in the paper cell (blue) is shifted to less negative potentials. This might be caused by the different RE utilized here (Ag wire vs. graphite foil). However, curves can be baseline-corrected (black lines) and peak intensities of 30 mA can be determined. Due to the unsymmetrical peak shape, the peaks were not fitted and the value at maximum peak height was chosen.

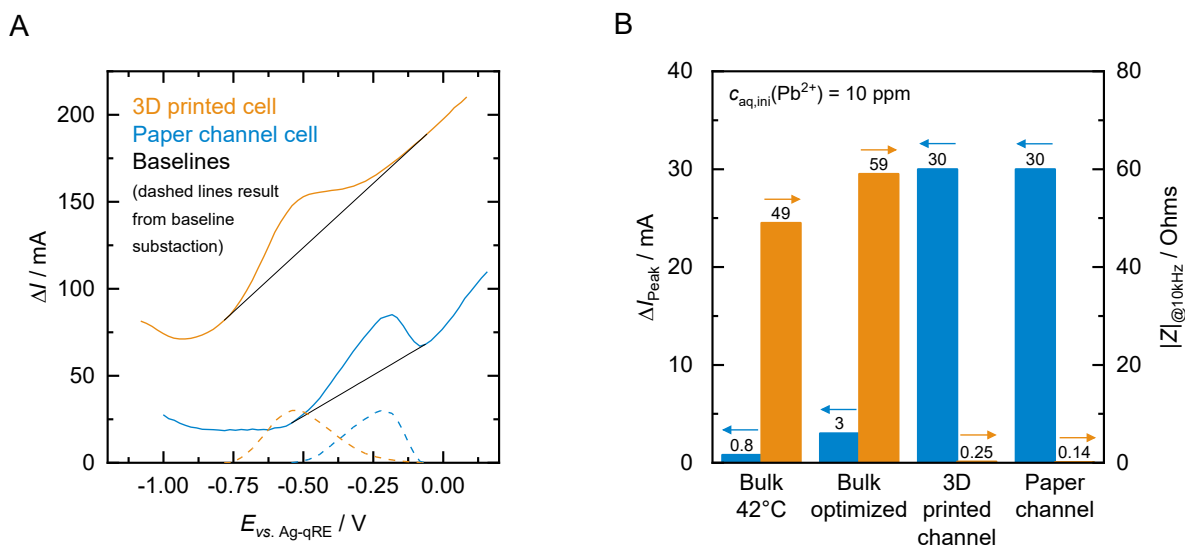


Figure 33: A: SWV current response curves for a 3D printed channel (1 mm thickness, orange) and a paper channel (eucalyptus/glass fibres, ca. 100 μm , blue), without (lines) and with (dashed) baseline correction for $c_{\text{aq,ini}}(\text{Pb}^{2+})=10 \text{ ppm}$, $V_{\text{aq,ini}}V_{\text{org,ini}}^{-1}=1$, RT and unmodified electrodes. B: Comparison of peak intensities (blue bars, left axis) and impedance at 10 kHz (orange bars, right axis) of the channel cells and results of the bulk cell. Note: SWV parameters as well as cell parameters are not identical.

The extracted peak intensities (blue bars) as well as the impedance at 10 kHz (unfilled bars) using the IL electrolyte and the new cells are plotted in Figure 33 B together with results from bulk cell experiments. It needs to be noted, that cell parameters as well as measuring parameters differ between the experiments leading to the shown values. Compared to the bulk cell optimized parameters (cf. Table 13), both paper channels show higher peak intensities and lower resistances. Peak intensities are one order of magnitude higher, impedances two magnitudes of order lower. The stripping peak in the paper channel cell was recorded after 60 s of deposition time. All other deposition times have 10 times longer duration. For 600 s, consequently, higher peak intensities can be assumed.

The lowered ohmic losses are a consequence of the change in cell parameters. In addition to the increased A_{geo} in the channel cells, also the electrode distances are reduced. The increased surface area by itself does not explain the higher peak intensities, as concluded from Figure 25 B. This demonstrates the advantage of the miniaturization by the introduction of a

channel, reducing the electrode distance and a higher A_{geo} , while still reducing the required electrolyte volume.

The higher peak intensity is supposed to be an indicator for high sensitivities, however, low LODs are achieved, when the peak intensity does change with a small incline for lower concentrations. The slope is not extractable from this data and thus an LOD cannot be determined for the paper channel cell. It needs to be stated, that only the results of two experiments conducted with channel cells are presented here. Most of the experiments in this context failed due to overloads of the potentiostat's amplifier. As found later, at least some of these forced automatic abortions might have been caused by malfunction of the hardware. Although, flow velocities could be increased by the addition of glass fibres, SWV experiments with electrolyte flow remain to be investigated. Despite, based on the shown data, the feasibility of the introduction of a paper channel for the electrochemical detection of Pb^{2+} in water saturated [HBet][NTf₂] could be demonstrated and promises a strong improvement of this approach.

6. Summary

Within this work, a proof of principle was demonstrated. The same thermomorphic IL, [HBet][NTf₂] could successfully be employed for analyte extraction and electrolyte in subsequent electrochemical detection. The model analyte Pb²⁺ could be extracted from the spiked aqueous phase via temperature induced single phase generation and separation, exploiting the upper critical solution temperature for homogeneous liquid-liquid extraction. The concentration of Pb²⁺ in the extractor was monitored via ICP-OES. It could be enriched by increasing the initial volume ratio of water to IL and the addition of zwitterionic betaine to the mixture.

Electrolyte Properties of [HBet][NTf₂]

Water saturated [HBet][NTf₂] was compared to other ILs and exhibits the lowest pH, due to the carboxylic functional group. Despite the relatively high water uptake compared to other ILs, water saturated [HBet][NTf₂] keeps its hydrophobicity and forms a two-phase system with water at room temperature. Moreover, the contact to water is necessary to allow for a stable liquid state of the (water saturated) IL. In this wet state the electrical conductivity is comparably high and the viscosity comparably low. Constructing the Walden plot for RT water saturated [HBet][NTf₂] reveals 'poor' to 'good' electrolyte qualities according to Angell's classification. This was possible by determination of the temperature dependent density, viscosity, electrical conductivity, and fitting of the Vogel-Fulcher-Tammann equation and allows for comparison with other electrolytes. The validity of the measurements was ensured by literature comparison of [BMIm][NTf₂], measured alongside.

Electrochemical Detection

The electrochemical detection of Pb²⁺ in water saturated [HBet][NTf₂] was performed by square wave anodic stripping voltammetry. Method parameters were therefore adapted from aqueous phase settings. Increasing the frequency, as well as pulse and step potential lead to higher peak intensities. This allows for easier detection of a single analyte, though widens the peak, and reduces the data density. If the analyte is selectively accumulated by the preceding extraction step, the interference with other stripping signals by the widened peak shapes can assumably be circumvented. Gaussian fitting of the data was carried out for compensating sparse data density. Three approaches were tested for increasing peak intensity and lowering the LOD in the bulk cell: temperature increase (1.), electrode modification (2.), and addition (3.) of an extracting agent.

1. As expected by the behaviour of physico-chemical properties, increasing the temperature facilitates SWV detection and reduces the limit of detection. Operating at elevated temperature as also an increase of the water content was found to be key for reducing the solution resistance in bulk cell experiments. Together with the temperature dependent

liquid-liquid extraction, temperature control is thus of major importance within the presented approach.

2. Well documented modifications of the sensing electrodes by drop coating inks, containing Nafion[®] and bismuth, further increase the peak intensities and are easy to fabricate. It was also found, that changing the carbon material might entail another assessment of the SWV parameter settings, as trends run counter in the sensitivity analysis.
3. The addition of zwitterionic betaine to the extraction mixture increases the analyte concentration in the electrolyte. At the same time, the electrolyte's electrical resistance increases. Parallely, an increase in pH is observed. After passing a peak intensity maximum, intensities decrease again with increasing mass fractions of the additive. Adding the extracting agent is hence beneficial, however, this benefit is limited.

Combining these three approaches, $T_{\text{SWV}}=42\text{ °C}$, Nafion[®]/Bi modified electrodes, addition of 5 wt-% zwitterionic betaine, with a higher initial volume ratio, allows for a LOD of 30 ppb. This is about one order of magnitude above WHO recommendations, though demonstrates the feasibility of combining HLL and SWV by [HBet][NTf₂] and reveals parameters for adjusting the sensitivity.

Paper Channel Electrochemical Cell

Finally, the electrochemical detection of Pb²⁺ after its extraction with [HBet][NTf₂] was transferred to a 3D paper channel cell design. Although no efforts were undertaken to modify the electrodes or to increase the analyte concentration, observed peak heights in the channel cell outperform bulk cell experiments. The miniaturized dimensions of the channel cell, due to the small thickness of the paper material, reduces the required amount of electrolyte and reduces the electrode distances and thereby the ohmic losses. Only a limited number of results could be generated from this series of experiments, however, they clearly indicate the potential of the introduction of a paper channel.

Outlook

To fully assess the capabilities of the combined extraction and electrochemical detection by the thermomorphic IL using a paper channel cell, the limit of detection as well as the selectivity towards the analyte are yet to be determined. Therefore, a reliable test set-up for paper channel cells needs to be realized. This series of experiments could combine extraction with a high volume ratio of aqueous phase (5-8 $V_{\text{org,ini}}$), addition of zwitterionic betaine (~5 wt-%), SWV at elevated temperatures (42 °C) and Nafion[®]/Bi-modified electrodes. Additionally, the phase behaviour at the changed conditions as well as SWV parameters in this new set-up might need to be re-examined.

7. References

- [1] World Health Organization (WHO). 10 chemicals of public health concern. <https://www.who.int/news-room/photo-story/photo-story-detail/10-chemicals-of-public-health-concern> (accessed February 13, 2023).
- [2] Publications Office. DIRECTIVE (EU) 2020/2184 OF THE EUROPEAN PARLIAMENT AND OF THE COUNCIL: of 16 December 2020 on the quality of water intended for human consumption (recast). *Official Journal of the European Union* **2020**.
- [3] Jenkins, S. H. Standard Methods for the Examination of Water and Wastewater. *Water Research* **1982**, *16*, 1495–1496. DOI: 10.1016/0043-1354(82)90249-4.
- [4] Pujol, L.; Evrard, D.; Groenen-Serrano, K.; Freyssinier, M.; Ruffien-Cizsak, A.; Gros, P. Electrochemical sensors and devices for heavy metals assay in water: the French groups' contribution. *Frontiers in chemistry* **2014**, *2*, 19. DOI: 10.3389/fchem.2014.00019.
- [5] Osteryoung, J. G.; Osteryoung, R. A. Square wave voltammetry. *Anal. Chem.* **1985**, *57*, 101–110. DOI: 10.1021/ac00279a004.
- [6] Da Róz, A. L.; Ferreira, M.; Leite, F. d. L.; Oliveira, O. N., Eds. *Nanoscience and its applications*; William Andrew: Kidlington, 2017.
- [7] Shen, L.-L.; Zhang, G.-R.; Li, W.; Biesalski, M.; Etzold, B. J. M. Modifier-Free Microfluidic Electrochemical Sensor for Heavy-Metal Detection. *ACS omega* **2017**, *2*, 4593–4603. DOI: 10.1021/acsomega.7b00611.
- [8] Shen, L.-L.; Zhang, G.-R.; Etzold, B. J. M. Paper-Based Microfluidics for Electrochemical Applications. *ChemElectroChem* **2020**, *7*, 10–30. DOI: 10.1002/celec.201901495.
- [9] Nie, Z.; Nijhuis, C. A.; Gong, J.; Chen, X.; Kumachev, A.; Martinez, A. W.; Narovlyansky, M.; Whitesides, G. M. Electrochemical sensing in paper-based microfluidic devices. *Lab on a chip* **2010**, *10*, 477–483. DOI: 10.1039/b917150a.
- [10] Baranwal, J.; Barse, B.; Gatto, G.; Broncova, G.; Kumar, A. Electrochemical Sensors and Their Applications: A Review. *Chemosensors* **2022**, *10*, 363. DOI: 10.3390/chemosensors10090363.
- [11] Gründler, P. *Chemical sensors: An introduction for scientists and engineers ; with 25 tables*; Springer: Berlin, Heidelberg, 2007.
- [12] World Health Organization (WHO). The public health impact of chemicals: knowns and unknowns - data addendum for 2019. <https://www.who.int/publications/i/item/WHO-HEP-ECH-EHD-21.01> (accessed April 28, 2023).
- [13] World Health Organization (WHO). Lead poisoning. <https://www.who.int/news-room/fact-sheets/detail/lead-poisoning-and-health> (accessed April 28, 2023).
- [14] Borrill, A. J.; Reily, N. E.; Macpherson, J. V. Addressing the practicalities of anodic stripping voltammetry for heavy metal detection: a tutorial review. *The Analyst* **2019**, *144*, 6834–6849. DOI: 10.1039/c9an01437c.
- [15] Haynes, W. M. *CRC handbook of chemistry and physics*, 95th ed.; CRC Press, an imprint of Taylor and Francis: Boca Raton, FL, 2014.
- [16] Bard, A. J.; Faulkner, L. R. *Electrochemical methods: Fundamentals and applications*, 2. edition; Wiley: New York, Weinheim, 2001.

-
- [17] Bansod, B.; Kumar, T.; Thakur, R.; Rana, S.; Singh, I. A review on various electrochemical techniques for heavy metal ions detection with different sensing platforms. *Biosensors & bioelectronics* **2017**, *94*, 443–455. DOI: 10.1016/j.bios.2017.03.031.
- [18] José Triviño, J. Voltammetric method for the determination of Pb²⁺ and Cd²⁺ in water samples using a nafion–guanine-coated mercury film electrode. *Int. J. Electrochem. Sci.* **2022**, ArticleID:220762. DOI: 10.20964/2022.07.71.
- [19] Lu, D.; Shomali, N.; Shen, A. Task specific ionic liquid for direct electrochemistry of metal oxides. *Electrochemistry Communications* **2010**, *12*, 1214–1217. DOI: 10.1016/j.elecom.2010.06.022.
- [20] Pandey, S. K.; Sachan, S.; Singh, S. K. Ultra-trace sensing of cadmium and lead by square wave anodic stripping voltammetry using ionic liquid modified graphene oxide. *Materials Science for Energy Technologies* **2019**, *2*, 667–675. DOI: 10.1016/j.mset.2019.09.004.
- [21] Rahm, C. E.; Gupta, P.; Gupta, V. K.; Huseinov, A.; Griesmer, B.; Alvarez, N. T. Impact of physical and chemical parameters on square wave anodic stripping voltammetry for trace Pb²⁺ detection in water. *The Analyst* **2022**, *147*, 3542–3557. DOI: 10.1039/d2an00724j.
- [22] Liu, N.; Zhao, G.; Liu, G. Coupling Square Wave Anodic Stripping Voltammetry with Support Vector Regression to Detect the Concentration of Lead in Soil under the Interference of Copper Accurately. *Sensors (Basel, Switzerland)* **2020**, *20*. DOI: 10.3390/s20236792.
- [23] Tan, Z.; Wu, W.; Feng, C.; Wu, H.; Zhang, Z. Simultaneous determination of heavy metals by an electrochemical method based on a nanocomposite consisting of fluorinated graphene and gold nanocage. *Mikrochimica acta* **2020**, *187*, 414. DOI: 10.1007/s00604-020-04393-6.
- [24] Shi, J.; Tang, F.; Xing, H.; Zheng, H.; Lianhua, B.; Wei, W. Electrochemical detection of Pb and Cd in paper-based microfluidic devices. *J. Braz. Chem. Soc.* **2012**, *23*, 1124–1130. DOI: 10.1590/S0103-50532012000600018.
- [25] Jovanovski, V.; Hočvar, S. B.; Ogorevc, B. Bismuth electrodes in contemporary electroanalysis. *Current Opinion in Electrochemistry* **2017**, *3*, 114–122. DOI: 10.1016/j.coelec.2017.07.008.
- [26] Wang, J. Stripping Analysis at Bismuth Electrodes: A Review. *Electroanalysis* **2005**, *17*, 1341–1346. DOI: 10.1002/elan.200403270.
- [27] Švancara, I.; Prior, C.; Hočvar, S. B.; Wang, J. A Decade with Bismuth-Based Electrodes in Electroanalysis. *Electroanalysis* **2010**, *22*, 1405–1420. DOI: 10.1002/elan.200970017.
- [28] Gao, W.; Nyein, H. Y. Y.; Shahpar, Z.; Fahad, H. M.; Chen, K.; Emaminejad, S.; Gao, Y.; Tai, L.-C.; Ota, H.; Wu, E.; *et al.* Wearable Microsensor Array for Multiplexed Heavy Metal Monitoring of Body Fluids. *ACS Sens.* **2016**, *1*, 866–874. DOI: 10.1021/acssensors.6b00287.
- [29] Fu, L.; Li, X.; Yu, J.; Ye, J. Facile and Simultaneous Stripping Determination of Zinc, Cadmium and Lead on Disposable Multiwalled Carbon Nanotubes Modified Screen-Printed Electrode. *Electroanalysis* **2013**, *25*, 567–572. DOI: 10.1002/elan.201200248.
- [30] Huangfu, C.; Fu, L.; Li, Y.; Li, X.; Du, H.; Ye, J. Sensitive Stripping Determination of Cadmium(II) and Lead(II) on Disposable Graphene Modified Screen-Printed Electrode. *Electroanalysis* **2013**, *25*, 2238–2243. DOI: 10.1002/elan.201300239.

- [31] Xie, R.; Zhou, L.; Lan, C.; Fan, F.; Xie, R.; Tan, H.; Xie, T.; Zhao, L. Nanostructured carbon black for simultaneous electrochemical determination of trace lead and cadmium by differential pulse stripping voltammetry. *Royal Society open science* **2018**, *5*, 180282. DOI: 10.1098/rsos.180282.
- [32] Chaiyo, S.; Mehmeti, E.; Žagar, K.; Siangproh, W.; Chailapakul, O.; Kalcher, K. Electrochemical sensors for the simultaneous determination of zinc, cadmium and lead using a Nafion/ionic liquid/graphene composite modified screen-printed carbon electrode. *Analytica Chimica Acta* **2016**, *918*, 26–34. DOI: 10.1016/j.aca.2016.03.026.
- [33] Foster, C. W.; Souza, A. P. de; Metters, J. P.; Bertotti, M.; Banks, C. E. Metallic modified (bismuth, antimony, tin and combinations thereof) film carbon electrodes. *The Analyst* **2015**, *140*, 7598–7612. DOI: 10.1039/c5an01692d.
- [34] María-Hormigos, R.; Gismera, M. J.; Procopio, J. R.; Sevilla, M. T. Disposable screen-printed electrode modified with bismuth–PSS composites as high sensitive sensor for cadmium and lead determination. *Journal of Electroanalytical Chemistry* **2016**, *767*, 114–122. DOI: 10.1016/j.jelechem.2016.02.025.
- [35] Kefala, G.; Economou, A.; Voulgaropoulos, A. A study of Nafion-coated bismuth-film electrodes for the determination of trace metals by anodic stripping voltammetry. *The Analyst* **2004**, *129*, 1082–1090. DOI: 10.1039/b404978k.
- [36] Tang, X.; Wang, P.-Y.; Buchter, G. Ion-Selective Electrodes for Detection of Lead (II) in Drinking Water: A Mini-Review. *Environments* **2018**, *5*, 95. DOI: 10.3390/environments5090095.
- [37] Guziński, M.; Lisak, G.; Kupis, J.; Jasiński, A.; Bocheńska, M. Lead(II)-selective ionophores for ion-selective electrodes: a review. *Analytica Chimica Acta* **2013**, *791*, 1–12. DOI: 10.1016/j.aca.2013.04.044.
- [38] Alshawi, J. M. S.; Mohammed, M. Q.; Alesary, H. F.; Ismail, H. K.; Barton, S. Voltammetric Determination of Hg²⁺, Zn²⁺, and Pb²⁺ Ions Using a PEDOT/NTA-Modified Electrode. *ACS omega* **2022**, *7*, 20405–20419. DOI: 10.1021/acsomega.2c02682.
- [39] Herrero, E.; Arancibia, V.; Rojas–Romo, C. Simultaneous determination of Pb²⁺, Cd²⁺ and Zn²⁺ by adsorptive stripping voltammetry using Clioquinol as a chelating-adsorbent agent. *Journal of Electroanalytical Chemistry* **2014**, *729*, 9–14. DOI: 10.1016/j.jelechem.2014.06.039.
- [40] Zhou, N.; Li, J.; Chen, H.; Liao, C.; Chen, L. A functional graphene oxide-ionic liquid composites-gold nanoparticle sensing platform for ultrasensitive electrochemical detection of Hg²⁺. *The Analyst* **2013**, *138*, 1091–1097. DOI: 10.1039/c2an36405k.
- [41] Xuan, X.; Hossain, M. F.; Park, J. Y. A Fully Integrated and Miniaturized Heavy-metal-detection Sensor Based on Micro-patterned Reduced Graphene Oxide. *Scientific reports* **2016**, *6*, 33125. DOI: 10.1038/srep33125.
- [42] Plechkova, N. V.; Seddon, K. R. Applications of ionic liquids in the chemical industry. *Chemical Society reviews* **2008**, *37*, 123–150. DOI: 10.1039/b006677j.
- [43] Boeck, G. Paul Walden (1863–1957): the man behind the Walden inversion, the Walden rule, the Ostwald-Walden-Bredig rule and Ionic liquids. *ChemTexts* **2019**, *5*. DOI: 10.1007/s40828-019-0080-9.
- [44] Koel, M. *Ionic Liquids in Chemical Analysis*; CRC Press, 2008.
- [45] Walden, P. Ueber die Molekulargroesse und elektrische Leitfaehigkeit einiger geschmolzenen Salze. *Bulletin de l'Académie Impériale des Sciences de St.-Petersbourg* **1914**, *8*, 405–422.

- [46] Werner, S.; Haumann, M.; Wasserscheid, P. Ionic liquids in chemical engineering. *Annual review of chemical and biomolecular engineering* **2010**, *1*, 203–230. DOI: 10.1146/annurev-chembioeng-073009-100915.
- [47] Earle, M. J.; Seddon, K. R. Ionic liquids. Green solvents for the future. *Pure and Applied Chemistry* **2000**, *72*, 1391–1398. DOI: 10.1351/pac200072071391.
- [48] Earle, M. J.; Esperança, J. M. S. S.; Gilea, M. A.; Lopes, J. N. C.; Rebelo, L. P. N.; Magee, J. W.; Seddon, K. R.; Widegren, J. A. The distillation and volatility of ionic liquids. *Nature* **2006**, *439*, 831–834. DOI: 10.1038/nature04451.
- [49] Wasserscheid, P. Volatile times for ionic liquids. *Nature* **2006**, 797.
- [50] Galiński, M.; Lewandowski, A.; Stepniak, I. Ionic liquids as electrolytes. *Electrochimica Acta* **2006**, *51*, 5567–5580. DOI: 10.1016/j.electacta.2006.03.016.
- [51] Welton, T. Room-Temperature Ionic Liquids. Solvents for Synthesis and Catalysis. *Chemical reviews* **1999**, *99*, 2071–2084. DOI: 10.1021/cr980032t.
- [52] Seddon, K. R.; Stark, A.; Torres, M.-J. Influence of chloride, water, and organic solvents on the physical properties of ionic liquids. *Pure and Applied Chemistry* **2000**, *72*, 2275–2287. DOI: 10.1351/pac200072122275.
- [53] Andanson, J.-M.; Meng, X.; Traïkia, M.; Husson, P. Quantification of the impact of water as an impurity on standard physico-chemical properties of ionic liquids. *The Journal of Chemical Thermodynamics* **2016**, *94*, 169–176. DOI: 10.1016/j.jct.2015.11.008.
- [54] Dobliger, S.; Donati, T. J.; Silvester, D. S. Effect of Humidity and Impurities on the Electrochemical Window of Ionic Liquids and Its Implications for Electroanalysis. *J. Phys. Chem. C* **2020**, *124*, 20309–20319. DOI: 10.1021/acs.jpcc.0c07012.
- [55] Jacquemin, J.; Husson, P.; Padua, A. A. H.; Majer, V. Density and viscosity of several pure and water-saturated ionic liquids. *Green Chem* **2006**, *8*, 172–180. DOI: 10.1039/B513231B.
- [56] Silvester, D. S.; Compton, R. G. Electrochemistry in Room Temperature Ionic Liquids: A Review and Some Possible Applications. *Zeitschrift für Physikalische Chemie* **2006**, *220*, 1247–1274. DOI: 10.1524/zpch.2006.220.10.1247.
- [57] Silvester, D. S.; Aldous, L. Electrochemical Detection Using Ionic Liquids. In *Electrochemical Strategies in Detection Science*; Arrigan, D. W. M., Ed.; The Royal Society of Chemistry, 2015; pp 341–386.
- [58] Khani, H.; Rofouei, M. K.; Arab, P.; Gupta, V. K.; Vafaei, Z. Multi-walled carbon nanotubes-ionic liquid-carbon paste electrode as a super selectivity sensor: application to potentiometric monitoring of mercury ion(II). *Journal of hazardous materials* **2010**, *183*, 402–409. DOI: 10.1016/j.jhazmat.2010.07.039.
- [59] Zhang, G.-R.; Etzold, B. J. Ionic liquids in electrocatalysis. *Journal of Energy Chemistry* **2016**, *25*, 199–207. DOI: 10.1016/j.jechem.2016.01.007.
- [60] Xu, K.; Xu, W.; Zhang, S. S. Austen Angell's legacy in electrolyte research. *Journal of Non-Crystalline Solids: X* **2022**, *14*, 100088. DOI: 10.1016/j.nocx.2022.100088.
- [61] MacFarlane, D. R.; Forsyth, M.; Izgorodina, E. I.; Abbott, A. P.; Annat, G.; Fraser, K. On the concept of ionicity in ionic liquids. *Physical chemistry chemical physics : PCCP* **2009**, *11*, 4962–4967. DOI: 10.1039/b900201d.
- [62] Harris, K. R. On the Use of the Angell-Walden Equation To Determine the "Ionicity" of Molten Salts and Ionic Liquids. *The journal of physical chemistry. B* **2019**, *123*, 7014–7023. DOI: 10.1021/acs.jpcc.9b04443.

-
- [63] Schreiner, C.; Zugmann, S.; Hartl, R.; Gores, H. J. Fractional Walden Rule for Ionic Liquids: Examples from Recent Measurements and a Critique of the So-Called Ideal KCl Line for the Walden Plot. *J. Chem. Eng. Data* **2010**, *55*, 1784–1788. DOI: 10.1021/je900878j.
- [64] Angell, C. A.; Imrie, C. T.; Ingram, M. D. From simple electrolyte solutions through polymer electrolytes to superionic rubbers: some fundamental considerations. *Polym. Int.* **1998**, *47*, 9–15. DOI: 10.1002/(SICI)1097-0126(199809)47:1<9:AID-PI69>3.0.CO;2-1.
- [65] Ludwig, R. *Ionic liquids in synthesis*, 2nd, completely rev. and enl. ed.; Wiley-VCH: Weinheim, 2008.
- [66] Gardas, R. L.; Coutinho, J. A. P. Group contribution methods for the prediction of thermophysical and transport properties of ionic liquids. *AIChE J.* **2009**, *55*, 1274–1290. DOI: 10.1002/aic.11737.
- [67] Sbartai, A.; Namour, P.; Sarrut, N.; Krejčí, J.; Kucerova, R.; Hamlaoui, M. L.; Jaffrezic-Renault, N. Direct detection of lead in RTIL using DPASV on BDD film microcells and determination of concentration factor after extraction from aqueous samples. *Journal of Electroanalytical Chemistry* **2012**, *686*, 58–62. DOI: 10.1016/j.jelechem.2012.09.024.
- [68] Baerns, M.; Behr, A.; Brehm, A.; Gmehling, J.; Hinrichsen, K.-O.; Hofmann, H.; Palkovits, R.; Onken, U.; Renken, A. *Technische Chemie*, Zweite, erweiterte Auflage; Wiley-VCH: Weinheim, 2013.
- [69] Fu, F.; Wang, Q. Removal of heavy metal ions from wastewaters: a review. *Journal of environmental management* **2011**, *92*, 407–418. DOI: 10.1016/j.jenvman.2010.11.011.
- [70] Zhao, H.; Xia, S.; Ma, P. Use of ionic liquids as ‘green’ solvents for extractions. *J. Chem. Technol. Biotechnol.* **2005**, *80*, 1089–1096. DOI: 10.1002/jctb.1333.
- [71] Visser, A. E.; Swatloski, R. P.; Reichert, W. M.; Willauer, H. D.; Huddleston, J. G.; Rogers, R. D. Room Temperature Ionic Liquids as Replacements for Traditional Organic Solvents and Their Applications Towards “Green Chemistry” in Separation Processes **2002**, 137–156. DOI: 10.1007/978-94-010-0127-4_8.
- [72] Domańska, U.; Rękawek, A. Extraction of Metal Ions from Aqueous Solutions Using Imidazolium Based Ionic Liquids. *J Solution Chem* **2009**, *38*, 739–751. DOI: 10.1007/s10953-009-9402-7.
- [73] Villemin, D.; Didi, M. Extraction of rare earth and heavy metals, using ionic solvents as extraction medium (A Review). *Orient. J. Chem* **2013**, *29*, 1267–1284. DOI: 10.13005/ojc/290402.
- [74] Scott Handy, Ed. *Ionic Liquids in Separation of Metal Ions from Aqueous Solutions*; IntechOpen: London, 2011.
- [75] Yudaev, P. A.; Chistyakov, E. M. Ionic Liquids as Components of Systems for Metal Extraction. *ChemEngineering* **2022**, *6*, 6. DOI: 10.3390/chemengineering6010006.
- [76] Schulz, W. W.; Horwitz, E. P. The Truex Process and the Management of Liquid Tru Uwaste. *Separation Science and Technology* **1988**, *23*, 1191–1210. DOI: 10.1080/01496398808075625.
- [77] Flora, S. J. S.; Pachauri, V. Chelation in metal intoxication. *International journal of environmental research and public health* **2010**, *7*, 2745–2788. DOI: 10.3390/ijerph7072745.
- [78] Iwantschegg, G. *Das Dithizon und seine Anwendung in der Mikro- und Spurenanalyse*, 2., verb. Aufl.; Verl. Chemie: Weinheim, 1972.

- [79] Harris, D. C. *Quantitative chemical analysis*, 7th ed, 3rd printing; W. H. Freeman; Palgrave distributor: New York, Basingstoke, 2007.
- [80] Wei, G.-T.; Yang, Z.; Chen, C.-J. Room temperature ionic liquid as a novel medium for liquid/liquid extraction of metal ions. *Analytica Chimica Acta* **2003**, *488*, 183–192. DOI: 10.1016/S0003-2670(03)00660-3.
- [81] Leyma, R.; Platzer, S.; Jirsa, F.; Kandioller, W.; Krachler, R.; Keppler, B. K. Novel thiosalicylate-based ionic liquids for heavy metal extractions. *Journal of hazardous materials* **2016**, *314*, 164–171. DOI: 10.1016/j.jhazmat.2016.04.038.
- [82] Diabate, P.; Dupont, L.; Boudesocque, S.; Mohamadou, A. Novel Task Specific Ionic Liquids to Remove Heavy Metals from Aqueous Effluents. *Metals* **2018**, *8*, 412. DOI: 10.3390/met8060412.
- [83] Vergara, M. A. V.; Lijanova, I. V.; Likhanova, N. V.; Viguera, D. J.; Xometl, O. O. The removal of heavy metal cations from an aqueous solution using ionic liquids. *Can. J. Chem. Eng.* **2014**, *92*, 1875–1881. DOI: 10.1002/cjce.22053.
- [84] Vander Hoogerstraete, T.; Wellens, S.; Verachtert, K.; Binnemans, K. Removal of transition metals from rare earths by solvent extraction with an undiluted phosphonium ionic liquid: separations relevant to rare-earth magnet recycling. *Green Chem.* **2013**, *15*, 919. DOI: 10.1039/c3gc40198g.
- [85] Parmentier, D.; Metz, S. J.; Kroon, M. C. Tetraalkylammonium oleate and linoleate based ionic liquids: promising extractants for metal salts. *Green Chem* **2013**, *15*, 205–209. DOI: 10.1039/C2GC36458A.
- [86] Giridhar, P.; Venkatesan, K. A.; Srinivasan, T. G.; Vasudeva Rao, P. R. Extraction of fission palladium by Aliquat 336 and electrochemical studies on direct recovery from ionic liquid phase. *Hydrometallurgy* **2006**, *81*, 30–39. DOI: 10.1016/j.hydromet.2005.10.001.
- [87] los Ríos, A. P. de; Hernández-Fernández, F. J.; Lozano, L. J.; Sánchez, S.; Moreno, J. I.; Godínez, C. Removal of Metal Ions from Aqueous Solutions by Extraction with Ionic Liquids. *J. Chem. Eng. Data* **2010**, *55*, 605–608. DOI: 10.1021/je9005008.
- [88] Mikkola, J.-P.; Virtanen, P.; Sjöholm, R. Aliquat 336®—a versatile and affordable cation source for an entirely new family of hydrophobic ionic liquids. *Green Chem* **2006**, *8*, 250. DOI: 10.1039/B512819F.
- [89] Visser, A. E.; Swatloski, R. P.; Reichert, W. M.; Davis Jr., J. H.; Rogers, R. D.; Mayton, R.; Sheff, S.; Wierzbicki, A. Task-specific ionic liquids for the extraction of metal ions from aqueous solutions. *Chem. Commun.* **2001**, 135–136. DOI: 10.1039/b008041l.
- [90] Hoogerstraete, T. V.; Onghena, B.; Binnemans, K. Homogeneous Liquid-Liquid Extraction of Metal Ions with a Functionalized Ionic Liquid. *The journal of physical chemistry letters* **2013**, *4*, 1659–1663. DOI: 10.1021/jz4005366.
- [91] Work, W. J.; Horie, K.; Hess, M.; Stepto, R. F. T. Definition of terms related to polymer blends, composites, and multiphase polymeric materials (IUPAC Recommendations 2004). *Pure and Applied Chemistry* **2004**, *76*, 1985–2007. DOI: 10.1351/pac200476111985.
- [92] Nockemann, P.; Thijs, B.; Pittois, S.; Thoen, J.; Glorieux, C.; van Hecke, K.; van Meervelt, L.; Kirchner, B.; Binnemans, K. Task-specific ionic liquid for solubilizing metal oxides. *The journal of physical chemistry. B* **2006**, *110*, 20978–20992. DOI: 10.1021/jp0642995.
- [93] Nockemann, P.; Binnemans, K.; Thijs, B.; Parac-Vogt, T. N.; Merz, K.; Mudring, A.-V.; Menon, P. C.; Rajesh, R. N.; Cordoyiannis, G.; Thoen, J.; *et al.* Temperature-driven

- mixing-demixing behavior of binary mixtures of the ionic liquid choline bis(trifluoromethylsulfonyl)imide and water. *The journal of physical chemistry. B* **2009**, *113*, 1429–1437. DOI: 10.1021/jp808993t.
- [94] Kohno, Y.; Ohno, H. Temperature-responsive ionic liquid/water interfaces: relation between hydrophilicity of ions and dynamic phase change. *Physical chemistry chemical physics : PCCP* **2012**, *14*, 5063–5070. DOI: 10.1039/C2CP24026B.
- [95] Richter, J.; Ruck, M. Dissolution of metal oxides in task-specific ionic liquid. *RSC advances* **2019**, *9*, 29699–29710. DOI: 10.1039/c9ra06423k.
- [96] Fan, F.-L.; Qin, Z.; Cao, S.-W.; Tan, C.-M.; Huang, Q.-G.; Chen, D.-S.; Wang, J.-R.; Yin, X.-J.; Xu, C.; Feng, X.-G. Highly Efficient and Selective Dissolution Separation of Fission Products by an Ionic Liquid HbetTf2N: A New Approach to Spent Nuclear Fuel Recycling. *Inorganic chemistry* **2019**, *58*, 603–609. DOI: 10.1021/acs.inorgchem.8b02783.
- [97] Sasaki, K.; Suzuki, T.; Mori, T.; Arai, T.; Takao, K.; Ikeda, Y. Selective Liquid–Liquid Extraction of Uranyl Species Using Task-specific Ionic Liquid, Betainium Bis(trifluoromethylsulfonyl)imide. *Chem. Lett.* **2014**, *43*, 775–777. DOI: 10.1246/cl.140048.
- [98] Vander Hoogerstraete, T.; Onghena, B.; Binnemans, K. Homogeneous liquid-liquid extraction of rare earths with the betaine-betainium bis(trifluoromethylsulfonyl)imide ionic liquid system. *International journal of molecular sciences* **2013**, *14*, 21353–21377. DOI: 10.3390/ijms141121353.
- [99] Onghena, B.; Binnemans, K. Recovery of Scandium(III) from Aqueous Solutions by Solvent Extraction with the Functionalized Ionic Liquid Betainium Bis(trifluoromethylsulfonyl)imide. *Ind. Eng. Chem. Res.* **2015**, *54*, 1887–1898. DOI: 10.1021/ie504765v.
- [100] Shkrob, I. A.; Marin, T. W.; Jensen, M. P. Ionic Liquid Based Separations of Trivalent Lanthanide and Actinide Ions. *Ind. Eng. Chem. Res.* **2014**, *53*, 3641–3653. DOI: 10.1021/ie4036719.
- [101] Ikeda, S.; Mori, T.; Ikeda, Y.; Takao, K. Microwave-Assisted Solvent Extraction of Inert Platinum Group Metals from HNO₃ (aq) to Betainium-Based Thermomorphic Ionic Liquid. *ACS Sustainable Chem. Eng.* **2016**, *4*, 2459–2463. DOI: 10.1021/acssuschemeng.6b00186.
- [102] Volia, M. F.; Tereshatov, E. E.; Boltoeva, M.; Folden, C. M. Indium and thallium extraction into betainium bis(trifluoromethylsulfonyl)imide ionic liquid from aqueous hydrochloric acid media. *New J. Chem.* **2020**, *44*, 2527–2537. DOI: 10.1039/C9NJ04879K.
- [103] Mikeli, E.; Balomenos, E.; Pnias, D. Utilizing Recyclable Task-Specific Ionic Liquid for Selective Leaching and Refining of Scandium from Bauxite Residue. *Molecules (Basel, Switzerland)* **2021**, *26*. DOI: 10.3390/molecules26040818.
- [104] Volia, M. F.; Tereshatov, E. E.; Mazan, V.; Folden, C. M.; Boltoeva, M. Effect of aqueous hydrochloric acid and zwitterionic betaine on the mutual solubility between a protic betainium-based ionic liquid and water. *Journal of Molecular Liquids* **2019**, *276*, 296–306. DOI: 10.1016/j.molliq.2018.11.136.
- [105] Fagnant, D. P.; Goff, G. S.; Scott, B. L.; Runde, W.; Brennecke, J. F. Switchable phase behavior of HBetTf2N-H₂O upon neodymium loading: implications for lanthanide separations. *Inorganic chemistry* **2013**, *52*, 549–551. DOI: 10.1021/ic302359d.

-
- [106] Onghena, B.; Jacobs, J.; van Meervelt, L.; Binnemans, K. Homogeneous liquid-liquid extraction of neodymium(III) by choline hexafluoroacetylacetonate in the ionic liquid choline bis(trifluoromethylsulfonyl)imide. *Dalton transactions (Cambridge, England : 2003)* **2014**, *43*, 11566–11578. DOI: 10.1039/c4dt01340a.
- [107] Whitesides, G. M. The origins and the future of microfluidics. *Nature* **2006**, *442*, 368–373. DOI: 10.1038/nature05058.
- [108] Martinez, A. W.; Phillips, S. T.; Butte, M. J.; Whitesides, G. M. Patterned paper as a platform for inexpensive, low-volume, portable bioassays. *Angewandte Chemie (International ed. in English)* **2007**, *46*, 1318–1320. DOI: 10.1002/anie.200603817.
- [109] Liana, D. D.; Raguse, B.; Gooding, J. J.; Chow, E. Recent advances in paper-based sensors. *Sensors (Basel, Switzerland)* **2012**, *12*, 11505–11526. DOI: 10.3390/s120911505.
- [110] López-Marzo, A. M.; Merkoçi, A. Paper-based sensors and assays: a success of the engineering design and the convergence of knowledge areas. *Lab on a chip* **2016**, *16*, 3150–3176. DOI: 10.1039/c6lc00737f.
- [111] Washburn, E. W. The Dynamics of Capillary Flow. *Phys. Rev.* **1921**, *17*, 273–283. DOI: 10.1103/PhysRev.17.273.
- [112] Böhm, A.; Carstens, F.; Trieb, C.; Schabel, S.; Biesalski, M. Engineering microfluidic papers: effect of fiber source and paper sheet properties on capillary-driven fluid flow. *Microfluid Nanofluid* **2014**, *16*, 789–799. DOI: 10.1007/s10404-013-1324-4.
- [113] Medina-Sánchez, M.; Cadevall, M.; Ros, J.; Merkoçi, A. Eco-friendly electrochemical lab-on-paper for heavy metal detection. *Analytical and bioanalytical chemistry* **2015**, *407*, 8445–8449. DOI: 10.1007/s00216-015-9022-6.
- [114] Brandt, A.; Ray, M. J.; To, T. Q.; Leak, D. J.; Murphy, R. J.; Welton, T. Ionic liquid pretreatment of lignocellulosic biomass with ionic liquid–water mixtures. *Green Chem.* **2011**, *13*, 2489. DOI: 10.1039/c1gc15374a.
- [115] Glas, D.; van Doorslaer, C.; Depuydt, D.; Liebner, F.; Rosenau, T.; Binnemans, K.; Vos, D. E. de. Lignin solubility in non-imidazolium ionic liquids. *J. Chem. Technol. Biotechnol.* **2015**, *90*, 1821–1826. DOI: 10.1002/jctb.4492.
- [116] Wang, H.; Gurau, G.; Rogers, R. D. Ionic liquid processing of cellulose. *Chemical Society reviews* **2012**, *41*, 1519–1537. DOI: 10.1039/c2cs15311d.
- [117] Zhao, H.; Baker, G. A.; Song, Z.; Olubajo, O.; Crittle, T.; Peters, D. Designing enzyme-compatible ionic liquids that can dissolve carbohydrates. *Green Chem.* **2008**, *10*, 696. DOI: 10.1039/b801489b.
- [118] Roselli, A. Extraction of Hemicelluloses from a Kraft Paper Pulp with an Ionic Liquid water Mixture. Doctoral, Aalto University, Finland, 2017.
- [119] Glińska, K.; Aqlan, M.; Giralt, J.; Torrens, E.; Fortuny, A.; Montané, D.; Stüber, F.; Fabregat, A.; Font, J.; Olkiewicz, M.; *et al.* Separation of cellulose from industrial paper mill wastewater dried sludge using a commercial and cheap ionic liquid. *Water science and technology : a journal of the International Association on Water Pollution Research* **2019**, *79*, 1897–1904. DOI: 10.2166/wst.2019.189.
- [120] Tobjörk, D.; Österbacka, R. Paper electronics. *Advanced materials (Deerfield Beach, Fla.)* **2011**, *23*, 1935–1961. DOI: 10.1002/adma.201004692.
- [121] Pettersson, F.; Keskinen, J.; Remonen, T.; Herten, L. von; Jansson, E.; Tappura, K.; Zhang, Y.; Wilén, C.-E.; Österbacka, R. Printed environmentally friendly supercapacitors

with ionic liquid electrolytes on paper. *Journal of Power Sources* **2014**, *271*, 298–304. DOI: 10.1016/j.jpowsour.2014.08.020.

- [122] Dossi, N.; Toniolo, R.; Pizzariello, A.; Carrilho, E.; Piccin, E.; Battiston, S.; Bontempelli, G. An electrochemical gas sensor based on paper supported room temperature ionic liquids. *Lab on a chip* **2012**, *12*, 153–158. DOI: 10.1039/c1lc20663j.
- [123] Tokuda, H.; Hayamizu, K.; Ishii, K.; Susan, M. A. B. H.; Watanabe, M. Physicochemical properties and structures of room temperature ionic liquids. 2. Variation of alkyl chain length in imidazolium cation. *The journal of physical chemistry. B* **2005**, *109*, 6103–6110. DOI: 10.1021/jp044626d.
- [124] Thermo Fisher Scientific. 12231 Bismuth(III) nitrate pentahydrate, ACS, 98% min: Chemische Eigenschaften. <https://www.alfa.com/de/catalog/012231/> (accessed May 12, 2023).

8. Appendix

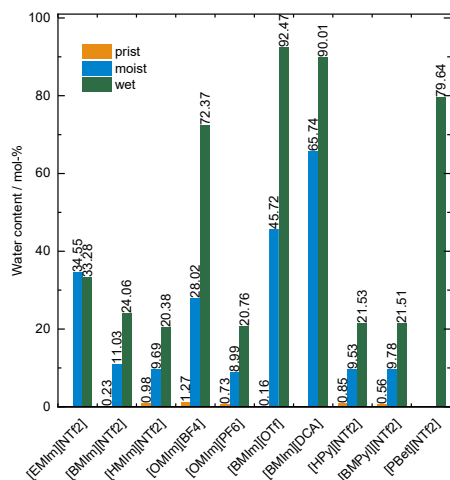
Materials and Disposables

Name	Manufacturer / Distributor
Graphite foil SIGRAFLEX NH	SGL Group
Carbon black Vulcan XC-72	Cabot
Graphite powder	unknown
Silver wire (4N, 1 mm)	TICAR Versand
Paper materials	Self prepared in the Laboratory of Macromolecular and Paper Chemistry, Ernst-Berl-Institut, Department of Chemistry, TU Darmstadt
3D printed cell	Self prepared by Daria Omralinov, Ernst-Berl Institut at TU Darmstadt
Electrochemical (bulk) cells	Self prepared by the mechanical workshop, Department of Chemistry at TU Darmstadt

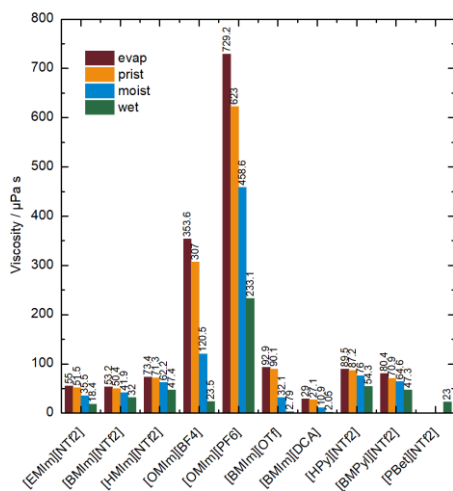
Chemicals

Name	Manufacturer / Distributor	Description
Water	VWR avantor	Ph. Eur., USP, JP
[HBet][NTf ₂]	IOLITEC	98 %
[BMIm][NTf ₂]	Sigma-Aldrich	≥ 98 %
Betaine, anhydrous	Sigma-Aldrich	≥ 99 %
Ethanol	Fischer Scientific	99 %
Bi(NO ₃) ₃ 5 H ₂ O	Sigma-Aldrich	98 %
Pb(NO ₃) ₂	Sigma-Aldrich	≥ 99 %
Nafion [®] (5 wt-%)	Sigma-Aldrich	

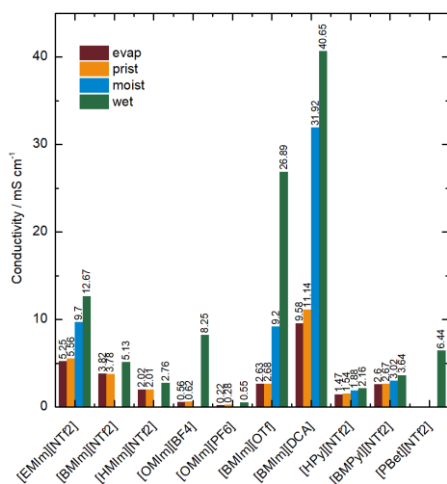
Water influence on Physico-chemical Properties of ILs



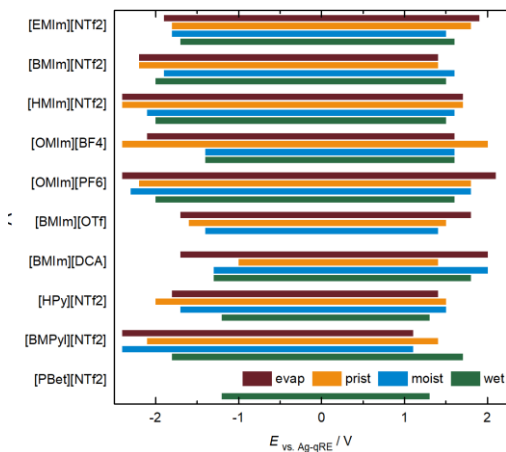
Mol ratios of water in different ILs at RT for the three stages of water content; pristine (prist), moist (50 % RH for 2 weeks) and wet (direct contact to liquid water); measured by Karl Fischer titration. Note: [DCA] and [OTf] containing ILs are completely water miscible.



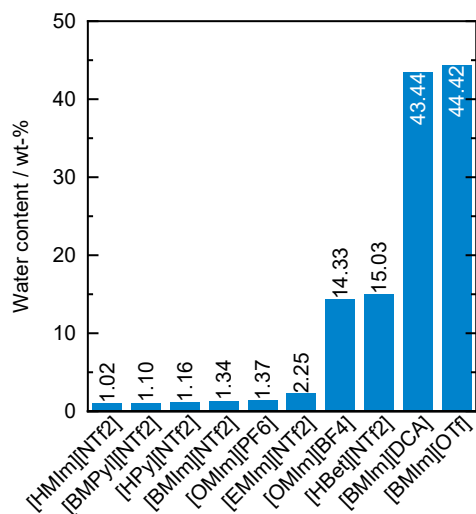
Viscosity of different ILs at RT for the four stages of water content; evaporated (evap), pristine (prist), moist (50 % RH for 2 weeks) and wet (direct contact to liquid water).



Electrical conductivity of different ILs at RT for the four stages of water content; evaporated (evap), praline (prist), moist (50 % RH for 2 weeks) and wet (direct contact to liquid water).

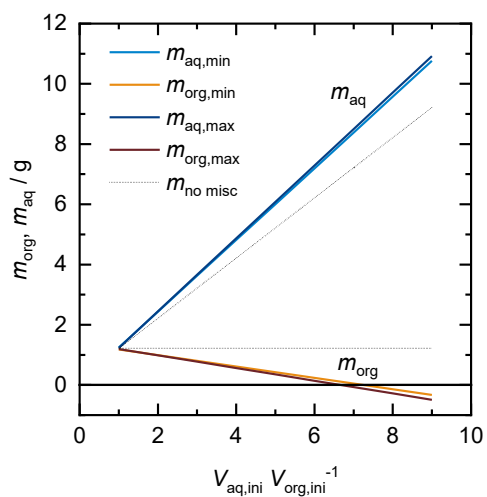


Electrochemical stability window of different ILs at RT for the four stages of water content; evaporated (evap), praline (prist), moist (50 % RH for 2 weeks) and wet (direct contact to liquid water).



Mass ratios of water in ILs after contact to a aqueous liquid phase measured by Karl Fischer titration. Note: [DCA] and [OTf] containing ILs are completely miscible.

Phase Behaviour of [HBet][NTf₂] and Water – Linearization

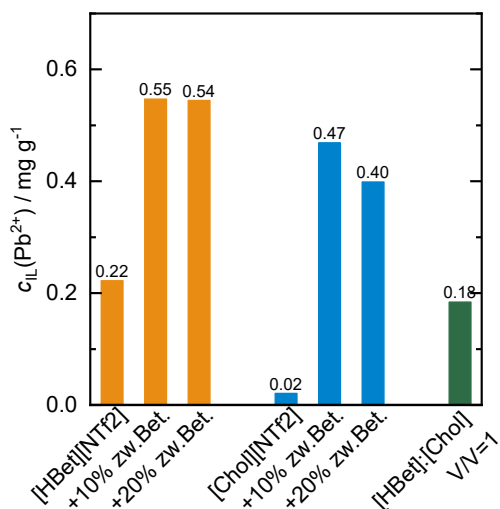


$$m_{\text{org min}} = -0.1892x + 1.3872 \rightarrow 7.33 \text{ mL added H}_2\text{O for complete IL dissolution}$$

$$m_{\text{org max}} = -0.2107x + 1.4059 \rightarrow 6.67 \text{ mL added H}_2\text{O for complete IL dissolution}$$

Extraction Behaviour of Choline [NTf₂]

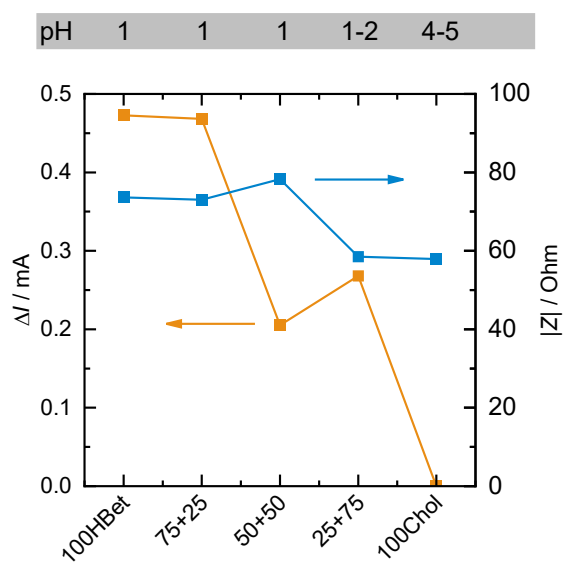
The addition of zwitterionic betaine transforms [Chol][NTf₂], an IL with an UCST of 72 °C and almost no intrinsic Pb²⁺ extraction capabilities to a suitable extractor.^[93] By the addition of 10 wt-% and 20 wt-% per mass of water saturated IL to a $V_{aq,ini}V_{org,ini}^{-1}=1$, concentrations of 0.47 mg g⁻¹ and 0.40 mg g⁻¹, respectively, were found in the organic phase, compared to 0.02 mg g⁻¹, without the additive. The extraction capabilities here could be boosted by a factor of 24. This extraction system has not been reported in the literature yet and transfers the findings of the betaine-based IL to a similar system, where the extraction performance could be enhanced even more by the addition of zwitterionic betaine. The procedure of the extraction with [Chol][NTf₂] follows the described routine of HLLC with [HBet][NTf₂] with an adjusted temperature programme for single phase generation. ONGHENA et al. reported a similar approach, based on [Chol][NTf₂] though with the addition of hexafluoroacetylacetonate as extractant for the extraction of Nd³⁺.^[106] Interestingly, the extraction performance of the mixture of both ILs is only slightly decreased compared to pure [HBet][NTf₂]. For a composition of 1/1 (V/V) of the water saturated ILs a Pb²⁺, a concentration of 0.18 mg g was measured. The extraction capabilities of [HBet][NTf₂] can almost be held, when diluted with [Chol][NTf₂].



Concentrations of Pb²⁺ in the IL phase after HLLC, $c_{aq,ini}(Pb^{2+}) = 1 \text{ mg L}^{-1}$, $V_{aq,ini}V_{org,ini}^{-1} = 1$, measured by ICP-OES.

Electrochemical Pb²⁺ Detection in Choline [NTf₂]

Water saturated [Chol][NTf₂] contains a low concentration of Pb²⁺ after HLLC, as examined via ICP-OES. Consequently, no peak can be found in SWASV detection. No signal can be assigned to Pb stripping even when zwitterionic betaine is added before the extraction, which was found to increase the Pb²⁺ concentration. Mixing this IL with the more intensively studied [HBet][NTf₂] leads to an assignable and evaluable peak signal. This might be caused by the higher pH of [Chol][NTf₂] and the parameter settings, which are optimized for [HBet][NTf₂]. However, [Chol][NTf₂] might be employed for temperature induced HLLC and electrochemical detection for pH adjustments.



Peak intensities, impedance @10 kHz and pH of water saturated [HBet][NTf₂] and [Chol][NTf₂] after HLLC in dependence of the IL volume fractions (abscissa).

$c_{aq,ini}(Pb^{2+}) = 10$ ppm, $V_{aq,ini}V_{org,ini}^{-1} = 1$, $E_{dep} = -1$ V vs. Ag-qRE for $t_{dep} = 600$ s, 42 °C, $E_{Step} = 30$ mV, $E_{Pulse} = 150$ mV, $f = 30$ Hz, blank WE.